Toward Improved Understanding of Aquifer Response Time Scales

by

Farhad Jazaei

A dissertation submitted to the Graduate Faculty of
Auburn University
in partial fulfillment of the
requirements for the Degree of
Doctor of Philosophy

Auburn, Alabama
August 5, 2017

Keywords: Groundwater, time scale, mean action time,
steady state, transient state

Approved by

T. Prabhakar Clement, Committee Chair, Professor of Civil Engineering
Jose Vasconcelos, Associate Professor of Civil Engineering
Xing Fang, Professor of Civil Engineering
Ming-Kuo Lee, Professor of Geoscience

ABSTRACT

Several methods are available in the published literature to analyze transient groundwater flow processes. These methods include both numerical and analytical approaches which describe how groundwater heads would transition from an initial unsteady state to a final steady state. The primary objective of this study is to quantify the time scale required for transient groundwater systems to approach its steady state conditions. Understanding these response time scales is important for managing different types of groundwater resources management problems. Since, in many cases, the governing equation for groundwater flow is identical to the well-known diffusion equation, the knowledge gained from this study is applicable for managing other systems that can be modeled using the diffusion equation. The diffusion equation is one of the most commonly used models for describing a variety of problems involving heat, solute, and water transport processes. When a diffusive system is transient, the dependent variable (e.g., temperature, concentration, or hydraulic head) varies with time; whereas at steady state, the temporal variations becomes negligible. In this work we generalize our steady state analyze and propose an intermediate state, called steady-shape state, which corresponds to situations where temporal variations in diffusive fluxes becomes negligible; however, the dependent variable might still remain transient. We present a general theoretical framework for quantifying the times scale needed for a diffusive system to approach both steady shape and steady state conditions.

ACKNOWLEDGMENTS

Foremost, I am sincerely grateful to my advisor Professor T. Prabhakar Clement for his continuous support of my PhD research, for his motivation, enthusiasm and for his patient mentorship. I am also grateful to Professor Matthew Simpson, at Queensland University of Technology, Australia, for working with me on this interesting research problem. They both helped me a lot to develop this research topic and guided me in writing this dissertation. I thank Dr. Mary Hughes for her words of encouragement and support. I would like to express my sincere gratitude to my dissertation committee: Professor Jose Vasconcelos, Professor Xing Fang and Professor Ming-Kuo Lee for their insightful comments and encouragement. Last but not the least, I would like to thank my caring parents, brothers and lovely wife for continuously supporting me spiritually throughout my life.

Finally, and without hesitation, I would like to dedicate this dissertation to Rebecca Kelly and to the memory of Bill Kelly, for all their love, kindness and support.

JOURNAL PUBLICATIONS FROM THIS DISSERTATION EFFORT

This research effort resulted in publication of the following four key journal articles:

1. Simpson, M.J., Jazaei, F. and Clement, T.P., 2013. How long does it take for aquifer recharge or aquifer discharge processes to reach steady state*? Journal of Hydrology*, 501, pp.241-248.

2. Jazaei, F., Simpson, M.J. and Clement, T.P., 2014. An analytical framework for quantifying aquifer response time scales associated with transient boundary conditions. *Journal of Hydrology*, 519, pp.1642-1648.

3. Jazaei, F., Simpson, M.J. and Clement, T.P., 2016. Spatial analysis of aquifer response times for radial flow processes: Nondimensional analysis and laboratory-scale tests. *Journal of Hydrology*, 532, pp.1-8.

4. Jazaei, F., Simpson, M.J. and Clement, T.P., 2017. Understanding time scales of diffusive fluxes and the implication for steady state and steady shape conditions. *Geophysical Research Letters*, 44(1), 174-180.

TABLE OF CONTENTS

LIST OF TABLES

LIST OF FIGURES

CHAPTER 1 **INTRODUCTION AND OBJECTIVES**

1.1 Background

One of the common issues in groundwater studies is to understand when a groundwater system would reach its steady state or equilibrium condition. Typically, when an aquifer system is perturbed by changing the external forcing (such as pumping or recharge) and/or boundary conditions, the aquifer will undergo a transient response until it reaches its steady state. The term "*steady state*" refers to the condition when the net inflows balances the outflows [*Currell et al.*, 2014]. However, although such definition seems to be definite, still there is an ambiguity in estimation of the time scale needed to reach steady state. The obscurity arises from the fact that from the mathematical view point a system which is in a transient state requires infinite amount of time to respond to the changes in the forcing conditions and to relax into a new steady state [*K Landman and McGuinness*, 2000; *McNabb*, 1993; *McNabb and Wake*, 1991; *Zhou*, 2009] (Figure 1-1). Therefore, this information may appear to be irrelevant since it is impossible to wait for infinite amount of time. Also, this information will not allow us to differentiate processes that act at different time scales (Figure 1-1). Therefore, a point of interest is to determine a finite time scale required for a the system to evolve "close to steady state" conditions [*Hickson et al.*, 2009a; b; *Rousseau-Gueutin et al.*, 2013]. Herein, this finite time scale for a system to effectively relax to its stead state is referred to as "*response time scale*."

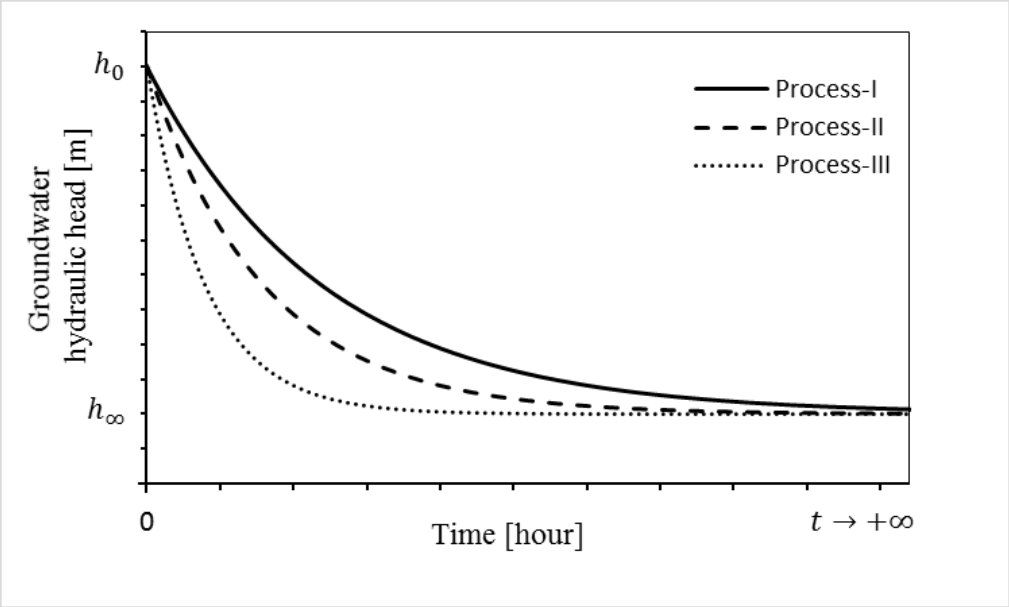

Figure 1-1: Three different groundwater processes. In all three processes hydraulic head drops from the initial condition h_0 to the steady state h_∞. As shown in this figure, when $t \to +\infty$ the hydraulic head in Process-III approaches to the steady state value of h_∞ faster than Process-I and Process-II.

Transient solutions of the groundwater head variation, when they are available, are considerably more complicated to implement. Therefore, in many studies, in order to simplify computational complexities, it is often assumed that the system is under steady state [*Schwartz et al.*, 2010]. Understanding the response time scales of the systems would allow one to decide whether such simplified steady state solutions are sufficient to model the systems of interest [*Alley et al.*, 2002; *Schwartz et al.*, 2010]. Furthermore, response time scales of the groundwater systems are useful parameters that can help us better characterize the interactions occurring between surface water and groundwater bodies [*Alley et al.*, 2002; *John Bredehoeft and Kendy*, 2008; *J Bredehoeft and Durbin*, 2009; *Kooi and Groen*, 2003; *Mario Sophocleous*, 2000; *Marios Sophocleous*, 2012].

1.2 Review of traditional approaches used to quantify aquifer response time scales

The methods available to evaluate response time scales of diffusive problems can be categorized into two groups: (1) explicit scaling methods, and (2) implicit computational methods.

1.2.1 Explicit scaling methods

Explicit scaling method first identifies a set of system parameters that impact the transient solution and uses them to derive an expression for estimating response time scales. Explicit scaling method has been used in several studies and some of these studies are reviewed in this section.

Theis, who pioneered early groundwater investigations, was one of the first who studied the response time of an aquifer to forcing boundary conditions [*C V Theis*, 1935]. In his classic work, the Theis-solution article, he analyzed a horizontal two-dimensional transient flow toward a well [*C V Theis*, 1935]. He discussed how storage coefficient, S, aquifer transmissivity, T, and the length scale of the system, L, would control the aquifer response time [*C V Theis*, 1940]. Theis analyses showed how pumping from a well would form a cone of depression which will spreads toward the boundary condition at a rate directly proportional with T and inversely proportional with S. In this study, he also clarified that points located further from the well, for example at the system boundaries, require more time than points closer to the well, to respond to pumping. In a later work, he analyzed the response of the boundary conditions (i.e. nearby stream) to pumping in terms of recharge rate variation at those locations [*C Theis*, 1941]. This work was followed by several other classic studies that analyzed the groundwater responses to pumping wells [*Glover and Balmer*, 1954; *C Jenkins*, 1968a; b; *C T Jenkins*, 1968].

Riley [1969] published an article in which he studied the compression characteristics of a vertical confined aquitard bounded by two aquifers in top and bottom. Once the bounded aquitard is perturbed by sudden head changes it required certain amount of time to dissipate the excess pore pressures. The author suggested that the excess hydraulic head dissipation time can be estimated using the expression: $S_S(b/2)^2/K$, where S_S is the specific storage, K is the hydraulic conductivity and b is the aquitard thickness. This time scale is considered in other porous media compression problems as "inelastic time constant" [*Hanson*, 1988; *Leake*, 1990].

Downing et al. [1974] was one of the first who evaluated the response time of the aquifer interacting with surface water bodies. They introduced a factor, T/SL^2, to analyze the capacity of aquifers in transferring the recharging fluxes. Later, this factor brought into use by *Rushton and Redshaw* [1979] as a parameter that controls the amount of time a system would require to achieve its steady state. The unit of presented response time is inverse of time. Therefore, *Erskine and Papaioannou* [1997] named it "aquifer response rate". They used this time scale to solve conjunctive surface water- groundwater problems.

The most widely used groundwater response time scale equation was introduced by *Gelhar and Wilson* [1974b]. They studied a generalized lumped groundwater (reservoir) model with one outflow. The primary objective of their work was to develop a framework for assessing the impact of forcing conditions on modeling outflow from a system. The authors defined the constant response time of the system as n/a, where n was aquifer porosity and a is a constant associated

with the hydraulic property of the system. They evaluated $a = 3T/L^2$ for a linearly responding aquifer (reservoir) and $a = \pi^2 T/4L^2$ for sinusoidal declining water tables.

Townly [1995] discussed the response of the aquifer to periodic sinusoidal hydraulic drivers at the boundary conditions. He analyzed the amplitude of head fluctuations and the phase lags between periodic forcing to represent a dimensionless characteristic parameter as $\tau = SL^2/TP$, where *P* was the period of the forcing boundary condition. He concluded that in a slow responding aquifer τ is large and steady-state models are sufficient to model the average condition of the system. On the other hand, if τ is small steady state models would miss-represent the average condition of the system [*Townley,* 1995].

Knight et al. [2005] applied a unit response approach to quantify the impacts of hydraulic parameters on the aquifer time scales. They specifically studied the effect of sloping on the aquifer response time scales and suggested the constant $SL^2/K\alpha$; where α was a constant expressing the change in the land surface elevation in the system. Recently, *Walker et al.* [2015] published a more comprehensive study and estimated the response time scale of a sloping aquifer system as $SL^2E^*/K\alpha$, where E^* is a constant associated with the land and surface elevation.

Marios Sophocleous [2012] reviewed the issues related to the response time scales of aquifers and concluded that it is an important groundwater management parameter and yet it is not fully understood. He pointed out the simple formula used for estimating the time scale of a one-dimensional diffusion system as L^2/D, where $D = T/S$, diffusivity of the aquifer. This formula has also been suggested by other researchers in the diffusion literature.

Recently, *Rousseau-Gueutin et al.* [2013] introduced a term as the "time to near steady state" as the time that 95% of the transition has accrued. Their works was focused on mixed aquifers, i.e. having confined and unconfined systems. He defined the characteristic time constant as $t_{ne} \approx 3S_u L_u / T(L_c + L_u/2)$, where S, T and L are specific storage, transmissivity and length of the systems. Subscripts c and u refer to confined and unconfined aquifers.

One of the major limitations of the above mentioned time scales is that they all provide a unique value for the entire aquifer system. However, one can intuitively expect the response time scale cannot be a constant at the entire domain. For example, point adjacent to a pumping well would respond faster than the points tens of meters away from the well. Time scale formulae derived using explicit scaling methods would show how the time would vary with aquifer some of hydraulic parameters, but they cannot explain how the time scale would vary spatially.

1.2.2 Implicit computational methods

Transient solutions for groundwater flow problems can be computed using traditional analytical solutions [e.g. *Theis,* 1934] or numerical codes such as MODFLOW [*McDonald and Harbaugh*, 2003]. To determine the response time scale of a groundwater system using implicit computational methods, one has to solve the transient groundwater problem first. Later, one requires to define a threshold value to estimate the response time. For example, one could assume that the system has effectively approached the steady state once 90% to 99% of the maximum possible variation is completed. One of the critical limitation of this approach is that such results significantly depends on the subjectively defined threshold value [*R Hickson et al.*, 2011; *K Landman and McGuinness*, 2000; *Lu and Werner*, 2013; *Watson et al.*, 2010]. Different threshold

values would result in different response time scale [*Ellery et al.*, 2012b]. Moreover, since the system is being analyzed at its close to steady state condition, small variation in the threshold value would result in significantly different computed response time. Another limitation of an implicit computational method is that it requires complex transient solution of the problem. Furthermore, this approach yields to a discrete time quantity, for example 20 hours or 100 days, which cannot be easily used to understanding the fundamental relationship between the response time scale and system parameters such *K, S, L* and the position.

Implicit computational methods have been used in several studies to estimate the response time scales under different forcing conditions. However, not all of them report the value of threshold parameter used in the computation processes. As an example, *J Bredehoeft and Durbin* [2009] applied an implicit computational method to estimate the response of an aquifer to pumping and surface recharges as a part of their study. However, the threshold value is not reported in the manuscript. *Riley* [1969] defined the response time of the aquifer as the moment at which 93% of the process was occurred. In another study, *Rousseau-Gueutin et al.* [2013] defined the response time of the aquifer as the moment at which 95% of the process was completed. Several other studies have also used numerical transient solutions to estimate the response times of groundwater systems [*Currell et al.*, 2014; *Konikow and Leake*, 2014; *Vasseur et al.*, 2015; *Zhou*, 2009].

1.3 Review of some novel approaches used to quantify time scales of heat and mass transport processes

Researchers studying heat and mass transport problems has also been interested in understanding the response time scale of their systems. In most heat and mass transport studies the required time to effectively reach the steady state is often referred to as “critical time” [*Hickson et*

al., 2009a; b; *R Hickson et al.*, 2011]. McNabb and Wake developed a novel theory, known as mean action time (MAT) theory, which can be used to evaluate the response time scale of heat transport processes as the first moment (mean) of the rate of temperature changes in the heat conductor [*McNabb and Wake*, 1991]. They defined the response time scale as a finite measurable time a heat transport process requires to transition from its initial state to a new equilibrium condition. The MAT theory does not have the limitation of the explicit mathematical and implicit computational methods. This theory can provide insight into the spatial variation of the response time scale. In contrary with implicit computational approaches, the MAT theory does not depend on any subjectively defined threshold values, and more importantly, it does not require any form of transient solutions (i.e. either analytical or numerical solution).

McNabb and Anderssen [1992] applied the MAT theory to investigate the relationships between the duration of cooling and freezing processes of homogeneous isotropic heat conductors. McNabb in his later study, used the MAT theory to study the amount of time natural resources, like methane gas resources, would require to diffuse out through fractured structures [*McNabb*, 1993]. Landman and coworkers used this to quantify the time scale of pressure filtering of flocculated suspensions [*K A Landman and White*, 1997]. During the pressure filtering process, void ratio of the material decreases with time, until the system reaches a steady state. The authors defined the time scale of the process by applying the MAT theory. McGuiness and coworkers pointed out that the MAT theory can provide useful insight for cooking processes. They discussed the applicability of the MAT theory to analyze heat and moisture movement equations and estimate a finite time scale for cooking grains [*K Landman and McGuinness*, 2000; *McGowan and McGuiness*, 1996].

Hickson and coworkers emphasized the need for a framework which can estimate the required time to reach the steady state in heat and mass transport problems [*Hickson et al.*, 2009a; b; *R Hickson et al.*, 2011; *R I Hickson et al.*, 2011]. In their studies, they considered a finite one-dimensional system having one and multiple layers. Their general objective was to define a finite time scale for heat transient models. Their definitions relied on the transient solutions and threshold values. However, *Ellery et al.* [2012b] discussed the limitations of each definition and suggested to use the MAT theory to avoid these limitations.

Recently, Berezhkovskii and coworkers introduced "local accumulation time [*Barenblatt*]" as the time scale of morphogen gradient formation for one-dimensional reaction diffusion processes [*Berezhkovskii*, 2011; *Berezhkovskii and Shvartsman*, 2011; *Berezhkovskii et al.*, 2010; *Gordon et al.*, 2011]. However, *Ellery et al.* [2012a] debated that their approaches were identical with *McNabb and Wake* [1991] framework simply reformulated for a different set of applications.

Later, Ellery and coworkers enhanced the MAT theory by defining the second moment of rate of variation about its mean as the variance of action time (VAT). The variance of action time can provide additional information about the time scale of the process. VAT can be used to quantify the spread of the distribution of process about the MAT. Hence, MAT and VAT together can provide another time scale of the process which can estimate the instant at which the system would effectively approach its steady state [*Ellery et al.*, 2012b].

1.4 Applying MAT theory to a classic problem

In this section, basic mathematics of the MAT theory is explained using a classic radio-active problem, known as first order reaction process. This process can be simply described by an ordinary differential equation as

$$\frac{\mathrm{d}C(t)}{\mathrm{d}t} = -kC(t), \tag{1}$$

where $C(t)$ [ML^3] is the concentration at time t [T], and K [T^{-1}] is the decay constant. We assume an initial value of $C(0) = C_0$. We know that, in this process, $C(t)$ approaches to its ultimate steady state of $C(\infty) = 0$ exponentially fast as $t \to +\infty$ [*Crank*, 1975]. Based on *McNabb et al.* [1990] the time scale of the process, MAT, can be determined as the mean of the rate of $C(t) - C(\infty) = C(t)$ variation,

$$MAT = \frac{\int_0^\infty t \frac{\mathrm{d}C(t)}{\mathrm{d}t}\mathrm{d}t}{\int_0^\infty \frac{\mathrm{d}C(t)}{\mathrm{d}t}\mathrm{d}t}. \tag{2}$$

To evaluate Eq.(2), first we rewrite the governing equation given in Eq.(1) as

$$C(t) = \frac{-1}{K}\frac{dC(t)}{dt}. \tag{3}$$

Applying integration by parts, we can rewrite Eq.(2) as

$$MAT = \frac{\left[tC(t)\Big|_0^\infty - \int_0^\infty C(t)dt \right]}{\int_0^\infty \frac{dC(t)}{dt}dt}. \tag{4}$$

Noting the fact that $C(t)$ approaches to $C(\infty)=0$ exponentially fast as $t \to +\infty$ makes the first term in the bracket vanish. Combining Eqs. (3) and (4) leads to

$$MAT = \frac{\frac{1}{K}\int_0^\infty \frac{\mathrm{d}C(t)}{\mathrm{d}t}\mathrm{d}t}{\int_0^\infty \frac{\mathrm{d}C}{\mathrm{d}t}\mathrm{d}t} = \frac{1}{K}. \tag{5}$$

Note that the time scale of the process, $1/K$, is estimated using the mean action time theory without using the transient solution. Answer is identical to the well-known time scale of first order decay processes known as the "mean life time" [*Purich and Allison,* 1999]. However, now we have a formal procedure to derive the time scale from the governing equation, Eq. (1).

1.5 Objectives of the study

The objective of this study is to apply the MAT theory to develop an approach which does not have the limitation of traditional approaches in characterizing the response time scale of aquifers. The goal of this dissertation is to improve our understanding of aquifer response time scales to different types of forcing conditions such as surface recharge and discharge, stream level variations at aquifer boundaries, and pumping or injection wells. Each of these conditions is expanded rigorously in Chapter 2, Chapter 3, Chapter 4, and Chapter 5. These chapters consist independent introduction, literature review, methods, results and discussion.

In Chapter 2, a one–dimensional, unconfined, Dupuit–Forchheimer model of groundwater flow through a saturated homogeneous porous medium having uniform areal recharge and discharge is considered. The main objectives of this chapter are to present the mathematical derivations and assumptions of the MAT theory, to define the aquifer response time scale to aerial

recharging and discharging forces, to show the explicit relationship between the aquifer response time scale and hydraulic and geometric properties of the system, and estimate the amount of time a recharging or discharging aquifer requires to approach its steady state[1].

Chapter 3 discusses that one of the major challenges in studying coupled groundwater and surface-water interactions arises from the considerable difference in the response time scales of surface-water and groundwater systems to external forcings. Despite of several studies which are focused on groundwater quantity or quality issues, this chapter is focused on the response time scales of the processes. In Chapter 3, a one–dimensional, unconfined, Dupuit–Forchheimer model of groundwater flow through a saturated homogeneous porous medium having varying boundary conditions at its both ends, is considered. In this chapter, variation at the boundary conditions represent surface water level variations (e.g. stream level variation). The main objectives of this chapter is to develop an analytical framework to estimate the response time scale of groundwater systems to changes in surface-water conditions[2].

Chapter 4 explores a groundwater system which is perturbed by a pumping or injecting well. The main objective of this chapter is to develop the non-dimensional MAT framework in a radial ystems. This chapter aims to investigate the pumping, injecting and recovery time scales to associated pumping rates[3].

---

[1] Chapter 2 is published in the *Journal of Hydrology* (2013), 519, 1642–1648.
[2] Chapter 3 is published in the *Journal of Hydrology* (2014), 519, 1642–1648
[3] Chapter 4 is published in the *Journal of Hydrology* (2016), 532, 1-8.

Unlike previous chapters which are focused on groundwater problems, Chapter 5 focuses on general form of diffusive processes. Therefore, results of this chapter are valid for all diffusive problems including groundwater, heat, and contaminant transport problems, to name a few. Along the common steady state condition, this chapter considers an intermediate state, called steady-shape state. Steady-shape state corresponds to situations where temporal variations in diffusive fluxes becomes negligible; however, the dependent variable might still remain transient. The concept of steady shape flow has been invoked heuristically by several researchers without any fundamental theoretical understanding of when steady shape conditions are relevant. The main objective of this chapter is to develop a general theoretical framework to address this fundamental limitation[4].

The main objective of the final chapter, Chapter (6), is to presents a summary of the general findings of this work, closing discussion and concluding remarks. This chapter also aims to point out the limitations of this work and possibilities for future researches.

[4] Chapter 5 is published in the *Geophysical Research Letters* (2017), 44(1), 174–180.

CHAPTER 2 HOW LONG DOES IT TAKE FOR AQUIFER RECHARGE AND DISCHARGE PROCESSES TO REACH STEADY STATE

2.1 Introduction

Groundwater flow systems, and the corresponding models used to study these systems, are typically characterized as being either transient or steady state [*Bear*, 1972; *Haitjema*, 1995; *Remson et al.*, 1971; *Strack*, 1989; *Wang and Anderson*, 1982; *Zheng and Bennett*, 2002]. This characterization is useful since the mathematical and computational techniques required to solve steady state groundwater flow models are generally much simpler than those required to solve transient groundwater flow models. Given that steady flow conditions correspond to the long time asymptotic limit of a transient response [*Wang and Anderson*, 1982], it is relevant to develop tools that can be used to estimate the amount of time required for a particular transient flow problem to effectively reach steady state. In the heat and mass transfer literature such a time is called a *critical time [Hickson et al., 2009a; 2009b; R Hickson et al., 2011]*.

A schematic diagram of a groundwater recharge problem is outlined in Figure 2-1 for an aquifer of length L. The aquifer is bounded by two rivers. River one, at $x = 0$, at river stage h_1, and river two, at $x = L$, at river stage h_2. The hypothetical phreatic surface without recharge is indicated by the curve marked $t = 0$. We consider initiating a transient response in the groundwater flow system by applying spatially uniform recharge at rate R. The result of this recharge is that the amount of water stored in the subsurface system increases with time and the phreatic surface rises to give the curve indicated by $t \to +\infty$. This kind of scenario, where recharge is applied to an existing unconfined groundwater flow system results in the saturated depth increasing with time which means that additional water is stored in the aquifer. The details

of how to design and operate such recharge systems has been described at length previously [*Bouwer*, 2002; *Daher et al.*, 2011; *Martín-Rosales et al.*, 2007; *Pedretti et al.*, 2012; *Vandenbohede and Van Houtte*, 2012]. The design of such recharge systems naturally leads us to the following questions:

(1) How long does it take for the water stored in the aquifer to essentially reach a maximum volume? (i.e. what is the critical time for this process?)

(2) How does this critical time depend on the parameters governing the flow processes and the geometry of the aquifer?

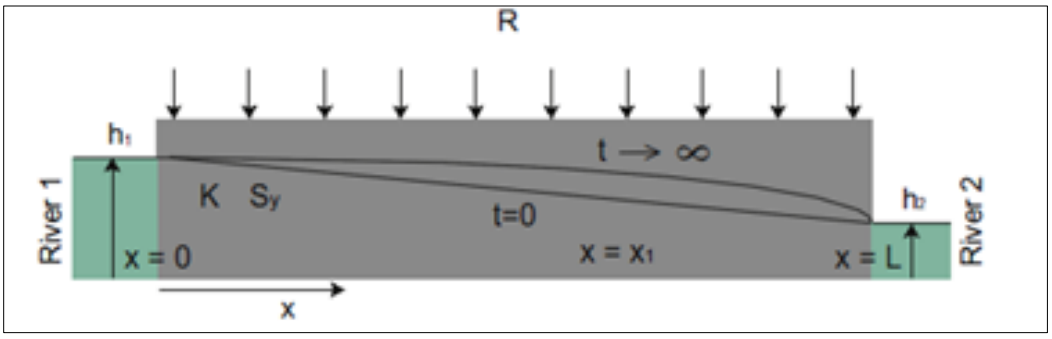

Figure 2-1: Schematic of an aquifer recharge process. The groundwater flow takes place on a one-dimensional domain, $0 \le x \le L$, and is assumed to correspond to a linearized, unconfined, Dupuit–Forchheimer description [*Bear*, 1972]. The saturated depth at $x = 0$ (river 1) is $h(0,t) = h_1$. The saturated depth at $x = L$ (river 2) is $h(L,t) = h_2$. The schematic depicts a transition where the initial phreatic surface, indicated by $t = 0$, asymptotes to a new steady state, indicated by $t \to +\infty$. This transition is associated with the application of uniform recharge, at rate R, for $t > 0$.

Strictly speaking, from a mathematical point of view, it takes an infinite amount of time for a transient response of a diffusive process to become steady [*McNabb*, 1993; *McNabb and Wake*, 1991]. Clearly, this strict mathematical definition is impractical and it would be useful to have a quantitative framework to estimate a finite time scale that indicates when the time rate of change of water stored in the aquifer to effectively reach zero [*Marios Sophocleous*, 2012; *Walton*, 2011].

Developing a method of analysis that avoids the need for relying on numerical computation to answer these questions would be useful since it is not obvious how, for example, changing the properties of the porous medium or the geometry of the groundwater flow system would affect the time taken for the rate of change of water stored in the aquifer to effectively reach zero. Understanding this time scale may have several practical uses; for example, if we were to design an artificial recharge program it would be of interest to monitor the increase in storage in the aquifer with time and to have a criterion to indicate when the system would effectively reach steady state.

Previous attempts to characterize critical times for groundwater flow models have relied on using numerical experimentation [*Buès and Oltean*, 2000; *Chang et al.*, 2011], laboratory–scale experimentation [*Chang and Clement*, 2012; *Goswami and Clement*, 2007; *Kim and Ann*, 2001; *M Simpson et al.*, 2003] or very simple mathematical definitions. One common mathematical approach is to define the critical time to be the amount of time taken for the transient solution to reach within ε% of the corresponding steady state value, where ε is some small user–defined tolerance [*R Hickson et al.*, 2011; *K Landman and McGuinness*, 2000; *Lu and Werner*, 2013; *Watson et al.*, 2010]. Although insightful, there are certain difficulties associated with this definition, namely:

(1) this definition depends upon a subjective choice of ε,

(2) this definition requires the complete solution of the transient groundwater flow problem, and

(3) this definition leads to a numerical framework that does not provide analytical insight into how the critical time varies with the parameters in the model.

In this work we introduce the concept of *mean action time* (MAT) which gives us a finite estimate of the amount of time required for a transient groundwater flow response to effectively reach steady state. The MAT was originally defined by McNabb and Wake as a tool to study linear heat transfer [*McNabb*, 1993; *McNabb and Wake*, 1991]. Here we demonstrate how to extend this theory to analyze groundwater flow processes. We will show, in a general framework, that:

(1) the MAT gives us an objective finite estimate of the amount of time required for a transient response to effectively reach steady state,

(2) the MAT can be found explicitly without solving the governing transient groundwater flow equation, and

(3) the mathematical expression for the MAT shows us how the time scale for different transitions, such as applying or removing different amounts of recharge, would depend on the parameters in the groundwater flow model.

Furthermore, once we have defined the MAT, we can define higher moments such as the variance of action time (VAT) which provides a measure of the spread of the distribution about the mean [*Ellery et al.*, 2012b; *M J Simpson et al.*, 2013b]. The VAT is insightful since we know that if the VAT is small then we are dealing with a low-variance distribution for which the mean value provides a useful estimate of the time scale of interest [*Ellery et al.*, 2012b; *Grimmett and Welsh*, 1986]. Alternatively, if the VAT is large then we are dealing with a high-variance distribution for which the mean value is less insightful [*Ellery et al.*, 2012b; *Grimmett and Welsh*,

1986]. For such high variance distributions we can improve our estimate of the time required for the system to approach steady state by incorporating information about the variance, as we shall demonstrate in Section 2.3 [*M J Simpson et al.*, 2013b].

In this work we aim to first present the mathematical derivations and assumptions in a general framework. Once we have developed the theoretical results we then apply these concepts to obtain specific MAT and VAT results for a new laboratory–scale experimental data set describing aquifer recharge and discharge processes.

2.2 Theoretical Methods

We consider a one–dimensional, unconfined, Dupuit–Forchheimer model of groundwater flow through a saturated homogeneous porous medium [*Bear*, 1972; 1979]

$$S_y \frac{\partial h}{\partial t} = K \frac{\partial}{\partial x}\left[h \frac{\partial h}{\partial x} \right] + R, \tag{6}$$

where $h(x,t) > 0$ [L] is the saturated thickness at position x and time t, $S_y > 0$ [-] is the specific yield, $K > 0$ [L/T] is the saturated hydraulic conductivity and $R > 0$ [L/T] is the recharge rate. For practical problems where the hydraulic gradient is very small, $\left|\partial h/\partial x\right| \ll 1$, this model is often linearized to give

$$S_y \frac{\partial h}{\partial t} = K\bar{h} \frac{\partial^2 h}{\partial x^2} + R, \tag{7}$$

where $\bar{h}$ is the average saturated thickness [*Bear*, 1972; 1979; *Haitjema*, 1995; *Strack*, 1989]. This simplification is sufficiently robust for solving many problems [*Haitjema*, 1995; *Strack*, 1989]

including laboratory–scale problems where the hydraulic gradient is not necessarily small [*Kim and Ann*, 2001]. For notational convenience we will re–write Eq. (7) in the form of a reaction–diffusion equation

$$\frac{\partial h}{\partial t} = D\frac{\partial^2 h}{\partial x^2} + W, \tag{8}$$

where $D = k\bar{h}/S_y$ [L^2/T] is the diffusivity and $W = R/S_y$ [L/T] is a zero order source term which is used to model recharge [*Bear*, 1979].

To apply our modelling framework to the schematic in Figure 2-1(a), we will consider a model of unconfined groundwater flow, Eq. (8), that describes an arbitrary transition from some initial condition, $h(x,0) = h_0(x)$, to some steady state $\lim_{t\to\infty} h(x,t) = h_\infty(x)$. This transition is sufficiently general that it could describe an aquifer recharge process, where $h_\infty(x) \geq h_0(x)$ for all locations x, such as the case where additional recharge applied by increasing R. Similarly, our framework could describe an aquifer discharge process, where $h_\infty(x) \leq h_0(x)$ for all locations x, such as the case where the recharge applied to the system is reduced, by decreasing R. We seek to characterize the amount of time required for such transitions to effectively reach steady state by considering the following quantities [*Ellery et al.*, 2012a; 2012b]:

$$\begin{aligned} F(t;x) &= 1 - \left[\frac{h(x,t) - h_\infty(x)}{h_0(x) - h_\infty(x)}\right], t > 0, \\ f(t;x) &= \frac{\partial F(t;x)}{\partial t} = -\frac{\partial}{\partial t}\left[\frac{h(x,t) - h_\infty(x)}{h_0(x) - h_\infty(x)}\right], t > 0. \end{aligned} \tag{9}$$

For many transitions $F(t;x)$ monotonically increases from $F=0$ at $t=0$ to $F\to 1^{-}$, as $t\to+\infty$ at all spatial locations x, as shown in Figure 2-2(b)–(c). This means that we can interpret $F(t;x)$ as a cumulative distribution function and $f(t;x)$ as the associated probability density function [*Ellery et al.*, 2012a; 2012b]. From a physical point of view, our interpretation of these definitions is as follows: at $t=0$, we have $F=0$, meaning that 0% of transient response has taken place. In the long time limit as $t\to+\infty$, we have $F\to 1^{-}$, meaning that effectively 100% of the transient response has occurred. For intermediate values of t we have $0<F<1$, meaning that $(100\times F)\%$ of the transient response has occurred. For example, if $F(t;x)=0.5$, then we can interpret this as 50% of the transient response has taken place by this time.

The MAT, $T(x)$, is the mean of this distribution which has the probability density function $f(t;x)$, and can be written as [*Ellery et al.*, 2012b]

$$T(x)=\int_0^{\infty} t f(t;x)\,\mathrm{d}t. \tag{10}$$

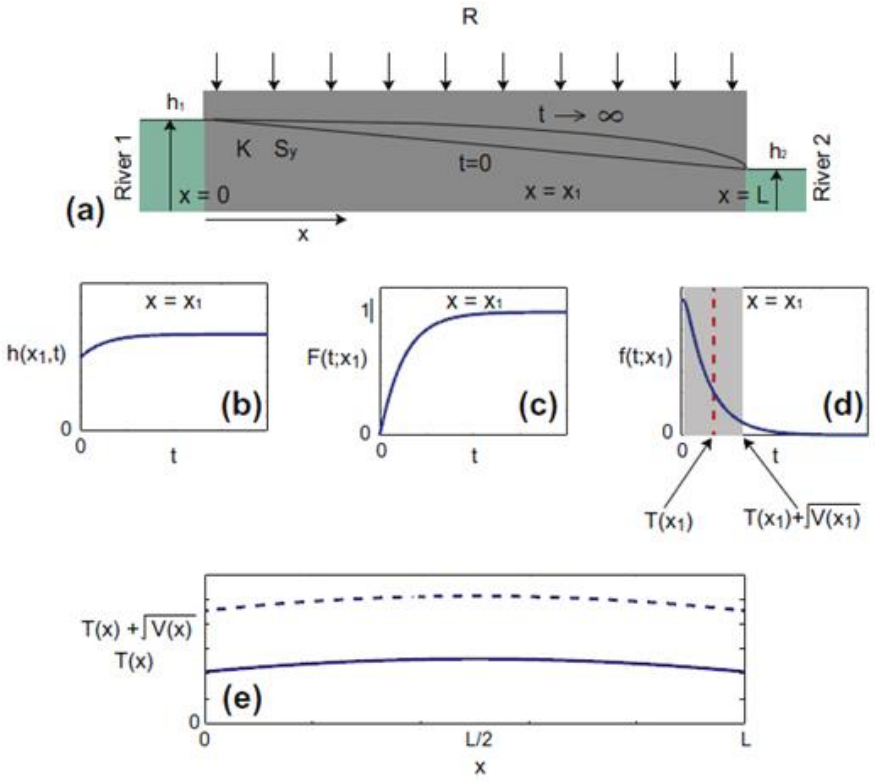

Figure 2-2 (a) Schematic showing an aquifer recharge process. (b) Schematic showing how the saturated thickness at a fixed location, $x = x_1$, in (a) varies with time, t. This schematic corresponds to a recharge transition since $h(x,t)$ increases with t. (c) For the schematic transition in (b) we show $F(t;x_1)$, which has the property that $F(0;x_1) = 0$ and $F(t;x_1) \to 1^-$ as $t \to +\infty$. (d) For the schematic transition in (b) we plot $f(t;x_1)$ using Eq. (22). The mean of this probability density function is indicated in the red vertical (dotted) line, and corresponds to the MAT, $T(x)$. The variance of this probability density function is indicated with the gray shading, which corresponds to one standard deviation about the mean $T(x) \pm \sqrt{V(x)}$ as indicated. Profiles in (e) show $T(x)$ (solid) and $T(x) + \sqrt{V(x)}$ (dashed) at all locations $0 \le x \le L$. (For interpretation of the references to color in this figure legend, the reader is referred to the web version of this article.)

Physically, we interpret the MAT to be the mean time scale required for the initial condition, $h_0(x)$, to asymptote to the steady state, $h_\infty(x)$. Intuitively, we expect that this time scale would depend on spatial location and we will see that the MAT is indeed a function of position, x. To evaluate the MAT we apply integration by parts to Eq. (10) to obtain

$$T(x)g(x) = \int_0^{\infty} h_{\infty}(x) - h(x,t)\,\mathrm{d}t, \tag{11}$$

where we have defined $g(x) = h_{\infty}(x) - h_0(x)$ for notational convenience. To arrive at Eq. (11) we made use of the fact that $h(x,t) - h_{\infty}(x)$ decays to zero exponentially fast as $t \to +\infty$ which is true for all linear reaction diffusion equations [*Ellery et al.*, 2012a; 2012b]. Differentiating Eq. (11) twice with respect to *x* and combining the resulting expression with Eq. (8), gives us

$$\frac{\mathrm{d}^2\left[T(x)g(x)\right]}{\mathrm{d}x^2} = -\frac{g(x)}{D}, \tag{12}$$

If we expand using the product rule, we can write this as

$$\frac{\mathrm{d}^2T(x)}{\mathrm{d}x^2} + \frac{\mathrm{d}T(x)}{\mathrm{d}x}\left[\frac{2}{g(x)}\frac{\mathrm{d}g(x)}{\mathrm{d}x}\right] + T(x)\left[\frac{1}{g(x)}\frac{\mathrm{d}^2g(x)}{\mathrm{d}x^2}\right] = -\frac{1}{D}, \tag{13}$$

which is a boundary value problem for the MAT, $T(x)$. We would like to emphasize that Eq. (13) is sufficiently general that it applies to any initial condition, $h_0(x)$, and any steady state, $h_{\infty}(x)$, such that $F(t;x)$ monotonically increases from $F = 0$ at $t = 0$ to $F \to 1^{-}$ as $t \to +\infty$ for all x. This means that Eq. (13) can be used to characterize the amount of time required for a transition to reach steady state for a very general class of aquifer recharge and discharge processes. Furthermore the approach is valid for any values of S_y, *K*, *R*, *L*, h_1 and h_2. We note that our derivation of Eq. (13) is very similar to previous work presented by Ellery and coworkers [*Ellery et al.*, 2012a; 2012b] except that those previous studies considered a first order linear source term in the governing equations whereas here we consider a zero order constant source term.

The theory of MAT relies on certain properties of the problem that allow us to evaluate the integral for $T(x)$, given by Eq. (10) is convergent. When we apply the definition of MAT in the present context we are guaranteed that the improper integral in Eq. (10) is convergent since $h(x,t)-h(x)$ decays to zero exponentially fast as $t \to +\infty$ for all such reaction diffusion equations [*Ellery et al.*, 2012a; 2012b; *Hickson et al.*, 2009a; 2009b; *R Hickson et al.*, 2011]. Alternative definitions of a critical time, such as considering the median of action time, where $F(t;x)=0.5$, do not allow us to make use of this asymptotic property and consequently we cannot solve for the critical time without having previously solved for the underlying partial differential equation.

In a similar way to calculating the mean of $f(t;x)$, we can also evaluate higher moments of $f(t;x)$, such as the variance, which quantifies the spread about the mean [*Ellery et al.*, 2012b; *M J Simpson et al.*, 2013b]. We begin by using the standard definition of the variance

$$V(x)=\int_0^\infty (t-T(x))^2 f(t;x)\,\mathrm{d}t, \tag{14}$$

Expanding the quadratic term in the integrand in Eq. (14) allows us to evaluate two of the three integral expressions on the right hand side of Eq. (14) in terms of the MAT, $T(x)$. The remaining integral can be simplified using integration by parts, making use of the fact that $h(x,t)-h(x)$ decays to zero exponentially fast as $t \to +\infty$ to give

$$\varphi(x)=2\int_0^\infty t(h_\infty(x)-h(x,t))\,\mathrm{d}t, \tag{15}$$

where we have made a change of variables, $\varphi(x) = V(x)g(x) + T(x)^2 g(x)$ to simplify the expression. To obtain a differential equation for $\varphi(x)$, we differentiate Eq. (15) twice with respect to x. Combining the resulting expression with Eq. (8) gives us

$$\frac{\mathrm{d}^2\varphi(x)}{\mathrm{d}x^2} = -\frac{2T(x)g(x)}{D}, \tag{16}$$

which, together with appropriate boundary conditions can be solved for $\varphi(x)$ and in turn rearranged to give $V(x)$, recalling that $V(x) = \varphi(x) \big/ g(x) - T(x)^2$. Once we have solved the relevant boundary value problems for the mean, $T(x)$, and the variance, $V(x)$, we can identify a mean time scale, $T(x)$ and a time interval about this mean time scale $t \in \left[T(x) - \sqrt{V(x)}, T(x) + \sqrt{V(x)} \right]$. Here, we take the time interval to be the mean plus or minus one standard deviation of the distribution $f(t;x)$ [*M J Simpson et al.*, 2013b].

To reiterate the practicality of our results, we would like to emphasize the following point. From a strict mathematical point of view, the transient solution of a reaction diffusion equation, such as Eq. (8), takes an infinite amount of time to reach steady state [*Hickson et al.*, 2009a; *McNabb*, 1993; *McNabb and Wake*, 1991]. Using this strict definition, it is completely unclear how to make a practical estimate of the duration of time that a transient groundwater process will require to reach steady state. Our result characterizes a mean time scale, the MAT, giving us a finite estimate of the amount of time required for the transient flow process to effectively reach steady state.

2.2.1 MAT and VAT for aquifer recharge

Although we have outlined the MAT theory in Section 2.2 for an arbitrary aquifer recharge or discharge process, we will now demonstrate the insight provided by the MAT framework by considering a specific application. We will examine the transition described by Eq. (8) on $0 \le x \le L$ with boundary conditions $h(0,t) = h_1$ and $h(L,t) = h_2$. We consider a transition from the initial condition,

$$h_0(x) = \frac{x(h_2 - h_1)}{L} + h_1, \tag{17}$$

to a new steady state that is driven by applying recharge, $R > 0$, for $t \ge 0$. The long time steady state for this transition is

$$\lim_{t\to\infty} h(x,t) = h_\infty(x) = -\frac{wx^2}{2D} + x\left[\frac{h_2 - h_1}{L} + \frac{WL}{2D}\right] + h_1, \tag{18}$$

where $D = K\bar{h}/S_y$ [L^2/T] is the diffusivity and $W = R/S_y$. This particular initial condition and steady state gives us

$$g(x) = \frac{Wx(L-x)}{2D}. \tag{19}$$

To find the MAT for this transition we note that $\mathrm{d}g(x)/\mathrm{d}x = W(L-2x)/2D$ and $\mathrm{d}^2g(x)/\mathrm{d}x^2 = -W/D$. Substituting these expressions for $g(x)$, $\mathrm{d}g(x)/\mathrm{d}x$ and $\mathrm{d}^2g(x)/\mathrm{d}x^2$ into Eq. (13) gives

$$\frac{\mathrm{d}^2T(x)}{\mathrm{d}x^2}+\frac{\mathrm{d}T(x)}{\mathrm{d}x}\left[\frac{2(L-2x)}{x(L-x)}\right]-T(x)\left[\frac{2}{x(L-x)}\right]=-\frac{1}{D}, \tag{20}$$

which is a variable coefficient second order boundary value problem that is singular at $x=0$ and $x=L$. We note that Eq. (20) is independent of W, and this can be explained by the fact that the coefficients of $\mathrm{d}T(x)/\mathrm{d}x$ and $T(x)$ in Eq. (13) are rational functions in which W cancels for our $g(x)$, given by Eq. (19).

To determine the relevant boundary conditions for Eq. (20) we multiply both sides of this equation by $x(L-x)$, which gives

$$x(L-x)\frac{\mathrm{d}^2T(x)}{\mathrm{d}x^2}+2(L-2x)\frac{\mathrm{d}T(x)}{\mathrm{d}x}-2T(x)=-\frac{x(L-x)}{D}. \tag{21}$$

Evaluating Eq. (21) at $x=0$ gives us

$$\frac{\mathrm{d}T(0)}{\mathrm{d}x}-\frac{T(0)}{L}=0. \tag{22}$$

which is a Robin condition for the boundary at $x=0$ [*Kreyszig*, 2008]. To determine the other boundary condition we substitute $x=L$ into Eq. (21) to give

$$\frac{\mathrm{d}T(L)}{\mathrm{d}x}-\frac{T(L)}{L}=0, \tag{23}$$

which is a Robin condition at $x=L$ [*Cullen and Zill*, 1992; *Kreyszig*, 2008].

The solution of Eq. (20) with Eqs. (22) and (23) is

$$T(x) = \frac{1}{12D}(L^2 + xL - x^2). \tag{24}$$

This solution shows that the MAT is spatially dependent and has a maximum value of $5L^2/48D$ at $x = L/2$. This expression is very revealing since it shows us exactly how the MAT depends on the parameters in the model and the boundary conditions. We see that the MAT is proportional to L^2/D, which is a diffusive time scale [*Barenblatt*, 2003], and we also see that the MAT depends explicitly on position x.

Now that we have solved for the MAT we can use Eq. (16), with the relevant boundary conditions $\varphi(0) = \varphi(L) = 0$, to solve for $\varphi(x)$ which can be rearranged to give

$$V(x) = \frac{1}{720D^2}(7L^4 + 2L^3x - 3L^2x^2 + 2x^3L - x^4). \tag{25}$$

The maximum VAT occurs at $x = L/2$ and is given by $119L^4/11520D^2$. The expression for the maximum variance can be used to find the maximum standard deviation, which is given by $\sqrt{119}L^2/\sqrt{11520}D \approx 0.1016\,L^2/D$.

2.2.2 MAT and VAT for aquifer discharge

We now consider a transition governed by Eq. (8) for the process of aquifer discharge. With the same domain and boundary conditions described for the recharge problem in Section 2.2.1, we consider the initial condition

$$h_0(x) = -\frac{Wx^2}{2D} + x\left[\frac{h_2 - h_1}{L} + \frac{WL}{2D}\right] + h_1, \tag{26}$$

which corresponds to the long term steady state profile from the recharge process described in Section 2.2.1, where $D = K\bar{h}/S_y$ and $W = R/S_y$. To initiate a discharge process, where the saturated thickness of the aquifer will decrease with time, we set $R = 0$ in Eq. (7), which is equivalent to setting $W = 0$ in Eq. (8), which gives

$$\lim_{t\to\infty} h(x,t) = h_\infty(x) = \frac{x(h_2 - h_1)}{L} + h_1, \tag{27}$$

and

$$g(x) = -\frac{Wx(L-x)}{2D}. \tag{28}$$

With these conditions, Eq. (13) can be written as

$$\frac{\mathrm{d}^2T(x)}{\mathrm{d}x^2} + \frac{\mathrm{d}T(x)}{\mathrm{d}x}\left[\frac{2(L-2x)}{x(L-x)}\right] - T(x)\left[\frac{2}{x(L-x)}\right] = -\frac{1}{D}, \tag{29}$$

which is exactly the same boundary value problem as we obtained previously in Section 2.2.1. The fact that the boundary value problem governing the MAT for the discharge process is exactly the same as the boundary value problem governing the MAT for the recharge process means that the exact same Robin boundary conditions and the exact same solution, namely Eq. (24), are relevant for both the recharge and discharge problems. Similarly, we can also solve Eq. (16) to find the VAT for this discharge problem. Following the same procedure to find the VAT we find that the solution of Eq. (16) for the discharge problem is exactly the same as for the recharge problem,

namely Eq. (25). This result shows that the important time scales associated with aquifer recharge and discharge processes are identical for the same physical problem.

2.3 Results

We now demonstrate the practicality of our theoretical predictions from Sections 2.2.1–2.2.2 by considering a new laboratory–scale data set describing aquifer recharge and discharge processes. We will perform experiments in a laboratory–scale aquifer model, packed with a homogeneous porous medium, by applying different amounts of recharge to the system and measuring the temporal response of the saturated depth in the system. Our experimental data will give us an indication of the amount of time required for the saturated thickness of the laboratory–scale aquifer to reach steady state and we will test these measurements against predictions made according to the MAT and VAT results developed in Section 2.2. We will test the MAT and VAT theory for both aquifer recharge and aquifer discharge experiments.

2.3.1 Case Study: Analysis of a new laboratory–scale data set

A laboratory–scale aquifer model, similar to the one used in several previous studies [*Abarca and Clement*, 2009; *Chang and Clement*, 2012; 2013; *Goswami and Clement*, 2007] was used, and an image of the physical model is shown in Figure 2-3(a). The tank consists of Pexiglass. The central porous chamber (50cm × 28cm × 2.2cm) was packed under wet conditions with uniformly–sized glass beads, where each bead has a diameter of 1.1 mm. We consider the glass bead system to be a homogeneous and isotropic porous medium [*Abarca and Clement*, 2009; *Chang and Clement*, 2012; 2013; *Goswami and Clement*, 2007]. A constant head boundary condition was applied at the left–hand vertical boundary, where $x = 0$ cm, to maintain an initial saturated depth

of approximately 18.7 cm. A no–flow boundary was imposed at the right–hand vertical boundary, where $x = 50$ cm.

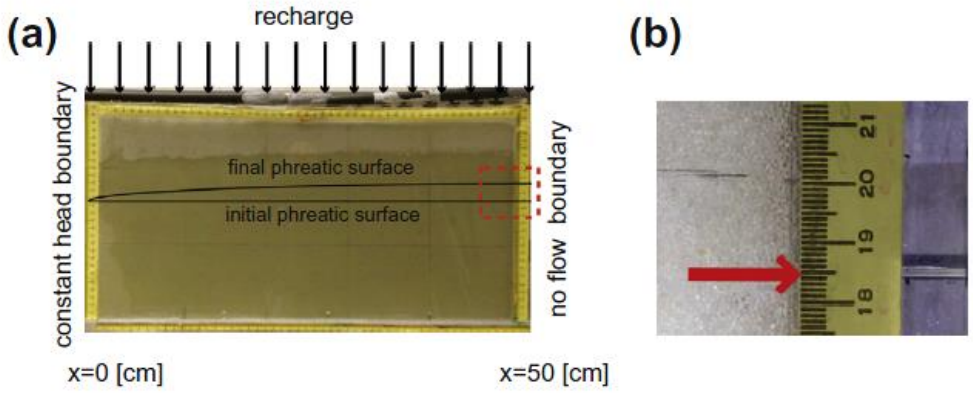

Figure 2-3 (a) Laboratory-scale apparatus. The porous media chamber was wet-packed with uniform glass beads. A constant head boundary was imposed at $x = 0$ cm and a no flow boundary was imposed at $x = 50$ cm. The initial condition corresponds to an approximately horizontal phreatic surface, as indicated. The recharge was applied approximately uniformly along the top of the porous media chamber and eventually the phreatic surface evolves to the final state, as indicated. Observations were made by monitoring the saturated depth of the fluid at $x = 50$ cm. The region contained within the (red) dashed square in (a) is shown in (b) where the saturated thickness is indicated by the red arrow. (For interpretation of the references to color in this figure legend, the reader is referred to the web version of this article.)

A recharge gallery along the upper boundary of the aquifer, consisting of approximately evenly spaced constant flow drippers, was installed. Water was delivered to the recharge outlets from a constant head tank. We considered two different kinds of experiments and repeated each experiment for three different pumping rates:

(1) For the recharge experiments, we considered the initial condition in the system to be a spatially uniform saturated depth $h_0(x) = h_1 \approx 18.7$ cm. At $t = 0$ the recharge was applied and the increase in saturated thickness at the right hand boundary, where $x = 50$ cm, was recorded using the scale shown in Figure 2-4(b). The recharge experiments were repeated three times using three different recharge rates: $R_1 = 1.23$ cm/min, $R_2 = 1.77$ cm/min, and $R_3 = 2.57$ cm/min.

(2) The *discharge experiments* were initiated by removing the recharge gallery at the conclusion of each recharge experiment. This means that after a sufficient period of time (approximately 5 minutes), at the conclusion of each recharge experiment, the phreatic surface was approximately parabolic and each discharge experiment involved observing the parabolic phreatic surface relaxing back to an essentially horizontal phreatic surface.

The recharge rates used in the experiments are very large, and the reason that we used such large recharge rates was so that we could make our measurements as accurate as possible. For the recharge experiments we expect that initial saturated depth, $h_0(x)$, will increase to $h_\infty(x)$ after a sufficient amount of time. Since we are aiming to make accurate measurements of the increase in $h(x,t)$, it is convenient for us to use relatively large recharge rates to ensure that the difference between $h_\infty(x)$ and $h_0(x)$, was approximately 2–3 cm (see Figure 2-4(b)) so that we could record these measurements as accurately as possible.

We first report results for the recharge experiments. Results in Figure 2-5(a)–(c) show the transient response at $x = 50$ cm in the laboratory–scale aquifer when applying three different recharge rates: $R_1 = 1.23$ cm/min, $R_2 = 1.77$ cm/min and $R_3 = 2.57$ cm/min, respectively. Comparing the profiles in Figure 2-5(a)–(c) indicates that each of the recharge experiments were initiated with $h(50,0) \approx 18.7$ cm, and we observe that the increase in saturated thickness at $x = 50$ cm depends on the recharge rate. For example, with $R_1 = 1.23$ cm/min we see that $h(50,t)$ eventually increases to approximately 19.9 cm, for $R_2 = 1.77$ cm/min we see that $h(50,t)$ eventually increases to approximately 20.5 cm and for $R_3 = 2.57$ cm/min $h(50,t)$ eventually increases to approximately 22.3 cm. Interestingly, a visual comparison of the three transient data

sets in Figure 2-5(a)–(c) indicates that it is very difficult to distinguish the differences in the time scales of the transient processes regardless of the differences in the recharge rate and the differences in the change in saturated thickness at $x = 50$ cm. This qualitative observation is consistent with our theoretical predictions from Section 2.12.2.1 where the MAT framework predicted that the recharge time scale is independent of the recharge rate. We will now quantitatively test this prediction using the data from Figure 2-5(a)–(c).

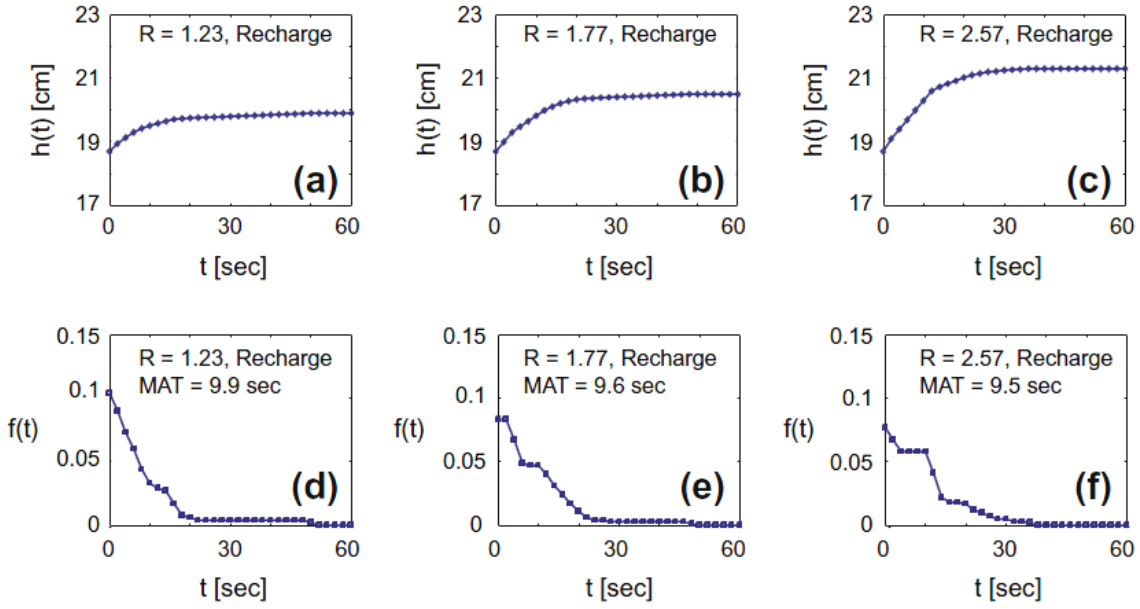

Figure 2-4: Results for the recharge experiments are given in (a)–(c) showing the evolution of $h(x,t)$, at $x = 50$ cm, for $R_1 = 1.23$ cm/min, $R_2 = 1.77$ cm/min and $R_3 = 2.57$ cm/min, respectively. Using the data in (a)–(c), collected at 2 s intervals, profiles of $f(t;x)$ at $x = 50$ cm were estimated using Eq. (30), and presented in (d)–(f). Estimates of the MAT at $x = 50$ cm were obtained by numerically integrating Eq. (10) and the results are reported in (d)–(f).

To compute the values of $f(t;x)$ we used the data from Figure 2-5(a)–(c), at $x = 50$ cm, and estimated $h_0(x)$ and $h_\infty(x)$ directly from these data. To reconstruct $f(t;x)$ for this data we rewrite Eq. (9) as

$$f(t;x) = \frac{1}{h_\infty(x) - h_0(x)} \frac{\partial h(x,t)}{\partial t}$$
$$\approx \frac{1}{h_\infty(x) - h_0(x)} \left[\frac{h(x,t+\Delta t) - h(x,t-\Delta t)}{2\Delta t} \right], \quad (30)$$

where we have used a central difference approximation to estimate $\partial h/\partial t$ [*Chapra and Canale*, 2012]. This discrete expression for $f(t;x)$ can be evaluated using the $h(x,t)$ time series data presented in Figure 2-5(a)–(c). The corresponding $f(t;x)$ profiles, at $x = 50$ cm, shown in Figure 2-5(d)–(f), are given for the three different recharge rates: $R_1 = 1.23$ cm/min, $R_2 = 1.77$ cm/min and $R_3 = 2.57$ cm/min, respectively. To quantitatively test our theoretical predictions from Section 2.2.1 we evaluate $T(x)$, at $x = 50$ cm, using Eq. (10) and the $f(t;x)$ data in Figure 2-5(d)–(f). The integral expression is evaluated numerically using a trapezoid rule with panel width of 2 seconds [*Chapra and Canale*, 2012]. The corresponding values of the MAT, estimated directly from the data are, 9.9, 9.6 and 9.5 seconds for each of the three recharge experiments, respectively. These results indicate that the MAT for the experiments appear to be independent of the recharge rate, as predicted by our theory in Section 2.2.1.

We now report the results of the discharge experiments. Results in Figure 2-5(a)–(c) show the transient response at $x = 50$ cm in the laboratory–scale aquifer after turning off the recharge at the conclusion of each of the three recharge experiments where different rates of recharge had been applied: $R_1 = 1.23$ cm/min, $R_2 = 1.77$ cm/min and $R_3 = 2.57$ cm/min. Comparing the profiles in Figure 2-5(a)–(c) confirms that each of the discharge experiments were initiated with different values of the saturated thickness at $x = 50$ cm. However, the data in Figure 2-5(a)–(c) indicates that after a sufficiently long period of time the saturated thickness at $x = 50$ cm asymptotes to

approximately 18.7 cm. A visual comparison of the three transient discharge data sets in Figure 2-5(a)–(c) indicates that the time scale of the transient processes are very similar regardless of the initial saturated depth at $x = 50$ cm. This qualitative observation is consistent with our theoretical predictions from Section 2.2.1–2.2.2 and we will now quantitatively test this prediction using the data from Figure 2-5(a)–(c).

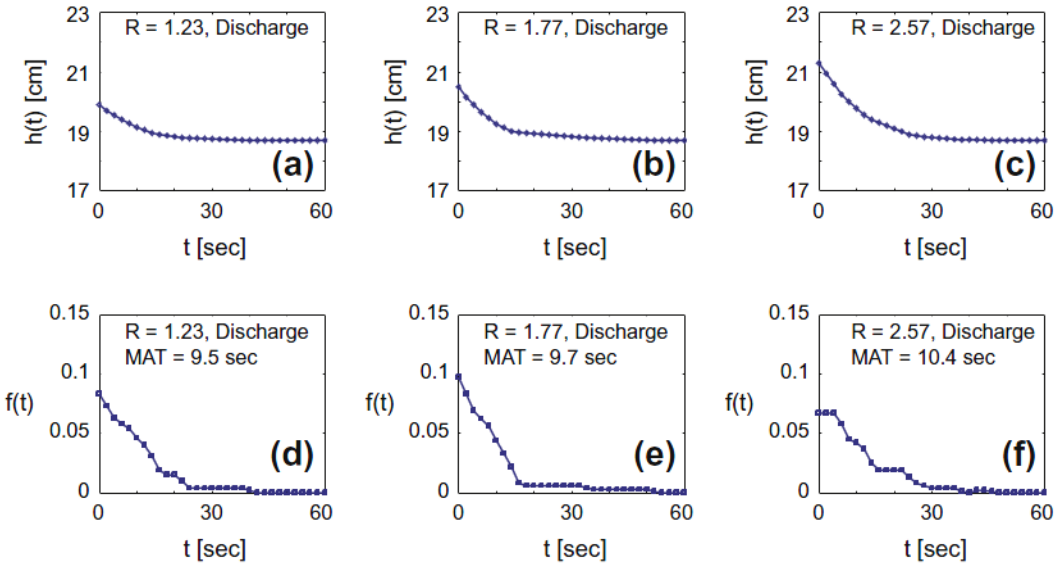

Figure 2-5: Results for the discharge experiments are given in (a)–(c) showing the evolution of $h(x,t)$, at $x = 50$ cm, for $R_1 = 1.23$ cm/min, $R_2 = 1.77$ cm/min and $R_3 = 2.57$ cm/min, respectively. Using the data in (a)–(c), collected at 2 s intervals, profiles of $f(t;x)$ at $x = 50$ cm were estimated using Eq. (30), and presented in (d)–(f). Estimates of the MAT at $x = 50$ cm were obtained by numerically integrating Eq. (10) and the results are reported in (d)–(f).

The profiles in Figure 2-5(d)–(f) show $f(t;x)$ at $x = 50$ cm, for each discharge experiment. To compute the values of $f(t;x)$ we used Eq. (10) with the data from Figure 2-5(a)–(c). For each discharge experiment we estimate $T(x)$, using Eq. (10) and our $f(t;x)$ data in Figure 2-5(d)–(f). To evaluate the integral in Eq. (10) we use the trapezoid rule with panel width of 2 seconds [*Chapra and Canale*, 2012]. The corresponding values of the MAT, estimated directly from the

data, are 9.5, 9.7 and 10.4 seconds for each of the three discharge experiments. These results are also consistent with our MAT predictions since our theoretical results in Sections 2.2.1–2.2.2 predicted that the mean time scale for the discharge process is identical to the mean time scale for the recharge process. Our laboratory data, described so far, qualitatively supports the theoretical predictions made using the MAT framework in Sections 2.2.1–2.2.2. To quantitatively test our theoretical predictions we must estimate the parameters describing the fluid flow in the laboratory scale model. We measured the saturated hydraulic conductivity using a standard column test which showed that the average saturated hydraulic conductivity is 980 m/day (68 cm/min). We independently measured the specific yield, $S_y \approx 0.2$, and we assumed that the average saturated depth was $\bar{h} \approx 19.0$ cm so that we can estimate $D = K\bar{h}/S_y$ to be 6460 cm^2/min. This gives a maximum MAT, $5L^2/48D$, of 9.7 seconds. Here we have used $L = 100$ cm to reflect the symmetry of the problem imposed by using a no flow boundary condition at $x = 50$ cm. This theoretical prediction agrees with our experimental measurements reported in Figure 2-4 and Figure 2-5.

If we wish to use our MAT and VAT results to quantify a critical time interval for the experimental data we take the critical time interval to be the mean plus or minus one standard deviation [*M J Simpson et al.*, 2013b]. Using $K = 980$ m/day, $S_y = 0.2$ and $\bar{h} = 19.0$ cm indicates that the maximum VAT is approximately 89.0 seconds for all our experimental systems. This means that we can take the critical time interval to be $9.7 \pm \sqrt{89} \approx 9.7 \pm 9.4$ seconds, which indicates that by 19.1 seconds the transient aquifer response has essentially finished.

Comparing this estimate with the data in Figure 2-4(a)–(c) and Figure 2-5(a)–(c) seems reasonable since we observe little transient response in the system after approximately 20 seconds for each experiment.

2.4 Discussion and Conclusions

The theory of MAT provides us with an objective tool to characterize the time scale required for a transient groundwater flow response to effectively reach steady state. This is a practical tool since it allows us to estimate the time scale required for a transient response to effectively reach steady state using an analytic framework that avoids the need for solving a time dependent partial differential equation describing the transient process.

The key advantage of the MAT framework is that it gives us an exact mathematical expression describing how the time scale depends on the particular aspects of the problem of interest. In this work we have shown that the MAT gives us an exact mathematical expression showing how the time scales of the process depend upon the parameters (e.g. K, $\bar{h}$, S_y, h_1, h_2, L and R) for a general aquifer recharge and aquifer discharge process. Our theoretical results yield some useful and possibly counterintuitive results. For example, we show that the MAT is not explicitly dependent upon the recharge rate, R, and we show that the MAT for a recharge process is equivalent to the MAT of the related discharge process. This is a surprising result since the steady state phreatic surface depends on the recharge rate R but the new theory indicates that the time taken to reach steady state is independent of R. These results are not obvious without the MAT framework.

In addition to providing more general insight into aquifer recharge and discharge processes, we also evaluated the MAT for a specific laboratory–scale data set describing an unconfined aquifer recharge and discharge process. The theory predicted that the MAT for the three recharge and the three discharge experiments should be 9.7 seconds. Despite experimental variabilities, all six MAT values (9.9, 9.6 and 9.5 seconds for recharge; and 9.5, 9.7, and 10.4 seconds for discharge) estimated from transient dataset are remarkably close to the theoretical prediction, demonstrating the validity of the theory.

The MAT analysis and results outlined here can be applied to study other linear models of groundwater flow, such as two–dimensional and three–dimensional models [*K Landman and McGuinness*, 2000]. For such models, the techniques outlined here for the one–dimensional case are directly applicable except that the boundary value problems governing the MAT will be two–dimensional and three–dimensional partial differential equations, similar to Poisson's equation [*Wang and Anderson*, 1982]. These kinds of models can be solved exactly using standard techniques, such as separation of variables, provided that the problems are considered on separable domains [*Kreyszig*, 2008]. Other problems, such as studying the MAT of genuinely nonlinear flow problems that are not readily linearized are far more challenging [*Ellery et al.*, 2012a; *M J Simpson et al.*, 2013b]. The application of the theory of MAT to such problems requires additional analysis and our future work will seek to address these problems.

The MAT analysis and results outlined here can be applied to study other linear models of groundwater flow, such as two-dimensional and three-dimensional models [*K Landman and McGuinness*, 2000]. For such models, the techniques outlined here for the one-dimensional case are directly applicable except that the boundary value problems governing the MAT will be two-

dimensional and three-dimensional partial differential equations, similar to Poisson's equation [*Wang and Anderson*, 1982]. These kinds of equations can be solved exactly using standard techniques, such as separation of variables, provided that the problems are considered on separable domains [*Kreyszig*, 2008]. Other problems, such as studying the MAT of genuinely nonlinear flow problems that are not readily linearized are far more challenging [*Ellery et al.*, 2012a; *M J Simpson et al.*, 2013b]. The application of the theory of MAT to such problems requires additional analysis and our future work will seek to address these problems.

An extension of our present study would be to consider the MAT for a heterogeneous groundwater flow problem. The heterogeneous analog of Eq. (6) can be written as

$$S_y \frac{\partial h}{\partial t} = \frac{\partial}{\partial x}\left[K(x) h \frac{\partial h}{\partial x} \right] + R(x), \tag{31}$$

where $K(x)$ is the spatially varying saturated hydraulic conductivity and $R(x)$ is the spatially varying recharge rate [*Bear*, 1979]. For practical problems where the hydraulic gradient is very small, $|\partial h/\partial x| \ll 1$, the linearized analog of this model can be written as

$$\frac{\partial h}{\partial t} = \frac{\partial}{\partial x}\left[D(x) \frac{\partial h}{\partial x} \right] + W(x), \tag{32}$$

where $D(x) = \bar{h}K(x)/S_y$ [L²/T] is a spatially-dependent diffusivity and $W(x) = R(x)/S_y$ is a spatially dependent zero order source term. If we apply the same mathematical procedure, outlined previously in Section 2.2, to find the boundary value problem governing the MAT for the heterogeneous flow model we arrive at

$$\frac{\mathrm{d}^2\left[T(x)g(x)\right]}{\mathrm{d}x^2}+\frac{1}{D(x)}\frac{\mathrm{dD}(x)}{\mathrm{d}x}\frac{\mathrm{d}\left[T(x)g(x)\right]}{\mathrm{d}x}=-\frac{g(x)}{D(x)}, \tag{33}$$

which is a generalization of Eq. (12) since the two boundary value problems are identical when $D(x)$, or equivalently $K(x)$, is a constant. Similar to the homogeneous flow problem, the MAT for the heterogeneous flow problem is independent of the recharge, but is now explicitly dependent on the form of the heterogeneity since the solution of Eq. (33) depends on the functional form of $D(x)$. Although we have outlined how the theory of MAT extends to deal with the heterogeneous flow, we leave a thorough exploration of the solution of Eq. (33) and a comparison of such a solution with physical measurements as a topic for future research.

$$S_y\frac{\partial h}{\partial t}=K\frac{\partial}{\partial x}\left[h\frac{\partial h}{\partial x}\right], \tag{34}$$

CHAPTER 3 AN ANALYTICAL FRAMEWORK FOR QUANTIFYING AQUIFER RESPONSE TIME SCALES ASSOCIATED WITH TRANSIENT BOUNDARY CONDITIONS

3.1 Introduction

Understanding the interactions between groundwater and surface-water systems is an important aspect of water resources management. Using mathematical models to study these interactions can help us better address associated water quality and quantity issues. In the published literature, groundwater and surface-water interactions have been studied using both physical and mathematical approaches [*Chang and Clement*, 2012; 2013; *Clement et al.*, 1994; *M J Simpson et al.*, 2003a; *Winter*, 1995] that involve invoking a range modeling simplifications and assumptions, such as assuming that groundwater flow takes place in a homogeneous porous medium, assuming that streams are fully penetrating, and assuming rainfall conditions are uniform. To provide further insight into real-world practical problems, some of these simplifications and assumptions need to be relaxed.

A major challenge in studying groundwater and surface-water interactions arises from the fact that there is a considerable difference in the response times of these systems [*Hantush*, 2005; *Rodríguez et al.*, 2006]. For example, after a rainfall event, surface-water levels can respond on the order of hours to days, whereas groundwater levels might respond on the order of weeks to months. Current approaches for studying these problems can be classified into four categories, each of which involve certain limitations: (i) field investigations, which can be expensive and time consuming; (ii) laboratory experiments, which can be limited by scaling issues; (iii) numerical modeling, which, due to the orders of magnitude differences in the response times, might lead to numerical instabilities or other convergence issues [*Hantush*, 2005]; and analytical modeling,

which may be efficient but can have serious limitations in considering practical scenarios involving variations in stream stage, recharge, or discharge boundary conditions [*Barlow and Moench*, 1998]. Several previous researchers have presented analytical solutions focusing on aquifer response times [*Lockington*, 1997; *Ojha*, 2000; *Pinder et al.*, 1969; *Rowe*, 1960; *Singh and Sagar*, 1977; *Swamee and Singh*, 2003].

In the groundwater literature, response time (or lag time) is defined as the time scale required for a groundwater system to change from some initial condition to a new steady state [*Marios Sophocleous*, 2012]. In the heat and mass transfer literature this time scale is known as the critical time [*Hickson et al.*, 2009a; 2009b; *R Hickson et al.*, 2011]. Simpson et al. (2013) summarized several previous attempts to estimate the groundwater response time into three categories: (i) numerical computation, (ii) laboratory-scale experimentation, and (iii) simple mathematical definitions or approximations. All three categories involve making subjective definitions of the response time by tracking transient responses and choosing an arbitrary tolerance ϵ and claiming that the response time is the time taken for the transient response to decay below this tolerance [*Chang et al.*, 2011; *R Hickson et al.*, 2011; *K Landman and McGuinness*, 2000; *Lu and Werner*, 2013; *Watson et al.*, 2010]. There are several limitations with this approach. The most obvious limitation is that the response time depends on a subjectively defined tolerance, ϵ. Secondly, this approach does not lead to a general mathematical expression to describe how the response time would vary with problem geometry, changes in boundary conditions or aquifer parameters. Finally, this approach requires an analytical or a numerical solution to the governing transient equation. To deal with these limitations, *M J Simpson et al.* [2013a] demonstrated the use of a novel concept, mean action time (MAT), for estimating aquifer response times.

The concept of MAT was originally proposed by [*McNabb and Wake,* 1991] to describe the response times of heat transfer processes. MAT provides an objective definition for quantifying response time scales of different processes [*McNabb,* 1993]. MAT analysis leads to an expression relating the response time to the various model parameters. [*M J Simpson et al.*, 2013a] used MAT to characterize the response time for a groundwater flow problem that was driven by areal recharge processes, but did not consider any groundwater and surface-water interactions. The objective of this study is to extend the work of [*M J Simpson et al.*, 2013a] and present a mathematical model which describes transient groundwater flow processes near a groundwater and surface-water boundary with time-dependent boundary conditions. We adapt existing MAT theory to deal with time-dependent boundary conditions and present expressions for MAT which describe spatial variations in response times for both linear and non-linear boundary forcing conditions. These theoretical developments are then tested using data sets obtained from laboratory experiments.

3.2 Mathematical development

We consider a one-dimensional, unconfined, Dupuit–Forchheimer model of saturated groundwater flow through a homogeneous porous medium [*Bear*, 1979], which can be written as,

$$S_y \frac{\partial h}{\partial t} = K \frac{\partial}{\partial x}\left[h \frac{\partial h}{\partial x} \right], \tag{35}$$

where $h(x,t)$ [L] is the groundwater head at position x [L], t [T] is time, S_y [–] is the specific yield and K [L/T] is the saturated hydraulic conductivity. When variations in the saturated thickness are small compared to the average saturated thickness, we can linearize the governing equation by introducing an average saturated thickness, $\bar{h}$, to yield [*Bear*, 1979],

$$S_y \frac{\partial h}{\partial t} = K\bar{h} \frac{\partial^2 h}{\partial x^2}, \tag{36}$$

which can be re-written as the linear diffusion equation,

$$\frac{\partial h}{\partial t} = D \frac{\partial^2 h}{\partial x^2}, \tag{37}$$

where $D = K\bar{h}/S_y$ $[\mathrm{L}^2/\mathrm{T}]$ is the aquifer diffusivity. In this work, we will use Eq. (37) to model a groundwater system which changes from an initial condition, $h(x,0) = h_0(x)$, to some steady state, $\lim_{t \to +\infty} h(x,t) = h_\infty(x)$. We will consider two different classes of boundary conditions (38)for Eq. (37): Case 1, in which both the left $(x = 0)$ and right $(x = L)$ boundary conditions vary as functions of time, and Case 2, in which one boundary condition is fixed and the other one is allowed to vary with time.

3.2.1 Case 1: two time varying boundary conditions

We first consider the case where the surface-water variations at both the left $(x = 0)$ and right $(x = L)$ boundaries vary with time,

$$B_L(t) = h(0,t), \tag{39}$$

$$B_R(t) = h(L,t), \tag{40}$$

We assume that, after a sufficient amount of time, both $B_L(t)$ and $B_R(t)$ approach some steady condition,

$$\lim_{t\to+\infty} B_L(t) = h_\infty(0), \tag{41}$$

$$\lim_{t\to+\infty} B_R(t) = h_\infty(L), \tag{42}$$

for which the steady solution of Eq. (37) is,

$$h_\infty(x) = \left(\frac{h_\infty(L) - h_\infty(0)}{L}\right)x + h_\infty(0). \tag{43}$$

A schematic of these initial, transient and steady-state conditions are shown in Figure 3-1.

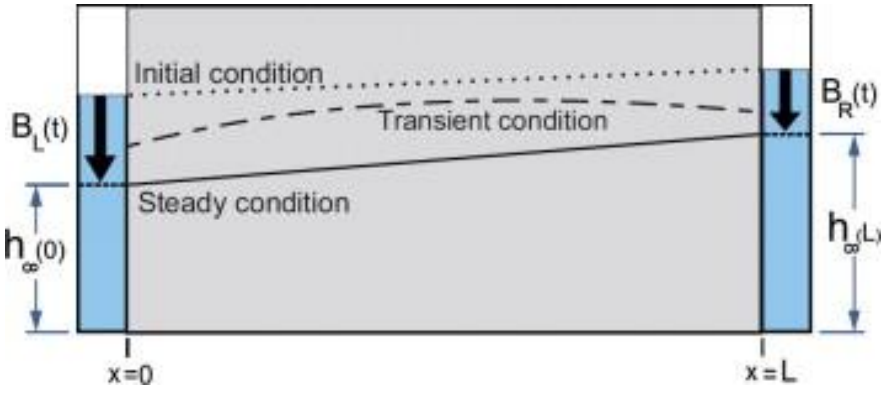

Figure 3-1: Schematic of the physical model showing initial (dotted), transient (dashed) and steady (solid) conditions. Changes in water head in the right and left boundaries are defined by functions of $B_R(t)$ and $B_L(t)$, respectively. At steady-state, the left and right boundary conditions reach the levels $h_\infty(0)$ and $h_\infty(L)$, respectively.

The purpose of this study is to present an objective framework to estimate the time scale required for the system to effectively relax to steady-state conditions. To begin our analysis we first consider the following two mathematical quantities [*Ellery et al.*, 2012a; 2012b; *M J Simpson et al.*, 2013a],

$$F(t;x) = 1 - \left[\frac{h(x,t) - h_\infty(x)}{h_0(x) - h_\infty(x)} \right], t > 0, \tag{44}$$

$$f(t;x) = \frac{\partial F(t;x)}{\partial t} = -\frac{\partial}{\partial t}\left[\frac{h(x,t) - h_\infty(x)}{h_0(x) - h_\infty(x)} \right], t > 0. \tag{45}$$

where $h(x,t)$ is the solution of Eq. (37), $h_0(x)$ is the initial groundwater level, and $h_\infty(x)$ is the steady-state level reached after a sufficiently long period of time and we require that $h_0(x) \neq h_\infty(x)$, ensuring that a transition takes place. Theoretically, the transient response will require infinite amount of time to reach steady-state. This implies that at all spatial locations, $F(t;x)$ changes from $F = 0$ at $t = 0$ to $F \to 1^-$ as $t \to +\infty$. We can interpret $F(t;x)$ as a cumulative distribution function (CDF) and $f(t;x)$ as a probability density function (PDF) [*Ellery et al.*, 2012a; 2012b; *M J Simpson et al.*, 2013a].

The MAT, $T(x)$, is the mean or the first moment of $f(t;x)$, which can be written as [*M J Simpson et al.*, 2013a],

$$T(x) = \int_0^\infty t f(t;x) \mathrm{d}t. \tag{46}$$

To solve for $T(x)$, we apply integration by parts to Eq. (46) and make use of the fact that $h(x,t) - h_\infty(x)$ decays to zero exponentially fast as $t \to +\infty$ [*Ellery et al.*, 2012a; 2012b; *Haberman*, 2004] to give,

$$T(x)g(x) = \int_0^\infty h_\infty(x) - h(x,t) \mathrm{d}t, \tag{47}$$

where we define $g(x) = h_\infty(x) - h_0(x)$. Differentiating Eq. (47) twice with respect to x and combining the result with Eq. (37) yields,

$$\frac{\mathrm{d}^2[T(x)g(x)]}{\mathrm{d}x^2} = -\frac{g(x)}{D}, \tag{48}$$

Expanding Eq. (48) by applying the product rule gives,

$$\frac{\mathrm{d}^2T(x)}{\mathrm{d}x^2} + \frac{\mathrm{d}T(x)}{\mathrm{d}x}\left[\frac{2}{g(x)}\frac{\mathrm{d}g(x)}{\mathrm{d}x}\right] + T(x)\left[\frac{1}{g(x)}\frac{\mathrm{d}^2g(x)}{\mathrm{d}x^2}\right] = -\frac{1}{D}, \tag{49}$$

which is a differential equation that governs the MAT for any change from $h_0(x)$ to $h_\infty(x)$, provided that $F(t;x)$ monotonically increases from $F = 0$ at $t = 0$ to $F \to 1^-$ as $t \to +\infty$.

To solve Eq. (49), we must specify boundary conditions at $x = 0$ and $x = L$. The appropriate boundary conditions can be found by evaluating Eq. (46) at $x = 0$ and $x = L$, recalling that the time variation in head at these locations is given by $B_L(t)$ and $B_R(t)$, respectively. We apply integration by parts, assuming that $B_L(t)$ and $B_R(t)$ approach $h_\infty(0)$ and $h_\infty(L)$, respectively, faster than t^{-1} decays to zero as $t \to +\infty$, to give,

$$A = \frac{1}{\alpha}\int_0^\infty h_\infty(0) - B_L(t)\mathrm{d}t, \text{ where } \alpha = h_\infty(0) - h_0(0), \tag{50}$$

$$B = \frac{1}{\beta}\int_0^\infty h_\infty(L) - B_R(t)\mathrm{d}t, \text{ where } \beta = h_\infty(L) - h_0(0). \tag{51}$$

The constants A and B represent the mean time scales of the boundary conditions. With these two constants we may solve Eq. (49) to give an expression for the effective time scale of the system,

$$T(x) = \underbrace{\frac{x(L-x)}{6D}}_{\text{intrinsic time scale of the aquifer}} + \underbrace{\frac{A\alpha(L-x)+B\beta x}{\alpha(L-x)+\beta x}}_{\text{intrinsic time scale of the boundary conditions}} + \underbrace{\frac{xL(L-x)(\alpha+\beta)}{6D\left[\alpha(L-x)+\beta x\right]}}_{\text{mixed time scale of the system}}. \quad (52)$$

The first term on the right of Eq.(52) is independent of the details of the boundary conditions, and so we interpret it as an intrinsic time scale of the aquifer. The second term on the right of Eq. (52) is independent of D, and depends on the details of the boundary conditions. Therefore, we interpret this term as an intrinsic time scale of the boundary conditions. We note that the intrinsic time scale of the boundary conditions can also be interpreted as the weighted average of A and B, $(Aw_a + Bw_a)/(w_a + w_b)$, with linear weight functions $w_a = \alpha(L-x)/L$ and $w_b = \beta x/L$. This interpretation implies the influence of the boundary conditions on the time scale of the process at any point within the system depends on the distances from the boundaries and also on the magnitude of the changes imposed at the boundaries. For example, the time scale at a point close to the left hand boundary, $x = 0$, will be dominated by the influence of the time scale of $B_L(t)$ and relatively unaffected by the influence of the time scale of $B_R(t)$, which is as we might expect intuitively. However, intuition alone cannot provide quantitative insight into the impact of the boundary conditions time scales at intermediate locations where the impact of both boundary conditions plays a role. Finally, the third term on the right of Eq. (52) depends on properties of the entire system including both D, the magnitudes of head changes at the

boundaries, but is independent of A and B, which are the mean time scales of the boundary conditions. Therefore, we consider this third term as the *mixed time scale of the system.*

To provide additional information about the response time we also consider the second moment of $f(t;x)$, known as the variance of action time (VAT), $V(x)$, and quantifies the spread about the MAT [Ellery et al., 2012a; 2012b]. VAT is defined as,

$$V(x) = \int_0^\infty (t - T(x))^2 f(t;x) \mathrm{d}t. \tag{53}$$

Using integration by parts and noting that $h(x,t) - h_\infty(L)$ decays to zero exponentially fast as $t \to +\infty$, Eq. (53) can be written as,

$$\varphi(x) = 2\int_0^\infty t(h_\infty(x) - h(x,t))\mathrm{d}t, \tag{54}$$

where have defined $\varphi(x) = g(x)[V(x) + T(x)^2]$. Differentiating Eq. (54) twice with respect to x and combining the result with Eq. (37) gives,

$$\frac{\mathrm{d}^2\varphi(x)}{\mathrm{d}x^2} = -\frac{2T(x)g(x)}{D}, \tag{55}$$

To solve Eq. (55), we require two boundary conditions, which are given by,

$$\varphi(0) = \alpha(C + A^2), \tag{56}$$

$$\varphi(L) = \beta(E + B^2), \tag{57}$$

where C and E are the VAT at $x=0$ and $x=L$, respectively. These constants are defined using Eq. (53), and can be written as,

$$C=\frac{1}{\alpha}\int_0^{\infty}\frac{\mathrm{d}B_L(t)}{\mathrm{d}t}(t-A)^2\,\mathrm{d}t, \tag{58}$$

$$E=\frac{1}{\beta}\int_0^{\infty}\frac{\mathrm{d}B_R(t)}{\mathrm{d}t}(t-B)^2\,\mathrm{d}t. \tag{59}$$

We solve Eq. (55) for $\varphi(x)$, recalling that $V(x)=\varphi(x)\big/g(x)-T(x)^2$ and that $h(x,t)-h_{\infty}(x)$ decays to zero exponentially fast as $t\to+\infty$, which gives us,

$$V(x)=\frac{1}{180D^2[\alpha(L-x)+\beta x]}(\gamma+\delta+\mu)-\theta, \tag{60}$$

where,

$$\begin{aligned}
c&=3x^5(\beta-\alpha)+15x^4\alpha L+180\alpha LD^2(C+A^2),\\
d&=10x^3(-\beta L^2-6\beta BD+6DA\alpha-2\alpha L^2)-180x^2\alpha LAD,\\
g&=x\left[180D^2(\beta E-\beta C+\beta B^2-\alpha A^2)+60L^2D(\beta B+2A\alpha)+L^4(7\beta+8\alpha)\right]\\
h&=\left[\frac{x^3(\beta-\alpha)+3x^2\alpha L-x(\beta L^2+6\beta BD-6DA\alpha+2\alpha L^2)-6\alpha LAD}{6D(x\beta-x\alpha+\alpha L)}\right]^2.
\end{aligned} \tag{61}$$

VAT is a measure of the spread of the PDF about the mean [*Ellery et al.*, 2013]. A small VAT implies that the spread about the mean is small, and that the MAT is a sufficient estimate of the time required for the system to effectively reach steady state [*Ellery et al.*, 2013; *M J Simpson et al.*, 2013a]. Alternatively, a large VAT indicates that the PDF has a large spread about the mean

and a better estimate of the response time is $T(x)+\sqrt{V(x)}$ [*Ellery et al.*, 2013; *M J Simpson et al.*, 2013a]. This framework gives an explicit estimate for the response time scale required for a groundwater system to respond to a relatively general set of boundary conditions. The method objectively describes the dependence of the time scale on various aquifer parameters, (e.g. K, S_y, $\bar{h}$, $B_L(t)$, $B_R(t)$ and L) and does not require any numerical or analytical transient solution of the governing equation.

Our MAT framework involves certain limitations which should be made explicit. The first limitation is that the boundary conditions must vary monotonically with time otherwise our definition of $F(t;x)$ cannot be interpreted as a CDF. The second limitation is that $B_L(t)$ and $B_R(t)$ must asymptote to the corresponding steady values faster than t^{-1} decays to zero as $t\to+\infty$. We also require that $B_L(t)$ and $B_R(t)$ both increase or decrease, or that one of the boundary conditions must remain fixed with time. If one boundary condition decreases and the other increases, there will be some points in the domain at which the head distribution does not vary monotonically and $F(t;x)$ cannot be interpreted as a CDF.

3.2.2 Case 2: one fixed boundary condition and one time varying boundary condition

Here we consider a fixed boundary condition at $x=0$ and a time-varying boundary condition at $x=L$. We consider the water level variation at $x=L$ to be given by $B_R(t)=h(L,t)$ which eventually asymptotes to some steady value, $h_\infty(L)$. As in Case 1, the differential equation governing the MAT is Eq. (49), which, in this case, simplifies to,

$$\frac{\mathrm{d}^2T(x)}{\mathrm{d}x^2}+\frac{2}{x}\frac{\mathrm{d}T(x)}{\mathrm{d}x}=-\frac{1}{D}, \tag{62}$$

Two boundary conditions are required to solve Eq. (62). The boundary condition at $x=L$ is the same as in Case 1, and given by Eq. (51). To determine the boundary condition at $x=0$, we multiply both sides of Eq. (62) by x, which gives,

$$x\frac{\mathrm{d}^2T(x)}{\mathrm{d}x^2}+2\frac{\mathrm{d}T(x)}{\mathrm{d}x}=-\frac{x}{D}. \tag{63}$$

Evaluating Eq. (63) when $x\to 0$ gives a Neumann boundary condition, $\mathrm{d}T/\mathrm{d}x=0$ at $x=0$. With these boundary conditions the solution of Eq. (62) is,

$$T(x)=\frac{L^2-x^2}{6D}+B. \tag{64}$$

To find the VAT we have $\varphi(0)=0$ and $\varphi(L)=\beta(B^2+E)$ as boundary conditions for Eq. (55). Recalling that $V(x)=\varphi(x)/g(x)-T(x)^2$, the VAT is given by,

$$V(x)=\frac{L^4-x^4}{90D^2}+E, \tag{65}$$

where β, B and E are defined by Eqs. (51) and (59), respectively.

3.3 Laboratory experiments

We now examine the validity of the theoretical developments presented in Section 3.2. To do this we consider two laboratory experiments performed in a rectangular soil tank, using methods

described previously [*Abarca and Clement*, 2009; *Chang and Clement*, 2013; *M J Simpson et al.*, 2013a]. An image of the physical tank is shown in Figure 3-2. The tank has three distinct chambers. The central porous media chamber (50 cm × 28 cm × 2.2 cm) was packed under wet conditions with a uniform fine sand. The hydraulic conductivity and specific yield of the porous medium are estimated to be 330 m/day and 0.2, respectively. Two chambers at either sides were separated using fine metal screens; these chambers were used to set up the boundary conditions. Our coordinate system is such that $x = 0$ and $x = L$ denotes the left and right boundaries, respectively. Siphon-type tubes connected to electronic manometers, shown in Figure 3-2, were used to monitor head at two internal points.

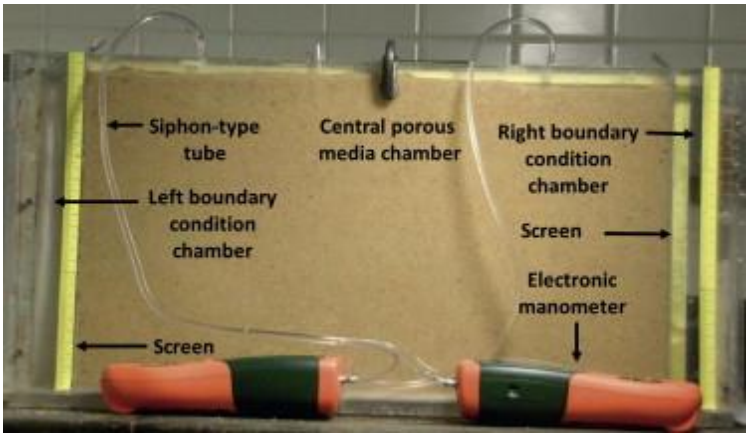

Figure 3-2: Experimental aquifer set up used in this study.

3.3.1 Experiment 1: Laboratory data for Case I

In this experiment, we consider a linearly varying boundary condition at $x = 0$ and a quadratically varying boundary condition at $x = L$. We model the right boundary condition as,

$$B_R(t) = \begin{cases} [h_\infty(L) - h_0(L)]\dfrac{t}{N} + h_0(L), & 0 \le t \le N, \\ h_\infty(L), \end{cases} \tag{66}$$

which is a linear change from $h_0(L)$ to $h_\infty(L)$ in N units of time. We model the left boundary condition as,

$$B_L(t) = \begin{cases} at^2 + bt + c, & 0 \le t \le N, \\ h_\infty(0), & t > M. \end{cases} \tag{67}$$

which is a nonlinear change from $h_0(0)$ to $h_\infty(0)$ in M units of time.

To represent a linear head variation, $B_R(t)$, a pump was used to evacuate water from the right chamber at a uniform rate. To represent a quadratically varying head condition, $B_L(t)$, we allow water to drain through an orifice in the left chamber. Using the Bernoulli equation, we derive a quadratic relationship between falling head and drainage time [*Bansal*, 2005]. To specify $B_L(t)$, experimental data for water elevation changes occurring at the left boundary were recorded. A quadratic expression, $B_L(t) = at^2 + bt + c$, was fitted to the data set. The initial state for the system was set to $h_0(x) = 22.5$ cm. The left boundary condition set to vary quadratically from $h_0(0) = 22.5$ cm to $h_\infty(0) = 19.1$ cm in 3 seconds, and the right boundary condition to vary linearly from $h_0(L) = 22.5$ cm to $h_\infty(L) = 19.1$ cm in 20 seconds. Table 1 summarizes the initial state, steady-state, transition time and transition function of each boundary used in this experiment. We measured the transient head data at two intermediate points, $x = 20$ cm and $x = 30$ cm, using digital manometers with 0.01 cm H_2O resolution.

Table 1: Experiment 1: Laboratory data for linearly varying right and quadratically varying left boundary conditions.

	Initial head (cm)	**Steady state head (cm)**	**Transition time (s)**	**Transition function (cm)**
Left boundary	22.5	19.1	3	$B_L(t) = 0.37t^2 - 2.22t + 22.48$
Right boundary	22.5	19.1	20	$B_R(t) = -0.17t + 22.50$

To quantitatively assess our framework, we calculated α, β, A and B to give,

$$\alpha = h_\infty(0) + h_0(0), \tag{68}$$

$$\beta = h_\infty(L) + h_0(L), \tag{69}$$

$$A = -\frac{1}{\alpha}\left[\frac{1}{3}aM^3 + \frac{1}{2}bM^2 + (c - h_\infty(0))\right], \tag{70}$$

$$B = \frac{N}{2}. \tag{71}$$

Values of α, β, A and B for this experiment were calculated as −3.4 cm, −3.4 cm, 1.1 s and 10.0 s, respectively. Using Eq. (52), we predict that the MAT at $x = 20$ cm and $x = 30$ cm are $T(20) = 11.2$ sec and $T(30) = 14.3$ sec, respectively. Similarly, after using Eqs. (58) and (59) and evaluating the constants $C = 0.4$ and $E = 33.3$, Eq. (60) gives $\sqrt{V(20)} = 10.4$ sec and $\sqrt{V(30)} = 8.6$ sec, respectively.

Predictions of MAT and $\sqrt{VAT}$ are summarized in Table 2. To test these predictions, we analyzed our laboratory data from Experiment 1 at $x = 20$ cm and $x = 30$ cm, as shown in

Figure 3-3. To compute $f(t;x)$, we used the data from Figure 3-3(a) and (b). We apply Eq. (45), using a central difference approximation to estimate $\partial h/\partial t$ [Chapra and Canale, *2012*]. Our estimates of $t \times f(t;x)$ at $x = 20\,\text{cm}$ and $x = 30\,\text{cm}$ are given in Figure 3-3(c) and (d). We applied Eqs. (46) and (53) to estimate $T(x)$ and $V(x)$ using the trapezoidal rule [Chapra and Canale, 2012] to estimate the integrals. The results are summarized in Table 2. Our results, reported in Figure 3-3(a) and (b), shows that the predicated effective time scale, $MAT + \sqrt{VAT}$, is a good approximation for the time required for the system to effectively reach steady state. Furthermore, the results in Table 2 show that the predicted estimates of MAT and VAT compare well with the values estimated directly from the experimental data set.

Table 2: Experimental and theoretical values of MAT, $\sqrt{VAT}$ and $MAT + \sqrt{VAT}$ at $x = 20\,\text{cm}$ and $x = 30$ cm for Experiment 1.

	MAT (s)		$\sqrt{VAT}$ (s)		$MAT + \sqrt{VAT}$ (s)	
	$x = 20$ (cm)	$x = 30$ (cm)	$x = 20$ (cm)	$x = 30$ (cm)	$x = 20$ (cm)	$x = 30$ (cm)
Experimental	12.3	14.3	9.1	8.7	21.4	23.0
Theoretical	11.2	14.3	10.4	8.6	21.6	22.9

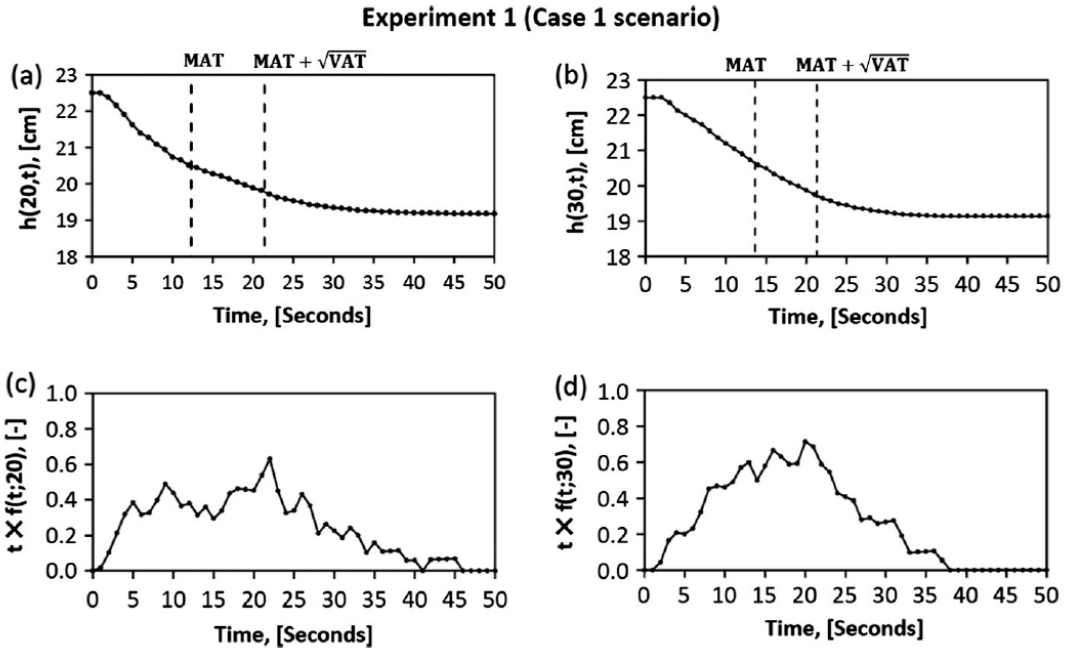

Figure 3-3: Laboratory data for Experiment 1 with initial condition $h_0(x) = 22.5$ cm, the left boundary condition varying quadratically from $h_0(0) = 22.5$ to $h_0(L) = 19.1$ in 3s, and the right boundary condition varying linearly from $h_0(L) = 22.5$ cm to $h_\infty(L) = 19.1$ cm in 20s. Results in (a) and (b) show the observed head changes at $x = 20$ cm and $x = 30$ cm, respectively. Results in (c) and (d) show $t \times f(t;20)$ and $t \times f(t;30)$; where $f(t;x)$ is the probability density function at location x. Integrating $t \times f(t;x)$ provides an estimate of the MAT at position x. An improved estimate of the effective time scale required for the system to reach steady-state is: $MAT + \sqrt{VAT}$.

3.3.2 Experiment 2: Laboratory data for Case II

In this experiment, a fixed boundary condition was maintained in the left chamber, and a linearly varying boundary condition at the right chamber. We used Eq. (66) to model the right boundary condition. A pump was used to evacuate water from the right chamber at a uniform rate. As shown in Table 3, in this experiment, the following conditions were used: $h_0(x) = 25$ cm, $h_\infty(x) = 23$ cm and $N = 25$ sec for the right boundary condition.

Table 3: Experiment 2: Laboratory data for linearly varying right and fixed left boundary conditions.

	Initial head (cm)	**Steady state head (cm)**	**Transition time (s)**	**Transition function (cm)**
Left boundary	25.0	25.0	–	$B_L(t) = 22.50$
Right boundary	25.0	23.0	25	$B_R(t) = 0.08t + 25.0$

To quantitatively assess our MAT predictions, we first calculated the constant B defined by Eq. (51) as $B = N/2 = 12.5$ sec. Using Eq. (64) we found $T(20) = 19.4$ sec and $T(30) = 17.7$ sec, respectively. Similarly, applying Eq. (59) we found $E = N^2/12 = 52.1$ sec^2 and $\sqrt{V(20)} = 9.9$ sec and $\sqrt{V(30)} = 9.7$ sec, respectively, using Eq. (65). Our predictions of MAT and $\sqrt{\text{VAT}}$ values are summarized in Table 4. The transient data collected from Experiment 2 are reported in Figure 3-4. Similar to Experiment 1, MAT, $\sqrt{\text{VAT}}$ and $\text{MAT}+\sqrt{\text{VAT}}$ at $x = 20$ cm and $x = 30$ cm were calculated and the results were compared against theoretical predictions. As shown in Table 4, the theoretical predictions are in good agreement with experimental results. Results in Figure 3-4(a) and (b) illustrate that the predicted time scale required for the system to effectively reach steady-state, $\text{MAT}+\sqrt{\text{VAT}}$, is consistent with our experimental observations.

Table 4: Experimental and theoretical values of MAT, $\sqrt{\text{VAT}}$ and $\text{MAT}+\sqrt{\text{VAT}}$ at $x = 20$ cm and $x = 30$ cm for Experiment 2.

	MAT (s)		$\sqrt{VAT}$ (s)		$MAT + \sqrt{VAT}$ (s)	
	$x = 20$ (cm)	$x = 30$ (cm)	$x = 20$ (cm)	$x = 20$ (cm)	$x = 30$ (cm)	$x = 20$ (cm)
Experimental	19.2	18.3	8.2	8.3	27.4	26.6
Theoretical	19.4	17.7	9.9	9.7	29.3	27.4

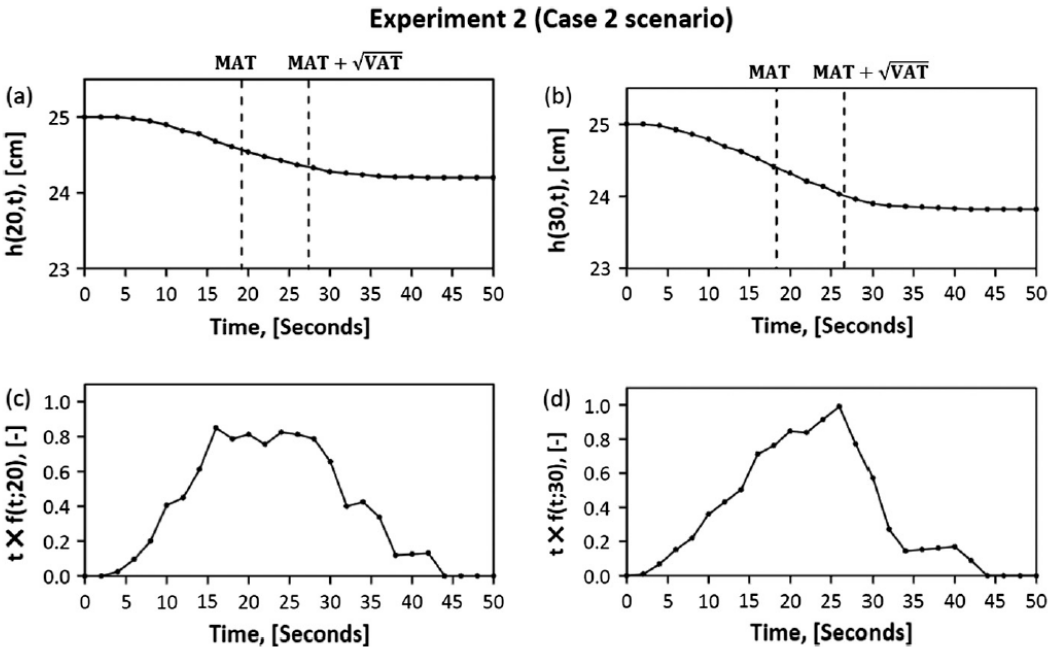

Figure 3-4: Laboratory data for Experiment 2 with initial condition $h_0(x) = 25$ cm, the left boundary condition fixed at $B_L(t) = 25$ cm, and the right boundary condition varying linearly from $h_0(L) = 22.5$ cm to $h_\infty(L) = 23$ cm in 25s. Results in (a) and (b) show the observed head changes at $x = 20$ cm and $x = 30$ cm, respectively. Results in (c) and (d) show $t \times f(t;20)$ and $t \times f(t;30)$; where $f(t;x)$ is the probability density function at location x. Integrating $t \times f(t;x)$ provides an estimate of the MAT at position x. An improved estimate of the effective time scale required for the system to reach steady state is: $MAT + \sqrt{VAT}$

3.4 Summary and conclusions

The focus of this study is to present a mathematical framework which can predict the response time scales of groundwater flow near a groundwater surface-water interface. To achieve this we applied the theory of MAT [*McNabb and Wake*, 1991] to estimate the time scale required for flow in a one-dimensional aquifer to respond to various types of surface-water boundary perturbations. We tested the proposed framework using two data sets collected from a laboratory-scale experiment. Results show that the experimental data are in good agreement with model predictions. A key limitation of previous approaches for estimating the response time scales is that

they gave no simple framework for studying the sensitivity of the time scale to various system parameters. Alternatively, our MAT framework provides a relatively straightforward mathematical relationship between the response time scale and various system parameters.

The limitations of our framework are that the boundary conditions must vary monotonically and that they must approach some steady value faster than t^{-1} decays to zero as $t \to +\infty$. Furthermore, we also require that both boundary conditions must either increase or decrease, or that one of the boundary conditions remains fixed. In practice, these limitations are not overly restrictive and a wide range of transient groundwater problems can be analyzed using the proposed framework. We also acknowledge that for all systems considered in this work we always considered an initial condition, $h_0(x)$, that was spatially constant, independent of position. We note that the same mathematical procedure used to find MAT and VAT also applies to other conditions where the initial condition is genuinely spatially variable and these mathematical details can be found in our previous work [*Ellery et al.*, 2012a; 2012b].

CHAPTER 4 SPATIAL ANALYSIS OF AQUIFER RESPONSE TIMES FOR RADIAL FLOW PROCESSES: NONDIMENSIONAL ANALYSIS AND LABORATORY-SCALE TESTS

4.1 Introduction

Population growth and associated industrial and agricultural activities can have considerable impact on groundwater resources. Since groundwater plays a significant role in our social and economic wellbeing, understanding groundwater responses to natural and anthropogenic changes is important. Several studies have examined various properties of groundwater flow processes using different tools including numerical or analytical models, field investigations and laboratory experiments [e.g. *Theis,* 1935*; Freeze and Witherspoon,* 1966*; Bredehoeft et al.,* 1982*; Hantush,* 2005]. Many of these studies have included radial flow problems to investigate pumping, injection and recovery processes.

A common concept used in groundwater modeling is defining a steady state (or equilibrium) flow condition. When a forcing condition on a system at equilibrium is changed, the system will undergo a transient response to approach a new equilibrium state. A point of interest is to understand the amount of time taken for the system to reach steady state. Strictly speaking, from a mathematical point of view, an infinite amount of time is required for the system to asymptote to steady state conditions. However, this strict mathematical definition is impractical because we can never wait for an infinite amount of time. Therefore, we wish to estimate a "sufficiently long period" of time that is required for the system to "effectively" reach steady state [*Schwartz et al.,* 2010]. However, the concept of a "sufficiently long period" is subtle.

A change in flow conditions at a pumping or injection well will eventually influence regions further away from the well, potentially over very large areas, including distant boundary conditions. When the flow rate at a pumping or injection well is altered, a transition pattern, often called a cone of depression, propagates through the aquifer with time. Understanding the amount of time required for a transient system to effectively relax to equilibrium can help us decide whether to use a steady state model or a more complicated transient model to describe the groundwater flow process [*Simpson et al.,* 2013*; Jazaei et al.,* 2014].

The concept of aquifer response time has been analyzed previously for various groundwater problems. Theis first considered the response of a groundwater system to pumping by solving a mathematical model describing the transient flow near a pumping well in an infinite aquifer [*Theis,* 1935]. After this initial study, Theis then considered the factors controlling the response time [*Theis,* 1940]. These factors include the aquifer transmissivity, T ; the storage coefficient, S; and the length scale of the problem. Theis concluded that the rate at which the cone of depression spreads is proportional to T and inversely proportional to S . Later, other researchers presented simpler scaling formulas to estimate the aquifer response time scale [e.*g. Gelhar and Wilson,* 1974*; Townley,* 1995*; Erskine and Papaionnau,* 1997*; Manga,* 1999*; Haitjema,* 2006]. For example, Gelhar and Wilson (1974) suggest that the hydraulic response time is $t_h = nL^2/3T$, where n is the average porosity and L is the aquifer length. Such scaling formulas suggest a constant time scale for the entire system and do not provide any information about how the time scale depends on position. Other studies [*e.g. Schwartz et al.,* 2010, *Kooi and Groen,* 2000*; Rousseau-Gueutin et al.,* 2013] define the response time as the amount of time taken for the difference between the transient and steady state solutions to fall below some tolerance. For example Rousseau-Gueutin

et al. (2013) define the aquifer response time to be the amount of time required for 95% of the transient head changes to have occurred. This definition does not lead to a simple closed form expression.

Recently, we presented a different framework to quantify the aquifer response time scale [*Simpson et al.,* 2013*; Jazaei et al.,* 2014]. Our analysis provides explicit mathematical expressions showing how the response time scale depends on position, aquifer properties and boundary conditions. This approach does not require any predefined thresholds, and avoids the need for solving the transient flow problem. However, our previous analyses were limited to one-dimensional Cartesian problems in which flows where driven by a surface recharge conditions, or changes at the interface between the surface water and groundwater. In contrast, here we analyze the time scale of a two–dimensional radial system, in which the transition between different steady state conditions is driven by flow changes at the pumping or injecting well. Our analysis is relevant for both converging and diverging flows and we employ a nondimensional framework which leads to more elegant, generalized results, which can be used to explain the difference between smaller scale laboratory flow conditions and larger scale field conditions.

Our approach involves analyzing the first and second moments of the transition time distribution, which is similar to the way in which some previous studies have used temporal moment analysis to investigate spatial variations in hydraulic conductivity [*Wei,* 2005*; Zhu and Yeh,* 2006]. We note, however, these previous studies were focusing on analyzing the hydraulic conductivity fields, and did not consider using moment analysis to derive expressions for the aquifer response time scales.

The objective of the present work is to develop a framework to quantify the spatial variations in response time scales under radial flow conditions. We investigate pumping, injection and recovery processes to understand how their response time scales depend on hydraulic and geometric properties of the aquifer. We employ two mathematical concepts, known as the mean action time (MAT) and the variance of action time (VAT) in this analysis. We employ a dimensionless framework that can be used to study both large scale field problems as well as small scale laboratory problems. Our theoretical predictions are tested using new datasets from laboratory scale experiments.

4.2 Mathematical model

In this section we first use a dimensional radial flow model to define a simpler and more general dimensionless model. Primed variables denote dimensional quantities and unprimed variables denote dimensionless quantities.

4.2.1 Dimensional model

Groundwater flow near a fully penetrating well of radius r_w' in a homogeneous confined aquifer can be analyzed using the following dimensional model [*Bear*, 1976],

$$S\frac{\partial h'(r',t')}{\partial t'} = \frac{T'}{r'}\frac{\partial}{\partial r'}\left[r'\frac{\partial h'(r',t')}{\partial r'}\right], \quad r_w' < r' < R', \tag{72}$$

where r' [L] is the radial distance from the center of the well, t' [T] is time, R' [L] is the radial distance between the center of the well and the boundary, $h'(r',t')$ [L] is the hydraulic head, T' [L

^{2}/T] is the aquifer transmissivity and S [-] is the aquifer storage coefficient. In this study we consider a Dirichlet boundary condition, $h'(R',t') = h'_0$.

For both pumping and injection processes we consider a spatially uniform initial condition, $h'_0(r') = h'_0$, and a constant flow rate denoted $Q' > 0$ for pumping and $Q' < 0$ for injection. For the radial problem the steady state solution is

$$\lim_{t'\to\infty} h'(r',t') = h'_\infty(r') = h'_0 + \frac{Q'}{2\pi T'}\ln(\frac{r'}{R'}). \tag{73}$$

The transient solution of Eq. (72) can be written as an infinite series involving Bessel functions [*Bear,* 1976]. We remark that the Theis solution is relevant only for aquifers of infinite extent and therefore does not apply to the finite problems considered here.

For the recovery process, we suppose that the flow rate at the well is stopped, giving $Q' = 0$. Furthermore, we assume that the initial condition corresponds to the steady state of the associated pumping or injection process, given by Eq. (73). The steady state solution of the recovery process is $h'_\infty(r') = h'_0$.

We explicitly model the effect of storage at the well by applying a boundary condition that couples the well storage to the flow at $r' = r'_w$,

$$2\pi r'_w T' \frac{\partial h'(r_w',t')}{\partial r'} - Q' = \pi r_w'^2 \frac{\partial h'(r'_w,t')}{\partial t'}. \tag{74}$$

The boundary condition at $r' = R'$ is given by

$$h'(R',t') = h'_0. \tag{75}$$

4.2.2 Dimensionless model

To simplify our analysis, we nondimensionalize the mathematical model by introducing the following characteristic length, time and head scales,

$$r^* = R', \qquad t^* = \frac{SR'^2}{T'}, \qquad h^* = h'_0. \tag{76}$$

We then define the following three dimensionless variables,

$$r = \frac{r'}{r^*}, \qquad t = \frac{t'}{t^*}, \qquad h = \frac{h'}{h^*}, \tag{77}$$

and two constants that are given by:

$$\alpha = \frac{r'_w}{R'}, \qquad \beta = \frac{Q'}{2\pi T' h'_0 \alpha}. \tag{78}$$

Physically, α is a positive constant representing the ratio of the well radius, r'_w, to the length of the domain, R'. For a small scale laboratory problem we have $\alpha \approx 0.01$ whereas in a field scale application $R' \gg r'_w$, so we are interested in the limiting condition, $\alpha \to 0$. Working in this dimensionless framework we can extend our analysis to both laboratory scale and field scale applications by simply varying α.

Substituting dimensionless variables and constants into Eqs. (72), (74) and (75), we obtain a simpler dimensionless model,

$$\frac{\partial h(r,t)}{\partial t} = \frac{1}{r}\frac{\partial}{\partial r}\left[r\frac{\partial h(r,t)}{\partial r} \right], \quad \alpha < r < 1, \tag{79}$$

$$\frac{\partial h(\alpha,t)}{\partial r} - \beta = \frac{\alpha}{2S}\frac{\partial h(\alpha,t)}{\partial t}, \qquad h(1,t) = 1. \tag{80}$$

The dimensionless initial condition for pumping and injection processes is $h_0(r) = 1$. The associated steady state solution is $h_\infty(r) = \alpha\beta \ln(r) + 1$. We assume that the initial condition for the recovery process is equivalent to the steady state condition for the pumping or injection process. The dimensionless steady solution of the recovery process is $h_\infty(r) = 1$.

4.3 Mean action time for a radial system

In this section we derive expressions for the MAT of the system using the dimensionless model. This approach leads to an expression for the dimensionless mean time scale, $M(r)$, which can be rescaled to give a dimensional time scale by multiplying by t^*. We begin by defining two mathematical quantities [*McNabb and Wake,* 1991*; McNabb,* 1993],

$$F(t \mid r) = 1 - \frac{h(r,t) - h_\infty(r)}{h_0(r) - h_\infty(r)}, \quad t \geq 0, \tag{81}$$

$$f(t \mid r) = \frac{dF(t \mid r)}{dt} = -\frac{\partial}{\partial t}\left[\frac{h(r,t) - h_\infty(r)}{h_0(r) - h_\infty(r)} \right], \quad t \geq 0. \tag{82}$$

To apply these quantities to a particular problem we require $h_0(r) \neq h_\infty(r)$ to ensure a transition occurs. Hence, for our problem, Eqs. (81) and (82) are indeterminate at $r = 1$ and we will explain how to deal with this later.

For all pumping and injection processes, $h(r,t)$ changes monotonically from $h_0(r)$ to $h_\infty(r)$. Therefore, $F(t\,|\,r)$ is a monotonically increasing function with an initial value of $F(0\,|\,r)=0$, and approaches unity as $t\to+\infty$. We interpret $F(t\,|\,r)$ as a cumulative distribution function (CDF). $F(t\,|\,r)$ quantifies the amount of action completed at a position *r*, after time *t*. Note that here we treat *t* as the independent variable and *r* as a parameter. At $t=0$, the transition is yet to begin, hence $F(0\,|\,r)=0$. As the process proceeds, the value of $F(t\,|\,r)$ increases. For example, we interpret $F(\delta\,|\,r)=0.5$ as indicating that 50% of the transient process is completed after $t=\delta$ at position *r*.

By definition, the first derivative of $F(t\,|\,r)$ with respect to *t*, given by Eq. (82), is the probability density function (PDF) [*Ellery et al.*, 2012*a*,*b*]. Mathematically, $f(t\,|\,r)$ is proportional to the time derivative of $h(r,t)$ at each position *r*. Therefore, $f(t\,|\,r)\to 0$ as $t\to+\infty$, and the system reaches steady state.

The MAT is the first moment of $f(t\,|\,r)$ (*McNabb and Wake, 1991; McNabb, 1993*),

$$M(r)=\int_0^\infty t f(t\,|\,r)\mathrm{d}t. \tag{83}$$

Since we know that $h(r,t)$ decays to $h_\infty(r)$ exponentially fast as $t\to+\infty$ [*Crank*, 1975], applying integration by parts to Eq. (83) leads to

$$M(r)g(r)=\int_0^\infty (h_\infty(r)-h(r,t))\mathrm{d}t, \tag{84}$$

where, $g(r)=h_\infty(r)-h_0(r)$. Differentiating Eq. (84) twice with respect to *r* gives,

$$\frac{d[M(r)g(r)]}{dr} = \int_0^\infty (\frac{dh_\infty(r)}{dr} - \frac{\partial h(r,t)}{\partial r})\mathrm{d}t, \tag{85}$$

$$\frac{d^2[M(r)g(r)]}{dr^2} = \int_0^\infty (\frac{d^2h_\infty(r)}{dr^2} - \frac{\partial^2 h(r,t)}{\partial r^2})\mathrm{d}t. \tag{86}$$

Multiplying Eq. (85) by $1/r$ and combining the resulting expression with Eqs.(79) and (86), we obtain a boundary value problem for the MAT:

$$\frac{d^2M(r)}{dr^2} + \frac{dM(r)}{dr}\left[\frac{1}{r} + \frac{2}{g(r)}\frac{dg(r)}{dr}\right] + \frac{M(r)}{g(r)}\left[\frac{1}{r}\frac{dg(r)}{dr} + \frac{d^2g(r)}{dr^2}\right] = -1. \tag{87}$$

Eq. (87) is valid for an arbitrary initial condition, $h_0(r)$. However, in this study we consider a spatially uniform initial condition, $h_0(r) = 1$, which allows us to simplify Eq. (87) *to*

$$\frac{d^2M(r)}{dr^2} + [\frac{2+\ln(r)}{r\ln(r)}]\frac{dM(r)}{dr} = -1. \tag{88}$$

To solve Eq. (88) we require boundary conditions at $r = \alpha$ and $r = 1$. At $r = \alpha$, we use Eqs. (80) and (85) to define a Robin condition given by

$$\frac{dM(\alpha)}{dr} + \frac{M(\alpha)}{\alpha\ln(\alpha)} = -\frac{\alpha}{2S}. \tag{89}$$

Since $h(r,t)$ decays to $h_\infty(r)$ exponentially fast as $t \to \infty$, $f(t \mid r)$ must also decay to zero exponentially fast as $t \to +\infty$. Therefore, $M(r)$, defined by Eq. (83), must be finite at all locations. The coefficient of $dM(r)/dr$ in Eq. (88) is infinite when $r \to 1$, implying that $M(r)$ is not well defined. To ensure that $M(r)$ is finite, we require

$$\frac{dM(1)}{dr} = 0. \tag{90}$$

Solving Eq. (88) with these boundary conditions gives us

$$M(r) = \underbrace{\frac{r^2(1-\ln(r))-1}{4\ln(r)}}_{\textit{geometry term}} + \underbrace{C_1}_{\textit{hydraulic term}}, \tag{91}$$

where the constant C_1 is given by

$$C_1 = \frac{\alpha^2(2\ln(\alpha)-1)}{4} - \frac{\alpha^2\ln(\alpha)}{2S}. \tag{92}$$

Our solution for $M(r)$ represents the dimensionless mean time scale for the radial flow process at each position, r. The expression for $M(r)$ is the sum of two distinct 'geometry' and 'hydraulic' terms. The geometry term describes the spatial variation of the mean time scale. Intuitively, we expect that points closer to the well will respond faster than points further away from the well and the geometry term reflects this. The constant hydraulic term is independent of position and describes the storage effects associated with both the aquifer and the well.

The mathematical expression for $M(r)$, given by Eq. (91), is independent of Q', indicating that the mean time scale is equivalent for pumping and injection processes. Furthermore, the boundary value problem is invariant if we switch the roles of $h_\infty(r)$ and $h_0(r)$, which is the same as replacing $g(r)$ with $-g(r)$ throughout. Therefore, not only $M(r)$ is equivalent for pumping and injection processes, but it is also equivalent for the associated recovery process [*Simpson et al.* 2013].

It is interesting to remark that we obtained our expression for $M(r)$ without solving the governing flow equation for $h(r,t)$. The expression for $M(r)$ is relatively straightforward and does not depend on any arbitrary thresholds. Since we did not make any subjective choice of thresholds, and we only used standard definitions of the mean of a PDF, our expression for $M(r)$ is a fundamental, objectively defined quantity that shows how the mean time scale depends on relevant hydraulic and geometric properties of the problem. Plots in Figure 4-1(a) illustrate how $M(r)$ varies with position for two different problems chosen to illustrate the differences between a field scale application, relevant for $\alpha \to 0$, and a laboratory scale application, with $\alpha > 0$. Both plots show that the mean time scale increases with r, as expected.

It is useful to note that Eq. (91) can be simplified when $\alpha \to 0$, for field scale applications, by evaluating the expression for C_1 in the limit as $\alpha \to 0$, giving $C_1 = 0$. Therefore, for a field scale problem, the MAT is totally independent of well storage effects because $C_1 = 0$. Therefore, for a field scale problem, $M(r)$ depends only on the geometry. Conversely, for smaller laboratory scale problems, well storage effects play a role and our general expression for $M(r)$ allows us to quantify the relative importance of these effects for problems at different scales simply by varying α.

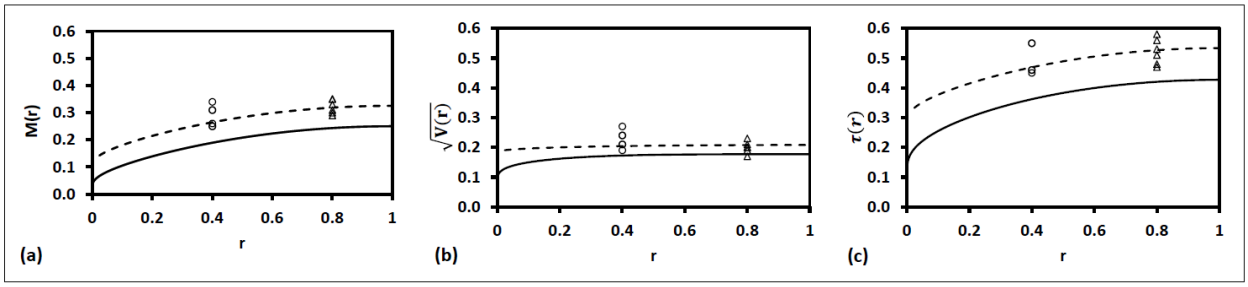

Figure 4-1: Comparison of: (a) $M(r)$, (b) $\sqrt{V(r)}$ and (c) $\tau(r) = M(r) + \sqrt{V(r)}$ for a large field scale application (solid) and a smaller laboratory scale application (dashed). The field scale application corresponds to $\alpha \to 0$ and is plotted for $0 < r < 1$. The laboratory scale application corresponds to $\alpha = 0.024$, and is plotted for $0.024 \le r < 1$. Experimental values of $M(0.4)$, $V(0.4)$ and $\sqrt{V(0.4)}$ (circle symbols), and $M(0.8)$, $\sqrt{V(0.8)}$ and $\tau(0.8)$ (square symbols) are superimposed from Table 5.

4.4 Variance of action time for a radial system

The VAT, $V(r)$, is the second moment of $f(t \mid r)$ [*Simpson et al.*, 2013*; Jazaei et al.*, 2014]. Once we have evaluated $V(r)$, we can compute $\sqrt{V(r)}$, which is a measure of the spread of $f(t \mid r)$ about $M(r)$. An estimate of the time needed to reach steady state, after accounting for both the mean and variance of the PDF, can be written as,

$$\tau(r) = M(r) + m\sqrt{V(r)}, \tag{93}$$

where m is a positive integer. In this study, we begin by making a simplest possible choice by setting $m = 1$, and we will discuss this choice later when we compare our theoretical predictions with our measurements from a physical model. This implies that our definition of time $\tau(r)$ is subjective since it depends on the choice of m. In contrast our definition of time scale $M(r)$ is completely objective.

The VAT is defined as [*Simpson et al.*, 2013*; Jazaei et al.*, 2014]

$$V(r) = \int_0^{\infty} (t - M(r))^2 \, f(t \mid r) \mathrm{d}t. \tag{94}$$

Using Eq. (83), together with the fact that $h(r,t)$ decays to $h_{\infty}(r)$ exponentially fast as $t \to +\infty$, we rewrite Eq. (94) as,

$$\varphi(r) = 2\int_0^{\infty} t(h_{\infty}(r) - h(r,t)) \mathrm{d}t, \tag{95}$$

where,

$$\phi(r) = g(r)[V(r) + M(r)^2]. \tag{96}$$

By combining the first and the second derivatives of $\phi(r)$ with Eqs. (79) and (83), we obtain a boundary value problem for $\phi(r)$,

$$\frac{d^2\phi(r)}{dr^2} + \frac{1}{r}\frac{d\phi(r)}{dr} = -2g(r)M(r). \tag{97}$$

To obtain the boundary conditions required to solve Eq. (97) we evaluate the first derivative of $\phi(r)$ at $r = \alpha$, and using Eq. (80), we obtain a Neumann boundary condition given by

$$\frac{d\phi(\alpha)}{dr} = -\frac{\alpha M(\alpha) g(\alpha)}{S}. \tag{98}$$

Since $h(r,t)$ decays to $h_\infty(r)$ exponentially fast as $t \to \infty$, Eq. (94), guarantees that $V(r)$ is finite at all locations. Since $g(1) = 0$, and $V(r) + M(r)^2$ is finite at all locations, the relevant boundary condition at $r = 1$ is:

$$\phi(1) = 0. \tag{99}$$

Solving Eq. (97) with these boundary conditions gives,

$$V(r) = \frac{1}{64}\left[\frac{128C_2}{S} - 2(r^4 + 32C_1^{\,2}) + \frac{(5r^4 + 128C_3 + 32C_1)}{\ln(r)} - \frac{4(r^2-1)^2}{\ln^2(r)}\right], \tag{100}$$

where C_1 is the hydraulic factor defined in Eq. (92) and,

$$C_2 = \frac{\alpha^2}{64}[4\ln(\alpha)(8SC_1 - S\alpha^2 + 2\alpha^2 - 8C_1) + S(5\alpha^2 - 16C_1 - 8) - 8\alpha^2 + 8], \tag{101}$$

$$C_3 = -\frac{5 + 32C_1}{128}. \tag{102}$$

It is interesting to note that $V(r)$ is also independent of Q', and this shows that the width of $f(t \mid r)$ is same for pumping, injection and recovery processes. Now that we have closed form solutions for $M(r)$ and $V(r)$, we can calculate $\tau(r) = M(r) + m\sqrt{V(r)}$. Similar to our expression for $M(r)$, the expression for $V(r)$ can be simplified considerably for field scale problems by considering the limit that $\alpha \to 0$, giving $C_1 = C_2 = 0$. However, unlike the expression for $M(r)$, the expression for $V(r)$ is more complicated and it is not obvious how to give these terms a meaningful interpretation like we did for $M(r)$.

Plots in Figure 4-1(b)–(c) illustrate how $\sqrt{V(r)}$ and $\tau(r)$ (with $m=1$) varies with position for two different problems chosen to illustrate the differences between a field scale application and a laboratory scale application. Comparing the results for $M(r)$ and $\sqrt{V(r)}$ we see that the spatial variations in the mean is more pronounced than the spatial variations in the standard deviation.

4.5 Laboratory experiments

We now apply our method of calculating $M(r)$, $V(r)$ and $\tau(r)$ to a set of laboratory scale pumping, injection and recovery experiments. The experiments involve a cylindrical confined flow system with a constant head boundary condition. Figure 4-2 shows horizontal and vertical cross sections through the flow tank. The tank has two distinct chambers separated by a fine screen. The lower layer was wet packed with homogeneously mixed silty sand to form a circular confined aquifer of thickness $B'=10$ cm, and a radius of $R'=25$ cm. The upper layer contained dry coarse sand and gravel material, primarily to support the confining plastic liner against the uplifting hydraulic pressure generated within the aquifer. A fully penetrating well of radius of 0.7 cm was located at the center of the aquifer. A thin tube with the radius of 0.3 cm connected to a peristaltic pump (Masterflex: L/S-7523-80) was inserted into the well to deliver water into or out of the aquifer. The effective radius of the well is approximately $r_w' = \sqrt{0.7^2 - 0.3^2} \approx 0.6$ cm. The well was only screened in the lower layer and the wall was sealed at the upper layer with a plastic liner. A layer of clay was used near to the wall to prevent water leaking from the aquifer to the upper layer. Two syphon-type tubes were connected to electronic manometers to monitor head changes at $r_1'=10$ cm and $r_2'=20$ cm. Head changes were monitored using 1 second time intervals, at a resolution of 0.1 mm. The ends of the syphon-type tubes were screened to prevent solid particles

to enter the tubes. The confined system was monitored for three days and no leakage was detected through the confining layer. The hydraulic conductivity of the silty sand material was independently measured to be $K' = 0.0008$ cm/sec using a falling head permeameter. Using our estimates of K' and B', we calculate the transmissivity, $T' = K'B'$. The value of the storage coefficient was estimated to be $S = 0.014$ by fitting a transient head dataset collected at $r_1' = 10$ cm under a constant injection rate of 30 ml/min.

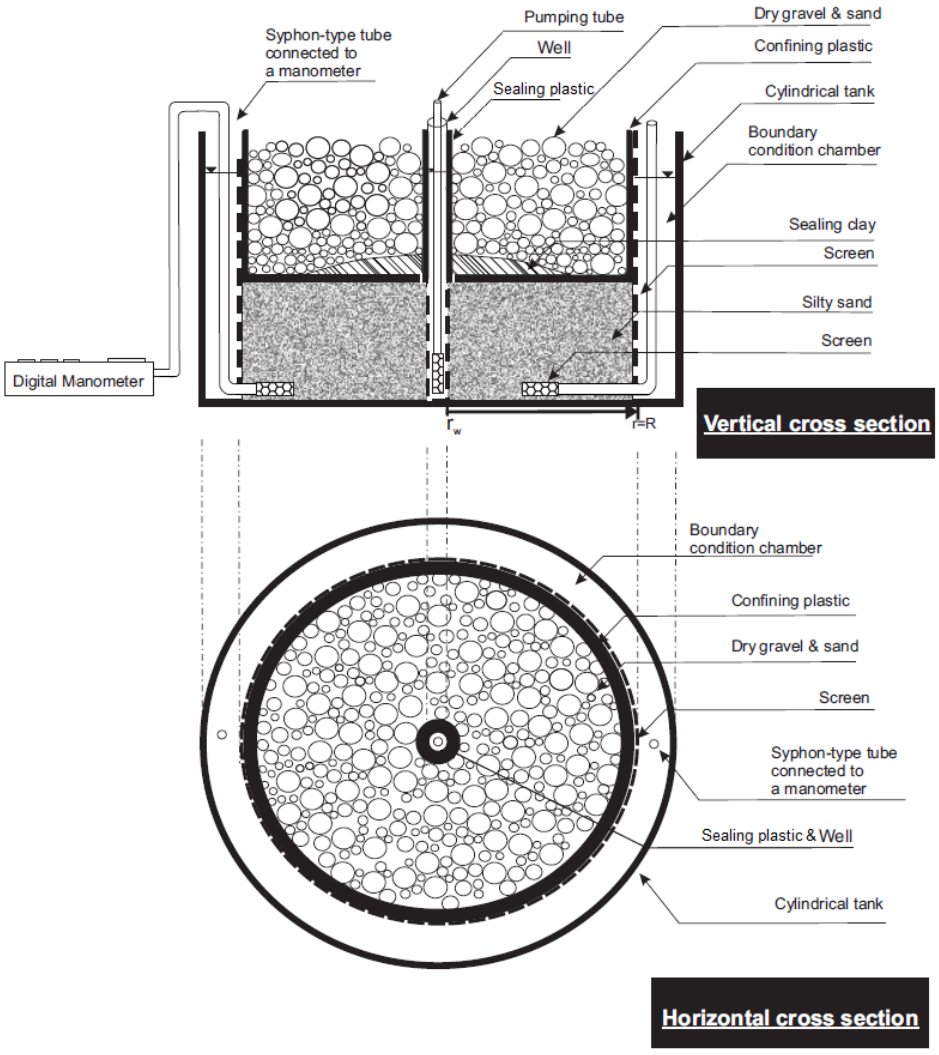

Figure 4-2: Vertical and horizontal cross sections of the laboratory model.

4.6 Analysis of transient head data

We performed one pumping and two injection experiments. We refer to these experiments as Experiment-P, Experiment-I1 and Experiment-I2, respectively. We also consider three associated recovery experiments, namely Experiment-RP, Experiment-RI1 and Experiment-RI2. The flow rates for Experiment-P, Experiment-I1 and Experiment-I2 are: $Q'_P = 15ml/min$, $Q'_{I1} = -30ml/min$, and $Q'_{I2} = -40ml/min$, respectively. The initial and boundary conditions for all experiments is $h'_0(r') = h'(R',t') = 35cm$. Using Eq. (76), the characteristic length, time, and head scales for our experiments are:

$$r^* = 25cm, \qquad t^* = 18.23min, \qquad h^* = 35cm. \tag{103}$$

These quantities allow us to define dimensionless *r*, *t* and *h* using Eq. (77). Transient head changes were measured at $r'_1 = 10cm$ and $r'_2 = 20cm$, or $r_1 = 0.4$ and $r_1 = 0.8$, respectively. For our experimental system we have $\alpha = 0.024$.

We predict the *theoretical* $M(r)$ and $V(r)$ values for six radial flow processes at two different positions using Eqs. (91) and (100), respectively. We also measured the observed time scales, which we refer to as *experimental* time scales using our laboratory datasets. To calculate MAT and VAT from our laboratory datasets we used the monitored transient head data to construct $f(t \mid r)$. To achieve this, we use a central difference approximation to estimate $\partial h/\partial t$. After constructing $f(t \mid 0.4)$ and $f(t \mid 0.8)$, we calculated the *experimental* $M(r)$ and $V(r)$ using Eqs. (83) and (94), evaluating the integrals using the trapezoid rule.

Theoretical and experimental values of $M(r)$, $\sqrt{V(r)}$ and $\tau(r)$ at $r_1 = 0.4$ and $r_2 = 0.8$ are summarized in Table 5, indicating that the experimental values match the theoretical predictions reasonably well. Our results also indicate that $M(r)$ and $\tau(r)$ are independent of Q' and therefore independent of whether we consider a pumping, injection or recovery process.

Table 5: Nondimensional theoretical and experimental values of $M(r)$, $\sqrt{V(r)}$ and $\tau(r)$ at $r_1 = 0.4$ and $r_2 = 0.8$.

	$r_1 = 0.4$ (-)			$r_2 = 0.8$ (-)		
	$M(r)$	$\sqrt{V(r)}$	$\tau(r)$	$M(r)$	$\sqrt{V(r)}$	$\tau(r)$
Theoretical values	0.26	0.21	0.47	0.32	0.22	0.54
Experiment-P $Q'_p = 15$ [ml/min]	0.31	0.24	0.55	0.35	0.23	0.58
Experiment-RP	0.26	0.19	0.45	0.31	0.20	0.51
Experiment-I1 $Q'_{I1} = -30$ [ml/min]	0.25	0.21	0.46	0.35	0.21	0.56
Experiment-RI1	0.31	0.24	0.55	0.30	0.17	0.47
Experiment-I2 $Q'_{I2} = -40$ [ml/min]	0.25	0.21	0.46	0.33	0.20	0.53
Experiment-RI2	0.34	0.27	0.61	0.29	0.19	0.48

Table 6 shows $F(t \mid r)$ after times $t = M(r)$ and $t = \tau(r)$ in all experiments at both monitoring points. Our data indicate that after $t = M(r)$, approximately 55–67% of the process has taken place. In contrast, after $t = \tau(r)$, approximately 84–89% of the process has taken place. These results show that setting $m = 1$ in Eq. (93) adequately estimates the amount of time required for the transient flow problem to effectively reach steady state conditions. We note that setting $m > 1$ would lead to larger values of $\tau(r)$. However, the simplest possible choice of $m = 1$ leads to a prediction of the time scale where about 87% of the transient response has taken place. Therefore,

for practical purposes, setting $m = 1$ leads to a useful and informative prediction of the relevant time at which the system effectively reaches the steady state.

Table 6: Cumulative distribution functions at two monitoring points, $r_1 = 0.4$ and $r_2 = 0.8$, indicating the proportion of each transition that has completed by $t = M(r)$ and $t = \tau(r)$ for all six experiments.

	$F(M(r)\mid r) = 1 - \frac{h(r, M(r)) - h_\infty(r)}{h_0(r) - h_\infty(r)}$		$F(\tau(r)\mid r) = 1 - \frac{h(r, \tau(r)) - h_\infty(r)}{h_0(r) - h_\infty(r)}$	
	$r_1 = 0.4$ (-)	$r_2 = 0.8$ (-)	$r_1 = 0.4$ (-)	$r_2 = 0.8$ (-)
Experiment-P $Q'_P = 15$ [ml/min]	57%	67%	88%	87%
Experiment-RP	61%	66%	85%	89%
Experiment-I1 $Q'_{I1} = -30$ [ml/min]	62%	64%	86%	85%
Experiment-RI1	61%	55%	84%	84%
Experiment-I2 $Q'_{I2} = -40$ [ml/min]	61%	63%	87%	88%
Experiment-RI2	61%	63%	87%	88%

Figure 4-3 shows the monitored transient head changes with the predicted theoretical values of $M(r)$ and $\tau(r)$ superimposed. Comparing the temporal head data and our estimates of $\tau(r)$ indicate that $\tau(r)$ is a useful estimate of the time required for the system to effectively reach steady state.

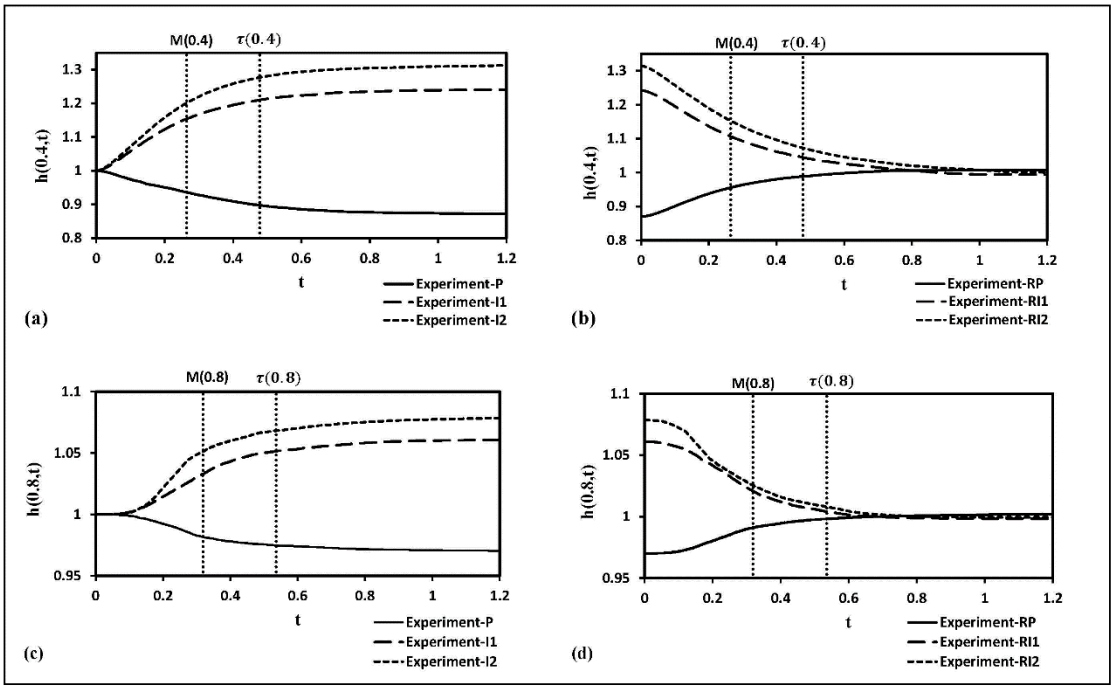

Figure 4-3: Results in (a)–(b) show dimensionless transient data gathered at $r_1 = 0.4$ for Summary and conclusions

4.7 Summary and conclusions

In this study we develop an analytical framework that can be used to: (1) estimate the time scale of the radial flow processes; (2) explicitly show how different hydraulic and geometric factors affect the time scales of the process; and (3) show how the time scales vary spatially within the flow domain. To achieve this we introduce two time scales: $M(r)$ and $\tau(r)$, using the concepts of mean action time (MAT) and variance of action time (VAT), respectively.

The key advantage of the MAT framework is that the mathematical expression for $M(r)$ explicitly shows how the geometry and hydraulic parameters affect the time scale of the flow process. In contrast, other definitions of the relevant time scale, such as using an arbitrary threshold, does not lead to mathematical expressions that are linked to hydraulic and geometric factors. Another limitation of using a threshold approach is that the time scale predicted itself

would depend upon the choice of the threshold. In contrast, MAT avoids the need for defining an arbitrary, subjective threshold.

We also define the VAT, $V(r)$, and use this information to estimate the actual time needed to reach steady state after accounting for both the mean and the width of the PDF that governs the transition. Given $M(r)$ and $V(r)$ we define $\tau(r) = M(r) + m\sqrt{V(r)}$, as an estimate of the instant that explicitly accounts for the spread in the PDF. Here, m is a positive integer, and to use this definition we must choose m. In this work we have used the simplest possible approach and have set $m = 1$, meaning that $\tau(r)$ corresponds to the mean plus one standard deviation. Comparing our estimate of $\tau(r)$ with our laboratory scale data confirms that setting $m = 1$ leads to a reasonable estimate of the time to reach steady state. For our test problem, $\tau(r)$ corresponds to the time required for approximately 84–89% of the transient response to have completed.

Our expressions for $M(r)$, $V(r)$ and $\tau(r)$ explicitly relate the aquifer response time scale to various parameters including aquifer transmissivity, storage coefficient, well diameter and the location of the boundary. Our analysis shows that the groundwater response time scales are equivalent for pumping, injection and recovery processes, and are independent of the flow rate at the well. Moreover, our mathematical expressions quantify the spatial variations in the aquifer response time for radial flow processes including pumping, injection and recovery processes. These predictions are confirmed by our laboratory–scale measurements.

One of the limitations of our work is that we consider groundwater flow driven by a single pumping or injection well. A possible extension of our present study is to consider flow processes driven by multiple pumping and/or injection wells. Under these conditions we have to consider a

more complicated two or three dimensional flow model in a Cartesian coordinate system. However, the general mathematical framework outlined here would still apply.

CHAPTER 5 UNDERSTANDING TIME SCALES OF DIFFUSIVE FLUXES AND IMPLICATION FOR STEADY STATE AND STEADY SHAPE CONDITIONS

5.1 Introduction

Environmental transport problems involving heat, solute or groundwater flow are typically classified as being either *transient* or *steady state*. Transient problems involve temporal variations in the dependent variable (temperature, concentration or hydraulic head), whereas steady state problems do not involve any temporal variations. In some geoscience fields (e.g., groundwater), previous researchers have postulated the existence of another state, often called *steady shape*, which has been used to describe the situation where the shape of the solution is steady, but the dependent variable may still vary with time, hence the system remains transient [*Bohling et al.*, 2002; *Heath*, 2009]. *Heath* [1983] refers to this as a *steady shape* condition, while *Kruseman and Ridder* [1990] refer to this as a *transient steady state* condition.

An important feature of the steady shape condition is that it is thought to be an intermediate state that arises well before the system reaches steady state. In the literature, it is also broadly assumed that the transport process during the steady shape period can be analyzed using simpler mathematical models that are normally used for describing steady problems [*Bohling et al.*, 2002; *Butler*, 1988]. The ability to use simpler models can have profound practical consequences since it can considerably reduce computational time and effort. However, despite its use, steady shape approximations are invoked heuristically, without any fundamental theoretical understanding of when steady shape conditions are relevant. The objective of this work is to address this fundamental limitation. To achieve this, we develop a formal theoretical basis for defining steady

shape conditions, and use this definition to examine the relevance of steady shape conditions when modeling a range of diffusive transport problems.

The cornerstone of the diffusion equation is the concept of flux, which, as defined by Fourier's law, relates the transport of an extrinsic property (e.g., heat) with the spatial gradient of an intrinsic property (e.g., temperature) [*Carslaw and Jaeger*, 1959; *Crank*, 1979]. The macroscopic quantity flux, which is proportional to the spatial gradient of the dependent variable, quantifies the amount of an extrinsic property transported across a unit area per unit time. The flux concept has been used for modeling several types of environmental transport systems including solute transport (where solute flow is linked with concentration gradient), and groundwater flow (where the groundwater flow is linked with hydraulic head gradient). In the groundwater literature, researchers have identified that pumping problems appear to first reach an intermediate steady shape condition where hydraulic fluxes are effectively steady, while the hydraulic head continues to vary with time [*Bohling et al.*, 2002; *Butler*, 1988]. Understanding how fluxes might approach steady state conditions at a different rate when compared to how the hydraulic head approaches steady state conditions is a fundamental issue that could shed some light on how steady shape conditions develop.

To quantify the time scales required for a diffusive process to approach steady state, we employ a concept called mean action time (MAT), which was originally proposed for analyzing heat transport [*McNabb and Wake*, 1991; *McNabb et al.*, 1991]. Later researchers adapted this approach for modeling more general transport problems [*Ellery et al.*, 2012a; *Jazaei et al.*, 2014; 2016; *K Landman and McGuiness*, 2000; *McGuiness et al.*, 2000; *McNabb and Keady*, 1994; *M J*

Simpson et al., 2013a]. However, all of these studies focus on quantifying the time scale associated with the dependent variable (e.g. hydraulic head, concentration or temperature). Here, we adapt the diffusion equation to model transient changes in diffusive fluxes. We hypothesize that the time scale associated with the dependent variable could be different from the time scale associated with the flux variable. These differences in time scales will be quantified using MAT theory to develop a formal mathematical basis for understanding the differences between steady shape and steady state conditions.

5.2 Development of a general mathematical framework of modeling steady state fluxes

We first review the mathematical framework needed for computing the time scale required for a diffusive variable to approach steady state. We then extend the framework to compute the time scale required for the flux to approach steady state. In this study we use non-dimensional variables to generalize the analysis. All dimensional variables are primed ($'$), and dimensionless variables are unprimed.

The aim of our analysis is to quantify the time scales required for a diffusive variable, ϕ', and the associated flux, $J' = -K'\partial\phi'/\partial x'$ (where the constant $K' > 0$ is a parameter), to effectively asymptote to their respective steady states. We begin with the dimensional form of the diffusion equation,

$$\frac{\partial\phi'(x',t')}{\partial t'} = D'\frac{\partial^2\phi'(x',t')}{\partial x'^2} + W', \quad 0 < x' < L', \tag{104}$$

where $\phi'(x',t')$ is the dependent variable at location x' and time t', $D' > 0$ is the diffusivity, W' is

the spatially uniform source/sink term, and L' is the length of the domain. We define three dimensionless variables,

$$x = \frac{x'}{L'}, \quad \phi(x,t) = \frac{\phi'(x',t')}{\Phi'}, \quad t = \frac{t'D'}{L'^2}. \tag{105}$$

Using these variables, the non-dimensional governing equation is

$$\frac{\partial \phi(x,t)}{\partial t} = \frac{\partial^2 \phi(x,t)}{\partial x^2} + w, \quad 0 < x < 1, \tag{106}$$

where, $w = W'L'^2 / D'\phi'$, and ϕ is a characteristic value of the dependent variable.

To quantify how the flux varies with time and position, we differentiate both sides of Eq. (106) with respect to *x*. Writing $g(x,t) = \partial\phi(x,t)/\partial x$, we obtain

$$\frac{\partial g(x,t)}{\partial t} = \frac{\partial^2 g(x,t)}{\partial x^2}, \quad 0 < x < 1, \tag{107}$$

where the dimensionless flux is $J = -g(x,t)$. Note that the equations governing the evolution of the dependent variable and the flux variable are similar for this Cartesian problem, except there is no source/sink term in Eq. (107). However, the solutions of Eq. (106) and Eq. (107) will differ because they involve a different set of initial and boundary conditions.

5.3 Application of the MAT theory to evaluate the time scales of diffusive fluxes

To derive an expression for the MAT of $\phi(x,t)$, we begin by considering two fundamental quantities [*Jazaei et al.*, 2014; 2016; *McNabb and Wake*, 1991; *M J Simpson et al.*, 2013a]

$$F_\phi(t \mid x) = 1 - \left[\frac{\phi(x,t) - \phi_\infty(x)}{\phi_0(x) - \phi_\infty(x)} \right], \quad t \geq 0, \tag{108}$$

$$f_\phi(t\,|\,x)=\frac{\mathrm{d}F_\phi(t\,|\,x)}{\mathrm{d}t}=-\frac{\partial}{\partial t}\left[\frac{\phi(x,t)-\phi_\infty(x)}{\phi_0(x)-\phi_\infty(x)}\right],\quad t\geq 0, \tag{109}$$

where $\phi_0(x)$ is the initial value of $\phi(x,t)$ (initial condition), and $\phi_\infty(x)$ is the long time steady state value of $\phi(x,t)$ (final steady state condition). MAT theory depends on interpreting $F_\phi(t\,|\,x)$ as a cumulative distribution function (CDF), and therefore this approach is valid for transitions where $F_\phi(t\,|\,x)$ increases monotonically from $F_\phi(0\,|\,x)=0$ and approaches $F_\phi(t\,|\,x)=1$, as $t\to+\infty$. Under these conditions, $f_\phi(t\,|\,x)$ can be interpreted as a probability density function (PDF). The mean, or first moment of this distribution gives a time scale that is called the MAT [*Ellery et al.*, 2012a; b; *Jazaei et al.*, 2014; 2016; *M J Simpson et al.*, 2013a]. This time scale provides an estimate of the amount of time required for $\phi(x,t)$ to asymptote from $\phi_0(x)$ to $\phi_\infty(x)$. The dimensionless MAT is

$$M_\phi(x)=\int_0^\infty t f_\phi(t\,|\,x)\mathrm{d}t. \tag{110}$$

One of the advantages of working with the MAT framework is that it is possible to solve for $M_\phi(x)$ without solving Eq. (106) for $\phi(x,t)$ [*Jazaei et al.*, 2016; *K Landman and McGuiness*, 2000; *M J Simpson et al.*, 2013a]. To solve for $M_\phi(x)$ we require explicit expressions for $\phi_0(x)$ and $\phi_\infty(x)$.

We now extend the MAT theory to evaluate the time scale associated with the transition in terms of the diffusive flux by defining

$$F_g(t\,|\,x)=1-\left[\frac{g(x,t)-g_\infty(x)}{g_0(x)-g_\infty(x)}\right],\quad t\geq 0, \tag{111}$$

$$f_g(t\,|\,x)=\frac{dF_g(t\,|\,x)}{dt}=-\frac{\partial}{\partial t}\left[\frac{g(x,t)-g_\infty(x)}{g_0(x)-g_\infty(x)}\right],\quad t\geq 0, \tag{112}$$

where $g_0(x)$ is the initial value of $g(x,t)$, and $g_\infty(x)$ is the steady value of $g(x,t)$. Once again, we interpret $F_g(t\,|\,x)$ as a CDF provided $F_g(t\,|\,x)$ increases monotonically from $F_g(0\,|\,x)=0$ and asymptotes to $F_g(t\,|\,x)=1$ as $t\to+\infty$. The MAT of the flux variable is,

$$M_g(x)=\int_0^\infty t f_g(t\,|\,x)\mathrm{d}t. \tag{113}$$

To compute $M_g(x)$, we first evaluate $M_\phi(x)$ and then develop a relationship between $M_\phi(x)$ and $M_g(x)$. To accomplish this, we combine Eq. (112) and Eq. (113) and interchange the order of differentiation. Since $g(x,t)=\partial\phi(x,t)/\partial x$, we obtain

$$M_g(x)=\frac{-1}{g_0(x)-g_\infty(x)}\frac{\partial}{\partial x}\int_0^\infty t\frac{\partial\left[\phi(x,t)-\phi_\infty(x)\right]}{\partial t}\mathrm{d}t. \tag{114}$$

Combining Eq. (109) and Eq. (114) gives,

$$M_g(x)=\frac{1}{g_0(x)-g_\infty(x)}\frac{\mathrm{d}}{\mathrm{d}x}\left[\left(\phi_0(x)-\phi_\infty(x)\right)\int_0^\infty t f_\phi(t\,|\,x)\,\mathrm{d}t\right]. \tag{115}$$

The integral in Eq. (115) is $M_\phi(x)$, as in Eq. (110). Therefore, Eq. (115) simplifies to

$$M_g(x)=M_\varphi(x)+\frac{C_\phi(x)}{\mathrm{d}C_\phi(x)/\mathrm{d}x}\left(\frac{\mathrm{d}M_\phi(x)}{\mathrm{d}x}\right), \tag{116}$$

where $C_\phi(x)=\phi_\infty(x)-\phi_0(x)$ and $\mathrm{d}C_\phi(x)/\mathrm{d}x=g_\infty(x)-g_0(x)$. Note that Eq. (116) is an important contribution of this work because it describes an explicit relationship between the time scales associated with the dependent variable, $M_\phi(x)$, and the time scale associated with the flux variable, $M_g(x)$. In Appendix-A chapter, we extend this analysis to solve a diffusion problem in radial coordinates and a two-dimensional diffusion problem in Cartesian coordinates (see Text S2 and Text S3).

5.4 Case studies

We apply the MAT expressions developed here to quantify the time scales associated with the dependent variable and the flux variable in two test cases. Case-I involves a diffusive problem with no source/sink term and a Dirichlet boundary condition at $x = 1$. The initial condition, $\phi(x, 0)$ or $\phi_0(x)$, is spatially uniform. Transient conditions are induced by applying a constant flux at $x = 0$. This test case could represent the hydraulic head in a confined aquifer with uniform initial condition, a fixed head at the right boundary, and a constant flux at the left boundary. Furthermore, this case could also represent the temperature distribution in thermal conductor with constant initial temperature, a fixed temperature at the right boundary, and the left boundary losing heat at a constant rate.

Case-II involves a spatially uniform initial condition, a zero flux condition at $x = 0$, and fixed head boundary conditions at $x = 1$. A constant source/sink term is included to induce a transient transition. This case could represent hydraulic head mounding in an aquifer with uniform initial condition and receiving areal recharge from above, or it could represent a thermal conductor heated from above. The initial and boundary conditions in these two test cases are

$$Case-I: \quad \text{IC} \quad \phi_0(x) = 1; \ \text{BCs} \ \frac{\partial \phi(0,t)}{\partial x} = \alpha \quad \text{and} \quad \phi(1,t) = 1; \quad w = 0, \tag{117}$$

$$Case-II: \quad \text{IC} \quad \phi_0(x) = 1; \ \text{BCs} \ \frac{\partial \phi(0,t)}{\partial x} = 0 \quad \text{and} \quad \phi(1,t) = 1; \quad w \neq 0, \tag{118}$$

where α and w are constants.

To solve for the MAT, we apply integration by parts to Eq. (110) and note that $\phi(x,t)$

approaches $\phi_\infty(x)$ exponentially fast as $t \to +\infty$ [*Crank, 1975; Simpson et al., 2013*], then differentiating the result twice with respect to *x*, and combining the resulting expression with Eq. (106) leads to a second order boundary value problem for $M_\phi(x)$,

$$\frac{\mathrm{d}^2\left[M_\phi(x)C_\varphi(x)\right]}{\mathrm{d}x^2} = -C_\phi(x). \tag{119}$$

To solve Eq. (119) we need to evaluate $C_\phi(x) = \phi_\infty(x) - \phi_0(x)$, where $\phi_\infty(x)$ is found by evaluating Eq. (106) at steady state. The $C_\phi(x)$ functions for the two cases are:

$$Case-I: \quad C_\phi = \alpha(x-1), \tag{120}$$

$$Case-II: \quad C_\phi = \frac{w(-x^2+1)}{2}. \tag{121}$$

The boundary conditions required to solve Eq. (119) are [*Jazaei et al.*, 2016; *M J Simpson et al.*, 2013a]

$$Case-I: \ \frac{\mathrm{d}\,M_\phi(0)}{\mathrm{d}x} - M_\phi(0) = 0; \qquad \frac{\mathrm{d}\,M_\phi(1)}{\mathrm{d}x} = 0, \tag{122}$$

$$Case-II: \ \frac{\mathrm{d}\,M_\phi(0)}{\mathrm{d}x} = 0; \qquad 2\,\frac{\mathrm{d}\,M_\phi(1)}{\mathrm{d}x} + M_\phi(1) = 0. \tag{123}$$

Further details of these boundary conditions are given in the Appendix-A chapter (see Text S1). The MAT expressions for the dependent variable, obtained using Eqs. (119) to (123), are

$$Case-I: \quad M_\phi(x) = \frac{1}{6}(2+2x-x^2), \tag{124}$$

$$Case-II: \quad M_\phi(x) = \frac{1}{12}(5-x^2). \tag{125}$$

In contrast, MAT expressions for the flux, obtained using Eqs. (116), (124) and (125), are

$$Case-I: \quad M_g(x) = \frac{1}{2}(2x - x^2), \tag{126}$$

$$Case-II: \quad M_g(x) = \frac{1}{6}(3 - x^2). \tag{127}$$

Note that these MAT expressions give non-dimensional time scales. If required, the dimensional time is given by $\tau'(x') = M(x'/L')(L'^2/D')$.

5.5 Results

5.5.1 Case-I

Figure 5-1 (a) shows the time scales required for the dependent variable and the diffusive flux variable, computed using Eq. (124) and Eq. (126), as functions of position. The data show considerable differences between the two time scales, with $M_g(x) < M_\phi(x)$. This is consistent with the conventional assumption that steady shape conditions arise before steady state conditions. To validate these findings we also solve the governing partial differential equations, with appropriate initial and boundary conditions, using an implicit finite difference method to estimate $\phi(x,t)$ and $g(x,t)$ for the two test problems. These two functions, evaluated at two fixed spatial locations, are given in Figure 5-1(b)-(c). The figures also show the time scales, $M_\phi(x)$ and $M_g(x)$, computed using the appropriate exact MAT expressions. These solutions confirm that the MAT elegantly characterize the time scales required for $\phi(x,t)$ and $g(x,t)$ to approach to their respective steady states. Furthermore, the numerical results confirm that, in this case, the time scales associated with the dependent variable and its flux can be different, and that $g(x,t)$

approaches steady state faster than $\phi(x,t)$.

5.5.2 Case-II

Figure 5-1(d) shows the time scales required for the dependent variable and the flux variable to approach their respective steady states at all locations for the second test problem. Unlike Case-1, the difference in the two time scales is relatively small, meaning that the steady shape condition is not so relevant in this case. Numerical data for $\phi(x,t)$ and $g(x,t)$ are given in Figure 5-1(e)-(f), confirming that $g(x,t)$ approaches steady state almost similar to $\phi(x,t)$.

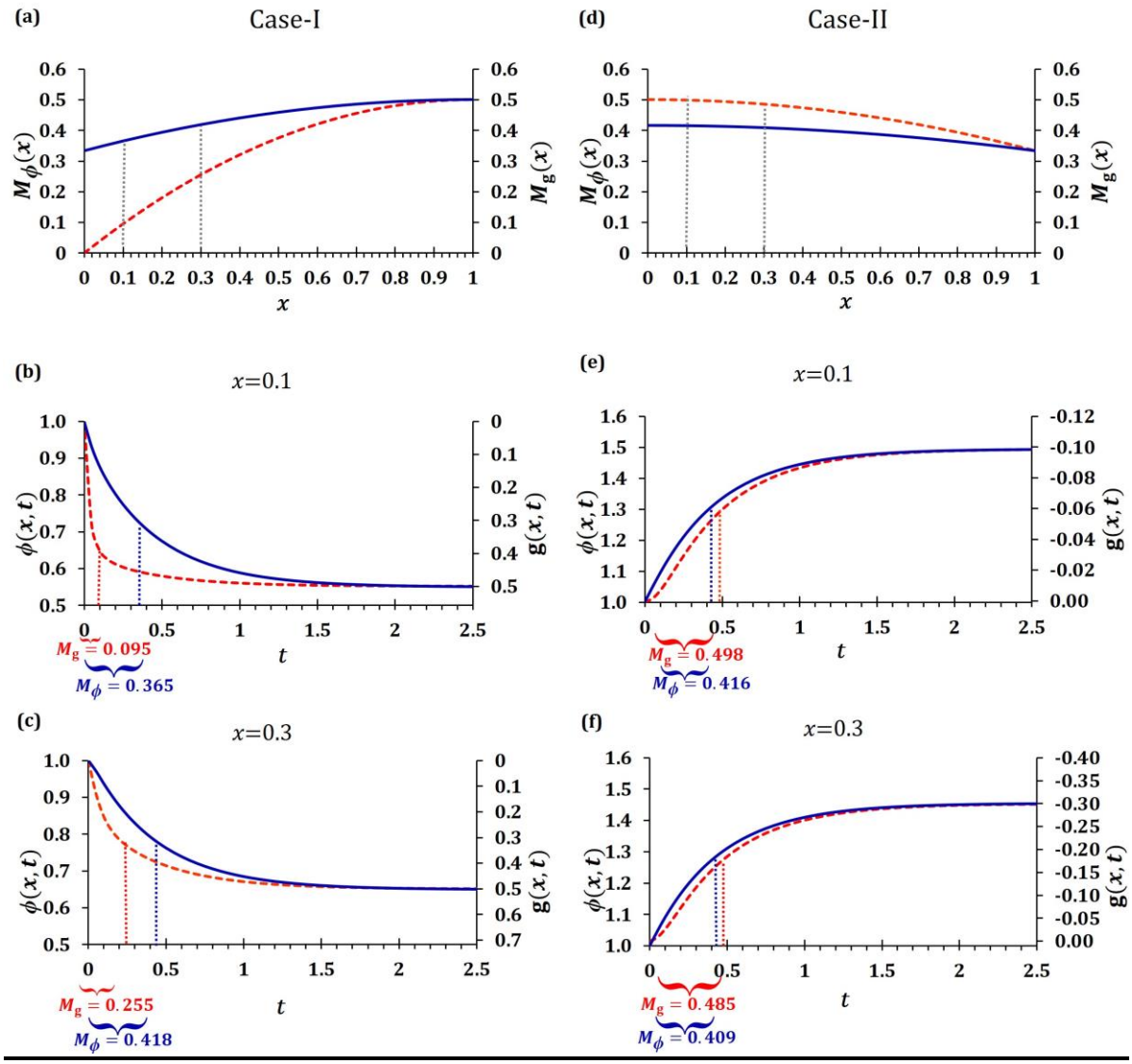

Figure 5-1: Left figures present Case-I results and right figures present Case-II results; (a) and (d) show the spatial variation in MAT for the dependent variable, $M_\phi(x)$ (solid blue), and the spatial variation in MAT for the flux, $M_g(x)$ (dashed red) for Case-I and Case-II, respectively. Results in (b) and (c) show numerical solutions of $\phi(x,t)$ (solid blue) and $g(x,t)$ (dashed red) for Case-I at *x=0.1* and, *x=0.3*, respectively. Results in (e) and (f) show numerical solutions of $\phi(x,t)$ (solid blue) and $g(x,t)$ (dashed red) for Case-II at *x=0.1* and, *x=0.3*, respectively. Parameters are $\Delta x = 0.0005, \Delta t = 0.05, w = 1$ and $\alpha = 0.5$.

5.6 Summary and conclusions

In this work we quantify differences in the time scales associated with the dependent variable and the flux variable to reach steady state conditions in a diffusive transport system. These two time scales are associated with the development of steady state, and steady shape conditions, respectively. We employ the theory of MAT to quantify these differences. These results are quite general, and applicable to any problem that can be modeled using the linear diffusion equation for which the transient solution asymptotes to a steady state solution. This includes problems such as groundwater flow in confined aquifers and heat flow in thermal conductors. In the groundwater literature, researchers have pointed out the possibility of groundwater flow systems reaching an intermediate condition, often called steady shape [*Bohling et al.*, 2002; *Butler*, 1988; *Heath*, 2009]. However, there has been no theoretical basis for objectively identifying steady shape conditions, nor has there been any theoretical framework developed to quantify the differences in time scales associated with steady shape and steady state conditions. Interestingly, of the two test problems we consider, only the first problem exhibits a clear and prolonged steady shape transition period. Therefore, the concept of steady shape conditions may not always be relevant. Understanding the relevance of steady shape conditions is difficult without the kinds of analytical tools presented in this work. Without a formal mathematical definition of steady shape conditions, and exact expressions for $M_{\phi}(x)$ and $M_{g}(x)$, we are limited to studying numerical solutions of transient partial differential equations on a case-by-case basis. In contrast, our formal mathematical framework provides very general insight, and can be adapted to apply to a range of other problems with different boundary conditions, initial conditions, as well as multi-dimensional problems (which are discussed in Appendix-A chapter--Text S2 and Text S3).

Previous analyses of transient diffusive problems have primarily employed scaling arguments to argue that the time scale required to reach steady state or steady shape conditions is proportional to L'^2 / D', where L' is a characteristic length scale [*Cussler*, 1997; *Gelhar and Wilson*, 1974a; *Heath*, 2009; *Manga*, 1999; *Turcotte and Schubert*, 1982]. However, it is unclear how to choose the proportionality constant. For example, *Heath* [2009] presents an empirical formula to estimate the critical time (in minutes) required for steady shape conditions to develop near a pumping well: $\tau' = 7500 r'^2 / D_a'$, where r' is distance (m) from the pumping well and D_a' is the aquifer diffusivity (m^2/day). Cussler [1997] states that diffusive systems are expected to approach steady state conditions when the Fourier number, $L'^2 / D't'$, is much less than unity. Our analysis shows that these empirical arguments neglect the fact that the proportionality term in the time scale relationship is not a constant, but it depends on position. Furthermore, the functional relationship itself is different for steady state or steady shape conditions. Our proposed mathematical framework provides an objective method for deriving analytical expressions for these relationships. Our analysis also quantifies the role of boundary conditions and demonstrates their importance in determining steady state and steady shape time scales.

A key aspect of our work is that we make use of the fact that if $\phi(x,t)$ evolves according to a linear diffusion equation then the diffusive flux also evolves according to a linear diffusion equation; however, with a different set of boundary conditions and a modified source term. These subtle differences in boundary conditions lead to the differences in the time scales. For example, if a diffusion equation describing the evolution of $\phi(x,t)$ involves a constant flux boundary

condition, then the corresponding equation describing the evolution of $\partial\phi/\partial x$ will involve a Dirichlet boundary condition. However, there are many cases for which transforming the boundary conditions for the equation governing the evolution of the dependent variable into the boundary conditions associated with the evolution of the flux is challenging. For example, consider a one-dimensional diffusion problem with two Dirichlet boundary conditions. Without solving the transient equation for $\phi(x,t)$, only the value of the dependent variable at the boundaries is known, whereas the value of the flux at the boundaries is unknown. This situation leads to complications while solving Eq. (10). An important contribution in this work is the development of Eq. (13), which circumvents this issue. In summary, the use of Eq. (13) avoids the need for solving Eq. (4). For example, *Simpson* [2016] recently analyzed the critical time scales for a problem involving morphogen gradients, which requires explicit analysis of the partial differential equation governing the evolution of the gradient variable. This approach cannot be used to solve the problems considered in the present study involving Dirichlet boundary conditions for the dependent variable. In contrast, our approach circumvents these issues.

Although all analyses presented here focus on one-dimensional Cartesian problems, the method can be extended to radial problems and multi-dimensional Cartesian problems. Two specific examples are presented in the Appendix-A chapter (see Text-S2 and Text S3). Furthermore, the applications described here involve homogeneous transport processes where D' and W' are constants. However, our framework also applies to more general heterogeneous problems provided $D'(x')$ and $W'(x')$ are sufficiently differentiable. Since the linear diffusion equation is routinely used to model several practical science and engineering problems including

consolidation (geotechnical literature) and corrosion (material science literature) processes, the proposed theoretical framework has practical relevance to a variety of practical problems across many applied fields.

CHAPTER 6 SUMMARY, CONCLUSIONS, AND RECOMMENDATIONS FOR FUTURE WORK

When a well-balanced diffusive system, such as a groundwater system, is perturbed by an external force, it undergoes a transient state and eventually relaxes into a new balanced steady state. Steady state has certain unique characteristics which are helpful for water resources scientists and hydraulic engineers who are interested in developing long term management plans. The term "*steady state*" refers to the condition when the overall external forcing effectively balance the discharges. In other words, once a system is in its steady state, the amount of water entering the system from boundaries are equal to the amount of water leaving the system via discharge boundaries. This fundamental characteristic of steady state is used to solve several mass transfer and mass balance problems. In addition, mathematical solutions of a steady state system is simpler than a transient solution. Therefore, steady state solutions have been extensively used to analyze complex and coupled flow and transport models.

The primary objective of this study is to explore a fundamental question – how long would it take an aquifer to transition from its initial condition to a new steady state? In the literature, the amount of time a system requires to transition from an initial state to a steady state is known as "*response time."* Determination of an aquifer response time is challenging. This is because from a mathematical viewpoint, a perturbed groundwater system requires an infinite amount of time to reach its ultimate steady state. This answer is, however, impractical, because it is impossible to wait for an infinite amount of time. In fact, to deal with practical problems, we need a finite quantity to express the time length of these process. Hence, researchers tried to define characteristic *time scales* of the diffusion process. The focus of this dissertation is to improve our

understanding of aquifer response time scales to different types of forcing conditions such as surface recharge and discharge, stream level variations at aquifer boundaries, and pumping or injection wells.

Traditional approaches available in the literature to determine response times scales can be categorized into two groups: (1) *explicit scaling* methods, and (2) *implicit computational* methods. Unfortunately, both methods have significant limitations. The first approach provides a unique time scale for the entire domain and cannot describe the spatially varying characteristics of the response time. The second approach requires transient solutions to the governing equation, and also it only provides subjective time scales that cannot explicitly show the relationship of the time scale with aquifer properties and geometric parameters. The framework developed in this dissertation does not have any limitations which are associated with traditional methods.

This study uses a novel theory known as mean action time (MAT) which defines the time scale of the processes as the first moment (or mean) of the rate of variation of action. The key advantage of the MAT framework is that it provides an exact mathematical expression describing how the response time scale depends on various aspects of the problem of interest. In Chapter 2, we use this method to analyze the response time scales of aquifer to surface recharge and discharge. The developed framework provides an analytical expression showing how the time scales of the process would depend upon various system variables (e.g. K, $\bar{h}$, S_y, h_1, h_2, L and R). The results yield several useful and possibly counterintuitive results. It shows that the response time scales of the recharge and discharge processes are not explicitly dependent upon the recharge rate, R . It also shows that the time scale for a recharge process is equivalent to the time scale of the related

discharge process. This is a surprising result since the steady state phreatic surface would depend on the recharge rate, *R*, however the time taken to approach the steady state is independent of *R*.

In Chapter 3 we use the framework to predict the response time scales of groundwater flow near a groundwater surface-water interface. This chapter analyzes response time scales of a one-dimensional aquifer to various types of perturbations at a surface-water boundary. The developed MAT framework provides a direct mathematical relationship relating the response time scale to various system parameters. Results show that aquifer systems have three fundamental time scales that depend on: (i) the intrinsic properties of the aquifer, (ii) the intrinsic properties of the boundary condition, and (iii) the global properties of the entire system.

The developed MAT framework in Chapter 4 is used to estimate the response time scales of a radial groundwater flow system. The derived response time scales explicitly show how different hydraulic and geometric factors affect the time scales of aquifers perturbed by a pumping or an injection well. Results show how response time scales vary spatially within the flow domain. Our analyses show that the groundwater response time scales are equivalent for pumping, injection and recovery processes, and are independent of the flow rate at the well. The MAT expressions presented in this chapter are developed in dimensionless forms and therefore, the results are applicable for small-scale laboratory problems as well as large-scale field problems.

Chapter 5 discusses a key general contribution, which is applicable for different types of diffusion problems including groundwater flow, heat flow and contaminant transport. The new framework is used to quantify the time scales of the dependent variable and its spatial derivative (flux) variation, which are associated with the development of steady state and steady shape

conditions, respectively. The MAT framework developed in Chapter 5 identifies steady shape conditions and quantifies the differences in time scales associated with both steady shape and steady state conditions. This chapter presents a formal mathematical tool to analyze steady shape conditions associated with any linear diffusive system.

This dissertation primarily focusses on cases in which the porous medium is assumed to be homogenous. A possible extension of present study is to consider the effects of heterogeneity within the system. Furthermore, this study has not investigated problems which have complex forcing conditions which would vary spatially or temporally (e.g. varying surface recharge/discharge or pumping/injection flows). MAT framework can be developed for such problems, provided differentiable expression for recharge function, $R(x)$ and heterogeneity function $K(x)$ are available. Future work can also address flows driven by multiple pumping/injection wells. Under these conditions, a more complicated two- or three-dimensional flow model in a Cartesian coordinate system must be considered. However, the general mathematical framework outlined in this dissertation would still apply. The developed techniques outlined in this dissertation for the one–dimensional case are applicable for multidimensional systems as well. However, in that case, the boundary value problems governing the response time scales will be a two–dimensional or a three–dimensional partial differential equation. In Appendix-A we briefly show the use of MAT theory for a two-dimensional Cartesian problem. This dissertation, however, does not include comprehensive analyses of multidimensional problems, which can be addressed in future efforts. Application of MAT to nonlinear problems that are not readily linearized are challenging and can be explored in future studies. There are also possibilities to extend the application of MAT theory for analyzing problems involving fluctuating boundary

conditions. Finally, this effort is mainly focused on groundwater problems. However, there are some obvious opportunities to extend the developed frameworks to other types of problems such as contaminant diffusion, heat flow and consolidation, to name a few.

REFERENCES

Abarca, Elena, and T. Prabhakar Clement. "A novel approach for characterizing the mixing zone of a saltwater wedge." Geophysical Research Letters 36.6 (2009).

Alley, William M., et al. "Flow and storage in groundwater systems." science 296.5575 (2002): 1985-1990.

Bansal, R. K. A textbook of fluid mechanics. Firewall Media, 2005.

Barenblatt, Grigory Isaakovich. Scaling. Vol. 34. Cambridge University Press, 2003.

Barlow, Paul M., and Allen F. Moench. Analytical solutions and computer programs for hydraulic interaction of stream-aquifer systems. No. 98-415-A. US Dept. of the Interior, US Geological Survey; Information Services [distributor], 1998.

Bear, J. "Dynamics of Fluids in Porous Media Dover Publications New York Google Scholar." (1972).

Bear, Jacob. "Hydraulics of Groundwater, 569." (1979).

Berezhkovskii, Alexander M. "Ordinary differential equation for local accumulation time." The Journal of chemical physics 135.7 (2011): 08B621.

Berezhkovskii, Alexander M., and Stanislav Y. Shvartsman. "Physical interpretation of mean local accumulation time of morphogen gradient formation." The Journal of chemical physics 135.15 (2011): 10B618.

Berezhkovskii, Alexander M., Christine Sample, and Stanislav Y. Shvartsman. "How long does it take to establish a morphogen gradient?." Biophysical journal 99.8 (2010): L59-L61.

Bohling, Geoffrey C., et al. "A field assessment of the value of steady shape hydraulic tomography for characterization of aquifer heterogeneities." Water Resources Research 43.5 (2007).

Bohling, Geoffrey C., et al. "Steady shape analysis of tomographic pumping tests for characterization of aquifer heterogeneities." Water Resources Research 38.12 (2002).

Bouwer, Herman. "Artificial recharge of groundwater: hydrogeology and engineering." Hydrogeology Journal 10.1 (2002): 121-142.

Bredehoeft, J. D., William Back, and B. B. Hanshaw. "Regional ground-water flow concepts in the United States: historical perspective." Geological Society of America Special Papers 189 (1982): 295-316.

Bredehoeft, John, and Eloise Kendy. "Strategies for offsetting seasonal impacts of pumping on a nearby stream." Ground Water 46.1 (2008): 23-29.

Bredehoeft, J., and T. Durbin. "Ground water development—The time to full capture problem." Ground water 47.4 (2009): 506-514.

Buès, M. A., and C. Oltean. "Numerical simulations for saltwater intrusion by the mixed hybrid finite element method and discontinuous finite element method." Transport in Porous Media 40.2 (2000): 171-200.

Butler, James J. "Pumping tests in nonuniform aquifers—The radially symmetric case." Journal of Hydrology 101.1-4 (1988): 15-30.

Carslaw, Horatio Scott, and John Conrad Jaeger. "Conduction of heat in solids." Oxford: Clarendon Press, 1959, 2nd ed. (1959).

Chang, Sun Woo, and T. Prabhakar Clement. "Experimental and numerical investigation of saltwater intrusion dynamics in flux-controlled groundwater systems." Water Resources Research 48.9 (2012).

Chang, Sun Woo, and T. Prabhakar Clement. "Laboratory and numerical investigation of transport processes occurring above and within a saltwater wedge." Journal of contaminant hydrology 147 (2013): 14-24.

Chang, Sun Woo, et al. "Does sea-level rise have an impact on saltwater intrusion?." Advances in water resources 34.10 (2011): 1283-1291.

Chapra, Steven C., and Raymond P. Canale. Numerical methods for engineers. Vol. 2. New York: McGraw-Hill, 1998.

Clement, T. P., William R. Wise, and Fred J. Molz. "A physically based, two-dimensional, finite-difference algorithm for modeling variably saturated flow." Journal of Hydrology 161.1-4 (1994): 71-90.

Crank, John. The mathematics of diffusion. Oxford university press, 1979.

Zill, Dennis, Warren S. Wright, and Michael R. Cullen. Advanced engineering mathematics. Jones & Bartlett Learning, 2011.

Currell, Matthew, Tom Gleeson, and Peter Dahlhaus. "A new assessment framework for transience in hydrogeological systems." Groundwater 54.1 (2016): 4-14.

Cussler, Edward Lansing. Diffusion: mass transfer in fluid systems. Cambridge university press, 2009.

Daher, Walid, et al. "Karst and artificial recharge: Theoretical and practical problems: A preliminary approach to artificial recharge assessment." Journal of Hydrology 408.3 (2011): 189-202.

Downing, R. A., et al. "Regional development of groundwater resources in combination with surface water." Journal of Hydrology 22.1-2 (1974): 155-177.

Ellery, Adam J., et al. "Critical time scales for advection-diffusion-reaction processes." Physical Review E 85.4 (2012a): 041135.

Ellery, Adam J., et al. "Moments of action provide insight into critical times for advection-diffusion-reaction processes." Physical Review E 86.3 (2012b): 031136.

Ellery, Adam J., et al. "Simplified approach for calculating moments of action for linear reaction-diffusion equations." Physical Review E 88.5 (2013): 054102.

Erskine, A. D., and A. Papaioannou. "The use of aquifer response rate in the assessment of groundwater resources." Journal of Hydrology 202.1 (1997): 373-391.

Freeze, R. Allan, and Paul Adams Witherspoon. "Theoretical analysis of regional groundwater flow: 1. Analytical and numerical solutions to the mathematical model." Water Resources Research 2.4 (1966): 641-656.

Gelhar, Lynn W., and John L. Wilson. "Ground-Water Quality Modeling." Ground Water 12.6 (1974): 399-408.

Glover, Robert E., and Glenn G. Balmer. "River depletion resulting from pumping a well near a river." Eos, Transactions American Geophysical Union 35.3 (1954): 468-470.

Gordon, Peter V., et al. "Local kinetics of morphogen gradients." Proceedings of the National Academy of Sciences 108.15 (2011): 6157-6162.

Goswami, Rohit R., and T. Prabhakar Clement. "Laboratory-scale investigation of saltwater intrusion dynamics." Water Resources Research 43.4 (2007).

Grimmett, G., and D. Welsh. "Probability: An Introduction. Clarendon." (1986): 19.

Haberman, Richard. Applied partial differential equations: with Fourier series and boundary value problems. Vol. 4. Upper Saddle River: Pearson Prentice Hall, 2004.

Haitjema, Henk M. Analytic element modeling of groundwater flow. Academic Press, 1995.

Haitjema, Henk. "The role of hand calculations in ground water flow modeling." Ground water 44.6 (2006): 786-791.

Hanson, Randall Tyler. "Aquifer-system compaction, Tucson Basin and Avra Valley, Arizona." (1988).

Hantush, Mohamed M. "Modeling stream–aquifer interactions with linear response functions." Journal of Hydrology 311.1 (2005): 59-79.

Heath, Ralph C. Basic ground-water hydrology. Vol. 2220. US Geological Survey, 1983.

Heath, Ralph C. "Another Look at Steady-Shape Conditions." Ground water 47.5 (2009): 612-614.

Hickson, Roslyn I., et al. "A comparison of critical time definitions in multilayer diffusion." The ANZIAM Journal 52.04 (2011): 333-358.

Hickson, R. I., S. I. Barry, and G. N. Mercer. "Critical times in multilayer diffusion. Part 1: Exact solutions." International Journal of Heat and Mass Transfer 52.25 (2009a): 5776-5783.

Hickson, R. I., S. I. Barry, and G. N. Mercer. "Critical times in multilayer diffusion. Part 2: Approximate solutions." International Journal of Heat and Mass Transfer 52.25 (2009b): 5784-5791.

Hickson, R. I., et al. "Critical times in single-layer reaction diffusion." International Journal of Heat and Mass Transfer 54.11 (2011): 2642-2650.

Jazaei, Farhad, Matthew J. Simpson, and T. Prabhakar Clement. "An analytical framework for quantifying aquifer response time scales associated with transient boundary conditions." Journal of Hydrology 519 (2014): 1642-1648.

Jazaei, Farhad, Matthew J. Simpson, and T. Prabhakar Clement. "Spatial analysis of aquifer response times for radial flow processes: Nondimensional analysis and laboratory-scale tests." Journal of Hydrology 532 (2016): 1-8.

Jazaei, Farhad, Matthew J. Simpson, and T. Prabhakar Clement. "Understanding time scales of diffusive fluxes and the implication for steady state and steady shape conditions." Geophysical Research Letters 44.1 (2017): 174-180.

Jenkins, C. T. Computation of rate and volume of stream depletion by wells. No. 04-D1. US Dept. of the Interior, Geological Survey: For sale by the Supt. of Docs., USGPO, 1968a.

Jenkins, C. T. "Techniques for computing rate and volume of stream depletion by wells." Ground Water 6.2 (1968b): 37-46.

Jenkins, Clifford Thaine. "Electric-Analog and Digital-Computer Model Analysis of Stream Depletion by Wells." Ground Water 6.6 (1968c): 27-34.

Kim, Dong-Ju, and Myeong-Joon Ann. "Analytical solutions of water table variation in a horizontal unconfined aquifer: Constant recharge and bounded by parallel streams." Hydrological Processes 15.13 (2001): 2691-2699.

Knight, John H., Mat Gilfedder, and Glen R. Walker. "Impacts of irrigation and dryland development on groundwater discharge to rivers—A unit response approach to cumulative impacts analysis." Journal of Hydrology 303.1 (2005): 79-91.

Konikow, Leonard F., and Stanley A. Leake. "Depletion and capture: revisiting "The source of water derived from wells"." Groundwater 52.S1 (2014): 100-111.

Kooi, H., and J. Groen. "Geological processes and the management of groundwater resources in coastal areas." Netherlands Journal of Geosciences 82.01 (2003): 31-40.

Kooi, H., J. Groen, and A. Leijnse. "Modes of seawater intrusion during transgressions." Water resources research 36.12 (2000): 3581-3589.

Kreyszig, Erwin. "Advanced Engineering Mathematics." Integration 9 (2008): 4.

Kruseman, Gideon P., and Nicolaas A. de Ridder. Analysis and evaluation of pumping test data. The Netherlands: International Institute for Land Reclamation and Improvement, 1979.

Landman, Kerry A., and Lee R. White. "Predicting filtration time and maximizing throughput in a pressure filter." AIChE Journal 43.12 (1997): 3147-3160.

Landman, Kerry, and Mark Mcguinness. "Mean action time for diffusive processes." Advances in Decision Sciences 4.2 (2000): 125-141.

Leake, S. A. "Interbed storage changes and compaction in models of regional groundwater flow." Water Resources Research 26.9 (1990): 1939-1950.

Li, Wei, Wolfgang Nowak, and Olaf A. Cirpka. "Geostatistical inverse modeling of transient pumping tests using temporal moments of drawdown." Water resources research 41.8 (2005).

Lockington, D. A. "Response of unconfined aquifer to sudden change in boundary head." Journal of Irrigation and Drainage Engineering 123.1 (1997): 24-27.

Lu, Chunhui, and Adrian D. Werner. "Timescales of seawater intrusion and retreat." Advances in Water Resources 59 (2013): 39-51.

Manga, Michael. "On the timescales characterizing groundwater discharge at springs." Journal of Hydrology 219.1 (1999): 56-69.

Martín-Rosales, W., et al. "Estimating groundwater recharge induced by engineering systems in a semiarid area (southeastern Spain)." Environmental Geology 52.5 (2007): 985-995.

McDonald, Michael G., and Arlen W. Harbaugh. "The history of MODFLOW." Ground water 41.2 (2003): 280-283.

McGowan, P., and M. McGuiness. "Modelling the cooking process of a single cereal grain." (1996).

McGuinness, M. J., et al. "Modelling the wetting and cooking of a single cereal grain." IMA Journal of Management Mathematics 11.1 (2000): 49-70.

McNabb, A. "Means action times, time lags, and mean first passage times for some diffusion problems." Mathematical and computer modelling 18.10 (1993): 123-129.

McNabb, A., and Graeme Charles Wake. "Heat conduction and finite measures for transition times between steady states." IMA Journal of Applied Mathematics 47.2 (1991): 193-206.

McNabb, Alex, and Grant Keady. "Diffusion and the torsion parameter." Journal of the Australian Mathematical Society-Series B 35.3 (1994): 289-301.

McNabb, Alex, and Robert S. Anderssen. "The Freezing Time for Pseudo-Ellipsoids." Mini-Conference on Free and Moving Boundary and Diffusion Problems. Centre for Mathematics and its Applications, Mathematical Sciences Institute, The Australian National University, 1992.

McNabb, A., et al. "Theoretical derivation of rules-of-thumb for freezing times." Inverse Problems 7.4 (1991): 633.

Moffat, B. A., et al. "Age-related changes in the kinetics of water transport in normal human lenses." Experimental eye research 69.6 (1999): 663-669.

Ojha, Chandra Shekhar P. "Explicit aquifer diffusivity estimation using linearly varying stream stage." Journal of Hydrologic Engineering 5.2 (2000): 218-221.

Pedretti, Daniele, et al. "A quick and inexpensive method to quantify spatially variable infiltration capacity for artificial recharge ponds using photographic images." Journal of hydrology 430 (2012): 118-126.

Pinder, George F., John D. Bredehoeft, and Hilton H. Cooper. "Determination of aquifer diffusivity from aquifer response to fluctuations in river stage." Water Resources Research 5.4 (1969): 850-855.

Purich, Daniel L., and R. Donald Allison. Handbook of biochemical kinetics: a guide to dynamic processes in the molecular life sciences. Academic Press, 1999.

Raghunath, Hassan Manjunath. Ground water. New Age International, 1987.

Remson, Irwin, George M. Hornberger, and Fred J. Molz. "Numerical methods in subsurface hydrology." (1971).

Riley, Francis S. "Analysis of borehole extensometer data from central California." Land subsidence 2 (1969): 423-431.

Rodríguez, Leticia B., Pablo A. Cello, and Carlos A. Vionnet. "Modeling stream-aquifer interactions in a shallow aquifer, Choele Choel Island, Patagonia, Argentina." Hydrogeology Journal 14.4 (2006): 591-602.

Rousseau-Gueutin, P., et al. "Time to reach near-steady state in large aquifers." Water Resources Research 49.10 (2013): 6893-6908.

Rousseau-Gueutin, P., et al. "Time to reach near-steady state in large aquifers." Water Resources Research 49.10 (2013): 6893-6908.

Rowe, P. P. "An equation for estimating transmissibility and coefficient of storage from river-level fluctuations." Journal of Geophysical Research 65.10 (1960): 3419-3424.

Rushton, Kenneth Ralph, and Seymour C. Redshaw. Seepage and groundwater flow: Numerical analysis by analog and digital methods. Chichester, 1979.

Schwartz, Franklin W., et al. "Ambiguous hydraulic heads and 14C activities in transient regional flow." Groundwater 48.3 (2010): 366-379.

Simpson, Matthew J. "Critical time scales for morphogen gradient formation: Concentration or gradient criteria?." International Journal of Heat and Mass Transfer 106 (2017): 570-572.

Simpson, Matthew J., et al. "Critical timescales and time intervals for coupled linear processes." The ANZIAM Journal 54.03 (2013): 127-142.

Simpson, Matthew J., Farhad Jazaei, and T. Prabhakar Clement. "How long does it take for aquifer recharge or aquifer discharge processes to reach steady state?." Journal of Hydrology 501 (2013): 241-248.

Simpson, Matthew J., T. Prabhakar Clement, and Francis E. Yeomans. "Analytical model for computing residence times near a pumping well." Ground water 41.3 (2003): 351-354.

Simpson, M. J., T. P. Clement, and T. A. Gallop. "Laboratory and Numerical Investigation of Flow and Transport Near a Seepage-Face Boundary." Ground water 41.5 (2003): 690-700.

Singh, Sita Ram, and Budhi Sagar. "Estimation of aquifer diffusivity in stream-aquifer systems." Journal of the Hydraulics Division 103.11 (1977): 1293-1302.

Singh, Vijay P., Il Won Seo, and Jung H. Sonu. Hydrologic Modeling: Proceedings of the International Conference on Water, Environment, Ecology, Socio-economics, and Health Engineering (WEESHE): October 18-21, 1999, Seoul National University, Seoul, Korea. Water Resources Publication, 1999.

Sophocleous, Marios. "Retracted: On Understanding and Predicting Groundwater Response Time." Groundwater 50.4 (2012): 528-540.

Sophocleous, Mario. "From safe yield to sustainable development of water resources—the Kansas experience." Journal of Hydrology 235.1 (2000): 27-43.

Strack, Otto DL. Groundwater mechanics. Prentice Hall, 1989.

Swamee, Prabhata K., and Sushil K. Singh. "Estimation of aquifer diffusivity from stream stage variation." Journal of Hydrologic Engineering 8.1 (2003): 20-24.

Theis, Charles V. "The effect of a well on the flow of a nearby stream." Eos, Transactions American Geophysical Union 22.3 (1941): 734-738.

Theis, Charles V. "The relation between the lowering of the Piezometric surface and the rate and duration of discharge of a well using ground-water storage." Eos, Transactions American Geophysical Union 16.2 (1935): 519-524.

Theis, Charles V. "The source of water derived from wells." Civil Engineering 10.5 (1940): 277-280.

Townley, Lloyd R. "The response of aquifers to periodic forcing." Advances in Water Resources 18.3 (1995): 125-146.

Turcotte, Donald L., and Geodynamics Schubert. "Geodynamics: Applications of continuum physics to geological problems, 450 pp." (1982).

Vandenbohede, Alexander, and Emmanuel Van Houtte. "Heat transport and temperature distribution during managed artificial recharge with surface ponds." Journal of hydrology 472 (2012): 77-89.

Vasseur, Guy, Pauline Rousseau-Gueutin, and Ghislain De Marsily. "Time constant of hydraulic-head response in aquifers subjected to sudden recharge change: application to large basins." Hydrogeology Journal 23.5 (2015): 915-934.

Waigh, Thomas Andrew. The Physics of Living Processes: A Mesoscopic Approach. John Wiley & Sons, 2014.

Walker, Glen R., et al. "Predicting Aquifer Response Time for Application in Catchment Modeling." Groundwater 53.3 (2015): 475-484.

Walton, William C. "Aquifer system response time and groundwater supply management." Ground Water 49.2 (2011): 126-127.

Wang, Herbert F., and Mary P. Anderson. Introduction to groundwater modeling: finite difference and finite element methods. Academic Press, 1995.

Watson, Ty A., Adrian D. Werner, and Craig T. Simmons. "Transience of seawater intrusion in response to sea level rise." Water Resources Research 46.12 (2010).

Winter, Thomas C. "Recent advances in understanding the interaction of groundwater and surface water." Reviews of Geophysics 33.S2 (1995): 985-994.

Zheng, Chunmiao, and Gordon D. Bennett. Applied contaminant transport modeling. Vol. 2. New York: Wiley-Interscience, 2002.

Zhou, Yangxiao. "A critical review of groundwater budget myth, safe yield and sustainability." Journal of Hydrology 370.1 (2009): 207-213.

Zhu, Junfeng, and Tian-Chyi J. Yeh. "Analysis of hydraulic tomography using temporal moments of drawdown recovery data." Water Resources Research 42.2 (2006).

APPENDIX-A

Contents of this Appendix

Introduction

This supporting information document provides additional details regarding how MAT theory can be used to determine the time scales associated with the dependent variable and the flux variable for multi-dimensional diffusion problems. In Text S1 we provide the detailed information on MAT boundary value problem development for Case-I and Case-II. In Text S2 we discuss a two-dimensional problem involving groundwater flow near a pumping well with radial symmetry. Text S3 discusses a rectangular two-dimensional Cartesian problem. Text S1, Text S2 and Text S3 are cited in the main text.

Text S1: Details of the boundary conditions for Case-I and Case-II

In the main text, Eqs. (117) and (118) introduce the initial and boundary conditions for Case-I and Case-II, respectively. To derive Eq. (119), we first employ the definition of $M_{\phi}(x)$ as

described in Eq. (110); we then apply integration by parts noting that $\phi(x,t)$ approaches $\phi_\infty(x,t)$ exponentially fast as $t \to +\infty$, which gives

$$M_\phi(x)C_\phi(x) = \int_0^\infty \phi_\infty(r) - \phi(r,t)\ \mathrm{d}t, \tag{128}$$

where, $C_\phi(x) = C_\infty(x) - C_0(x)$. Differentiating Eq. (128) twice with respect to x gives

$$\frac{\mathrm{d}\left[M_\phi(x)C_\phi(x)\right]}{\mathrm{d}x} = \int_0^\infty \left(\frac{\mathrm{d}\phi_\infty(x)}{\mathrm{d}x} - \frac{\partial\phi(x,t)}{\partial x}\right)\ \mathrm{d}t, \tag{129}$$

$$\frac{\mathrm{d}^2\left[M_\phi(x)C_\phi(x)\right]}{\mathrm{d}x^2} = \int_0^\infty \left(\frac{\mathrm{d}^2\phi_\infty(x)}{\mathrm{d}x^2} - \frac{\partial^2\phi(x,t)}{\partial x^2}\right)\ \mathrm{d}t. \tag{130}$$

Combining Eq.(130) and Eq. (106) gives the boundary value problem for $M_\phi(x)$, which is given by Eq. (119). To solve the boundary value problem, two boundary conditions at $x = 0$ and $x = 1$ are required for each case. For Case-I, the boundary condition at $x = 0$ can be determined by combining Eqs.(129), (117) and (120), noting that $\mathrm{d}\phi_\infty(0)/\mathrm{d}x = \partial\phi(0,t)/\partial x$. Combining Eqs. (119) and (120) and evaluating the result at $x = 1$ leads to the second boundary condition of Case-I. Both boundary conditions for Case-I are presented in Eq. (117). Similarly, for Case-II the boundary condition at $x = 0$ can be determined by combining Eqs. (129), (118) and (121), noting that $\mathrm{d}\phi_\infty(0)/\mathrm{d}x = \partial\phi(0,t)/\partial x$. Also, combining Eqs. (119) and (121), and evaluating the result at $x = 1$ leads to the second boundary condition for Case-II. These two boundary conditions for Case-II are presented in Eq. (123).

Text S2: MAT theory for analyzing fluxes near a pumping well

In the main text, the theory of MAT is applied to estimate the time scales required for the dependent variable and the associated flux to approach their respective steady states for several

one-dimensional Cartesian problems. Here, the framework is expanded to solve multi-dimensional problems. In this test case we exploit radial symetry to transform and solve a groundwater problem involving a pumping well into a one-dimenional radial flow problem. We have employ the notations used by *Jazaei et al., (2016)* and we extended their work to derive the MAT for diffusive fluxes. Consider groundwater flow near a fully penetrating well of radius, r'_w, at the center of a confined homogenous aquifer of radius R'. The aquifer has transmissivity and storativity values of T', and S, respectively. The dimensional groundwater flow head, $\phi'(r',t')$, at time t', and at distance r' from the well, can be modeled by

$$S\frac{\partial \phi'(r',t')}{\partial t'} = \frac{T'}{r'}\frac{\partial}{\partial r'}\left[r'\frac{\partial \phi'(r',t')}{\partial r'}\right], \quad r'_w < r' < R'. \tag{131}$$

To simplify the analysis, the non-dimensional form of Eq. (130) is

$$\frac{\partial \phi(r,t)}{\partial t} = \frac{1}{r}\frac{\partial}{\partial r}\left[r\frac{\partial \phi(r,t)}{\partial r}\right], \quad \delta < r < 1, \tag{132}$$

where,

$$r = \frac{r'}{R'},\ t = \frac{t'T'}{SR'^{2}},\ \phi = \frac{\phi'}{\Phi'},\ \sigma = \frac{r'_w}{R'}. \tag{133}$$

In Eq. (130) Φ' is a characteristic value of the dependent variable. We consider a constant flow rate, Q', at the well located at, $r = \delta$, a Dirichlet boundary condition at $r = 1$, and a uniform initial condition. The initial and boundary conditions for Eq. (132) can be summarized as (*Jazaei et al., 2016):*

$$IC:\ \ \phi(r,0) = \phi_0(r) = 1,\ \ \text{BCs:}\ \ \frac{\partial \phi(\sigma,t)}{\partial r} - \lambda = \frac{\sigma}{2S}\frac{\partial \phi(\sigma,t)}{\partial t} \quad \text{and} \quad \phi(1,t) = 1, \tag{134}$$

where $\lambda = Q'/(2\pi T'\Phi'\delta)$. The steady solution of Eq. (132) is

$$\phi_\infty(r) = 1 + \delta\lambda \ln(r), \quad \delta < r < 1. \tag{135}$$

We define $F_\phi(t\,|\,r)$ and $f_\phi(t\,|\,r)$ for the radial process in the usual way,

$$F_\phi(t\,|\,r) = 1 - \left[\frac{\phi(r,t) - \phi_\infty(r)}{\phi_0(r) - \phi_\infty(r)}\right], \quad t \geq 0, \tag{136}$$

$$f_\phi(t\,|\,r) = \frac{\mathrm{d}F_\phi(t\,|\,r)}{\mathrm{d}t} = -\frac{\partial}{\partial t}\left[\frac{\phi(r,t) - \phi_\infty(r)}{\phi_0(r) - \phi_\infty(r)}\right], \quad t \geq 0. \tag{137}$$

The MAT for $\phi(r,t)$ is

$$M_\phi(r) = \int_0^\infty t f_\phi(t\,|\,r)\,\mathrm{d}t. \tag{138}$$

Since $\phi(r,t)$ decays to $\phi_\infty(r)$ exponentially fast as $t \to +\infty$ [*Crank*, 1979], applying integration by parts to Eq. (138) leads to

$$M_\phi(r) C_\phi(r) = \int_0^\infty \phi_\infty(r) - \phi(r,t)\;\mathrm{d}t, \tag{139}$$

where, $C_\phi(r) = C_\infty(r) - C_0(r).$

Differentiating Eq. (139) twice with respect to r gives

$$\frac{\mathrm{d}\left[M_\phi(r) C_\phi(r)\right]}{\mathrm{d}r} = \int_0^\infty \left(\frac{\mathrm{d}\phi_\infty(r)}{\mathrm{d}r} - \frac{\partial\phi(r,t)}{\partial r}\right)\mathrm{d}t, \tag{140}$$

$$\frac{\mathrm{d}^2\left[M_\phi(r) C_\phi(r)\right]}{\mathrm{d}r^2} = \int_0^\infty \left(\frac{\mathrm{d}^2\phi_\infty(r)}{\mathrm{d}r^2} - \frac{\partial^2\phi(r,t)}{\partial r^2}\right)\mathrm{d}t, \tag{141}$$

and combining the results with Eq. (132), gives a boundary value problem for $M_\phi(r)$,

$$\frac{\mathrm{d}^2 M_\phi(r)}{\mathrm{d}r^2} + \frac{\mathrm{d}M_\phi(r)}{\mathrm{d}r}\left[\frac{2 + \ln(r)}{r\ln(r)}\right] = -1. \tag{142}$$

Appropriate boundary conditions required to solve Eq. (142) are [*Jazaei et al.*, 2016]:

$$\frac{\mathrm{d}M_{\phi}(\delta)}{\mathrm{d}r}+\frac{M(\delta)}{\delta\ln(\delta)}=\frac{-\delta}{2S}, \tag{143}$$

$$\frac{\mathrm{d}M_{\phi}(1)}{\mathrm{d}r}=0. \tag{144}$$

The solution of Eq. (142), using Eqs. (143) and (144) can be written as

$$M_{\phi}(r)=\frac{r^2[1-\ln(r)]-1}{4\ln(r)}+\frac{\delta^2[2\ln(\delta)-1]}{4}-\frac{\delta^2\ln(\delta)}{2S}. \tag{145}$$

As explained in the main text, Eq. (116) can be used to express the relationship between the time scales of dependent variable, $M_{\phi}(x)$, and the associated gradient variation, $M_g(x)$, in a one-dimensional Cartesian system. Here we extend this analysis to develop a similar relationship for radial flow. To accomplish this, we first define appropriate CDF, PDF and MAT variables,

$$F_g(t\,|\,r)=1-\left[\frac{g(r,t)-g_{\infty}(r)}{g_0(r)-g_{\infty}(r)}\right],\quad t\geq 0, \tag{146}$$

$$f_g(t\,|\,r)=\frac{\mathrm{d}F_g(t\,|\,r)}{\mathrm{d}t}=-\frac{\partial}{\partial t}\left[\frac{g(r,t)-g_{\infty}(r)}{g_0(r)-g_{\infty}(r)}\right],\quad t\geq 0, \tag{147}$$

$$M_g(r)=\int_0^{\infty}t f_g(t\,|\,r)\ \mathrm{d}t, \tag{148}$$

where $g_0(r)$, $g_{\infty}(r)$ and $g(r,t)$ are the initial condition, steady state solution and transient solution of the equation governing the evolution of $\partial\phi/\partial r$. Combining Eqs. (147) and (148), and interchanging the order of the differentiation gives

$$M_g(r)=\frac{-1}{g_0(r)-g_{\infty}(r)}\frac{\partial}{\partial r}\int_0^{\infty}t\frac{\partial\left[\phi(r,t)-\phi_{\infty}(r)\right]}{\partial t}\ \mathrm{d}t. \tag{149}$$

Combining Eq. (149) and Eq. (138) gives the relationship between $M_\phi(r)$ and $M_g(r)$,

$$M_g(r) = M_\phi(r) + \frac{C_\phi(r)}{\mathrm{d}C_\phi(r)/\mathrm{d}r}\left(\frac{\mathrm{d}M_\phi(r)}{\mathrm{d}r}\right). \tag{150}$$

We use Eq. (145) and Eq. (150) to compute the time scales of the dependent variable and the flux variable, and the results are summarized in Figure 4-1a. The results show a clear difference between the two time scales, with $M_g(r) < M_\phi(r)$, which is consistent with the conventional assumption that, in radial groundwater flow systems, steady shape conditions are attained before steady state conditions. To further validate these findings, we solve Eq. (132), with appropriate boundary and initial conditions, numerically. The $\phi(r,t)$ and *g(r,t)* functions, evaluated at two specific locations are given in Figure A-1 (b) and (c), respectively. These figures also show MAT values, $M_\phi(r)$ and $M_g(r)$, computed using Eq. (145) and Eq. (150).

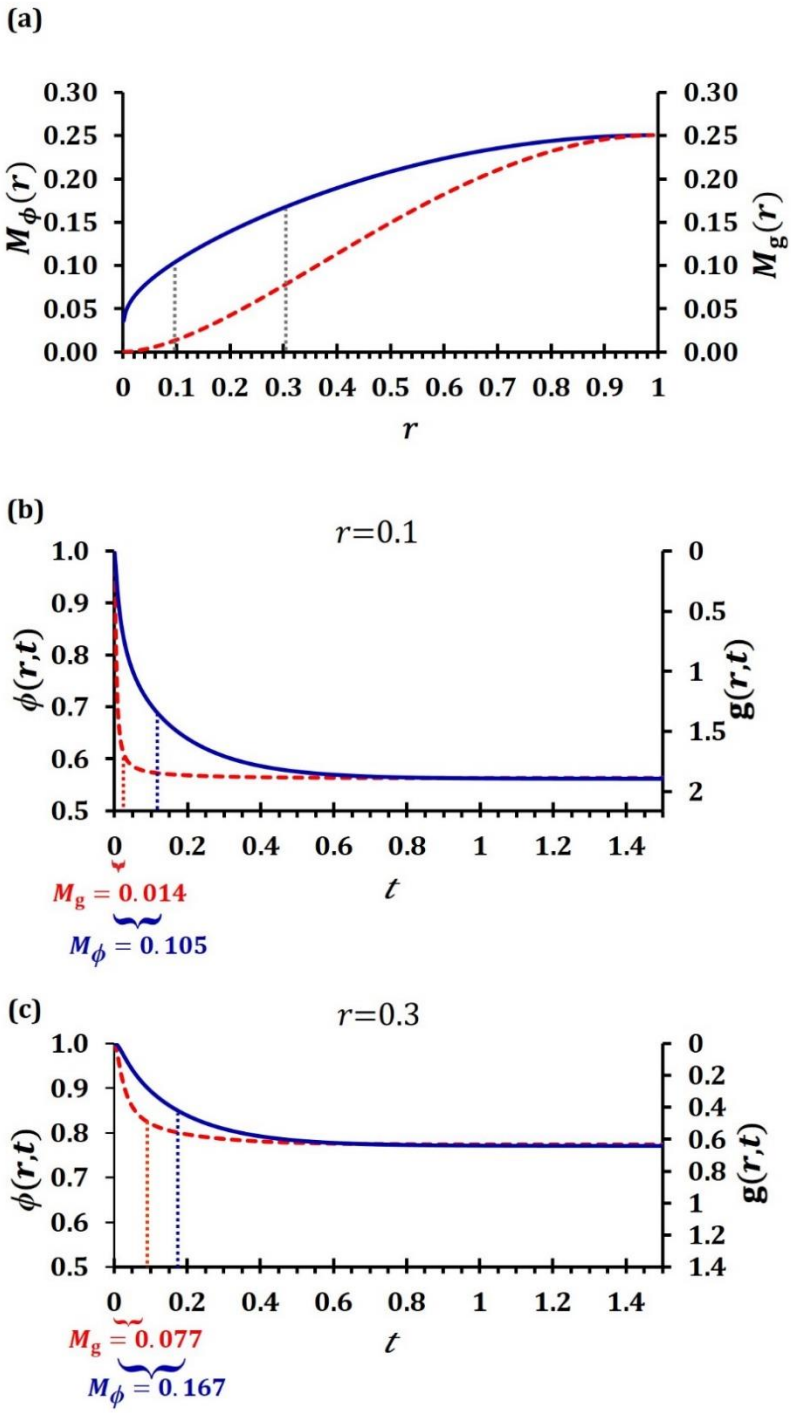

Figure A-1 Time scales of diffusive process in a radial problem; (a) shows the spatial variation in $M_\phi(r)$ (solid blue) and $M_g(r)$ (dashed red). Results in (b) and (c) show the numerical solution of $\varphi(r,t)$ (solid blue) and $g(r,t)$ (dashed red) at $r=0.1$ and $r=0.3$, respectively. Parameters are: $\Delta r=0.001$, $\Delta t=0.003$, $\delta=0.001$, $\lambda=0.8$ and $S=0.05$.

Text S3: MAT theory for analyzing fluxes in a two-dimensional Cartesian problem

We now demonstrate the use of MAT theory for solving a two-dimensional Cartesian problem. The problem considered is shown in Figure A-2, and involves three Dirichlet and one Neumann boundary conditions. The non-dimensional diffusion equation and the associated boundary conditions are

$$\frac{\partial \phi(x,y,t)}{\partial t} = \frac{\partial^2 \phi(x,y,t)}{\partial x^2} + \frac{\partial^2 \phi(x,y,t)}{\partial y^2}, \quad 0 < x < 1,\ 0 < y < 1, \tag{151}$$

$$\phi(x,0,t) = 1, \ \ \phi(0,y,t) = 1, \ \ \phi(1,y,t) = 1, \ \ \frac{\partial \phi(x,1,t)}{\partial y} = \eta, \tag{152}$$

where, η is a constant flux at $y = 1$ (Figure A-2). The initial condition is given by $\phi_0(x,y) = 1$. To find the MAT for the dependent variable, $M_\phi(x,y)$, we define

$$F_\phi(t \mid x,y) = 1 - \left[\frac{\phi(x,y,t) - \phi_\infty(x,y)}{\phi_0(x,y) - \phi_\infty(x,y)} \right], \quad t \geq 0, \tag{153}$$

$$f_\phi(t \mid x,y) = \frac{\mathrm{d}F_\phi(t \mid x,y)}{\mathrm{d}t} = -\frac{\partial}{\partial t}\left[\frac{\phi(x,y,t) - \phi_\infty(x,y)}{\phi_0(x,y) - \phi_\infty(x,y)} \right], \quad t \geq 0, \tag{154}$$

where $\phi_\infty(x,y)$ is the steady solution of Eqs. (151) and (152), which could be found numerically or by using separation of variables. The MAT is given by

$$M_\phi(x,y) = \int_0^\infty t f_\phi(t \mid x,y)\mathrm{d}t. \tag{155}$$

Combining Eqs. (154) and (155), applying integration by parts, and noting that $\phi(x,y) - \phi_\infty(x,y)$ decays to zero exponentially fast as $t \to +\infty$ [*Crank*, 1979], we obtain

$$C_\phi(x,y) M_\phi(x,y) = \int_0^\infty \phi(x,y,t) - \phi_\infty(x,y) \ \ \mathrm{d}t, \tag{156}$$

where $C_\phi(x,y) = \phi_\infty(x,y) - \phi_0(x,y)$. Differentiating Eq. (156) twice with respect to x and y gives

$$\frac{\partial^2\left[C_\phi(x,y)M_\phi(x,y)\right]}{\partial x^2} = \int_0^\infty \frac{\partial^2\phi(x,y,t)}{\partial^2 x} - \frac{\partial^2\phi_\infty(x,y)}{\partial^2 x}\ \mathrm{d}t, \tag{157}$$

$$\frac{\partial^2\left[C_\phi(x,y)M_\phi(x,y)\right]}{\partial y^2} = \int_0^\infty \frac{\partial^2\phi(x,y,t)}{\partial^2 y} - \frac{\partial^2\phi_\infty(x,y)}{\partial^2 y}\ \mathrm{d}t. \tag{158}$$

Summing Eqs. (157) and (158), combinng the result with Eq. (151), and recalling that

$$\frac{\partial^2\phi_\infty(x,y,t)}{\partial x^2} + \frac{\partial^2\phi_\infty(x,y,t)}{\partial y^2} = 0, \tag{159}$$

we obtain a boundary value problem for $M_\phi(x,y)$,

$$\frac{\partial^2\left[M_\phi(x,y)C_\phi(x,y)\right]}{\partial x^2} + \frac{\partial^2\left[M_\phi(x,y)C_\phi(x,y)\right]}{\partial y^2} = C_\phi(x,y). \tag{160}$$

Four boundary conditions are required to solve Eq. (160). Boundary conditions for three Dirichlet boundaries at $x=0,\ x=1,$ and $y=0$ can be defined by noting the fact that $M_\phi(x,y)$ is finite at all locations, leading to

$$\frac{\partial^2 C_\phi(0,y)}{\partial^2 x} M(0,y) + 2\frac{\partial C_\phi(0,y)}{\partial x}\frac{\partial M(0,y)}{\partial x} = 0, \tag{161}$$

$$\frac{\partial^2 C_\phi(1,y)}{\partial^2 x} M(1,y) + 2\frac{\partial C_\phi(1,y)}{\partial x}\frac{\partial M(1,y)}{\partial x} = 0, \tag{162}$$

$$\frac{\partial^2 C_\phi(x,0)}{\partial^2 y} M(x,0) + 2\frac{\partial C_\phi(x,0)}{\partial y}\frac{\partial M(x,0)}{\partial y} = 0. \tag{163}$$

Differentiating Eq. (156) with respect to y, at $y=1$ (the Neumann boundary), and noting that $\partial\phi(x,y,t)/\partial y = \partial\phi_{\infty}(x,y)/\partial y$ along this boundary, leads to the fourth boundary condition,

$$\frac{\partial\left[C_{\phi}(x,1)M_{\phi}(x,1)\right]}{\partial y}=0. \tag{164}$$

Therefore, by solving Eq. (160) subject to the four boundary conditions given by Eqs. (161) -(164), we obtain $M_{\phi}(x,y)$ which is the time scale associated with the dependent variable. Unlike the previous one-dimensional problems, here the equation governing the distribution of $M_{\phi}(x,y)$ is a two-dimensional boundary value problem (partial differential equation), and it is probably more convenient to solve this problem numerically rather than working with an infinite series solution that could be obtained using separation of variables. In the next section we will explain how to use this information to evaluate the time scales of associated flux variations.

Unlike the one-dimensional systems that we previously considered, two-dimensional problems can involve gradient variations in two directions since the flux variable is a vector. For brevity we will refer to these directions as the i^{th} directions, and we note that setting $i=x$ allows us to work with the gradient in the x-direction, whereas setting $i=y$ allows us to work with the gradient in the y-direction. Due to the boundary conditions imposed on the original problem, different i^{th}-direction fluxes, $g_{i^{th}}(x,y,t)$, may be associated with different time scales. The framework we present can be used to estimate different time scales for each of the i^{th}-direction gradients, $M_{g_{i^{th}}}(x,y)$. To accomplish this, we define:

$$F_{g_{i^{th}}}(t\mid x,y)=1-\left[\frac{g_{i^{th}}(x,y,t)-g_{i^{th}\infty}(x,y)}{g_{i^{th}0}(x,y)-g_{i^{th}\infty}(x,y)}\right],\quad t\geq 0, \tag{165}$$

$$f_{g_{i^{th}}}(t \mid x,y) = \frac{\mathrm{d}F_{g_{i^{th}}}(t \mid x,y)}{\mathrm{d}t} = -\frac{\partial}{\partial t}\left[\frac{g_{i^{th}}(x,y,t) - g_{i^{th}\infty}(x,y)}{g_{i^{th}0}(x,y) - g_{i^{th}\infty}(x,y)}\right], \tag{166}$$

$$M_{g_{i^{th}}}(x,y) = \int_0^\infty t f_{g_{i^{th}}}(t \mid x,y)\ \mathrm{d}t, \tag{167}$$

where $g_{i^{th}0}(x,y)$, $g_{i^{th}\infty}(x,y)$ and $g_{i^{th}}(x,y,t)$ represent the initial condition, steady state and solutions of the flux variable in the i^{th}-direction, respectively. We then combine Eq. (154) and Eq. (167), and interchange the order of differentiation to obtain

$$M_{g_{i^{th}}}(x,y) = \frac{-1}{g_{i^{th}0}(x,y) - g_{i^{th}\infty}(x,y)} \frac{\partial}{\partial i}\int_0^\infty t \frac{\partial\left[\phi(x,y,t) - \phi_\infty(x,y)\right]}{\partial t}\ \mathrm{d}t, \tag{168}$$

where $\partial/\partial i$ refers to the derivative in the i^{th}-direction. The integral in Eq. (168) is $M_\phi(x,y)$, as in Eq. (155). Therefore, $M_{g_{i^{th}}}(x,y)$, for the two-dimensional problem is given by

$$M_{g_{i^{th}}}(x,y) = M_\phi(x,y) + \frac{C_\phi(x,y)}{\partial C_\phi(x,y)/\partial i}\left(\frac{\partial M_\phi(x,y)}{\partial i}\right). \tag{169}$$

In summary, once we have solved Eq. (160) for $M_\phi(x,y)$, we can then use Eq. (169) to calculate the time scales associated with the flux variable in any direction.

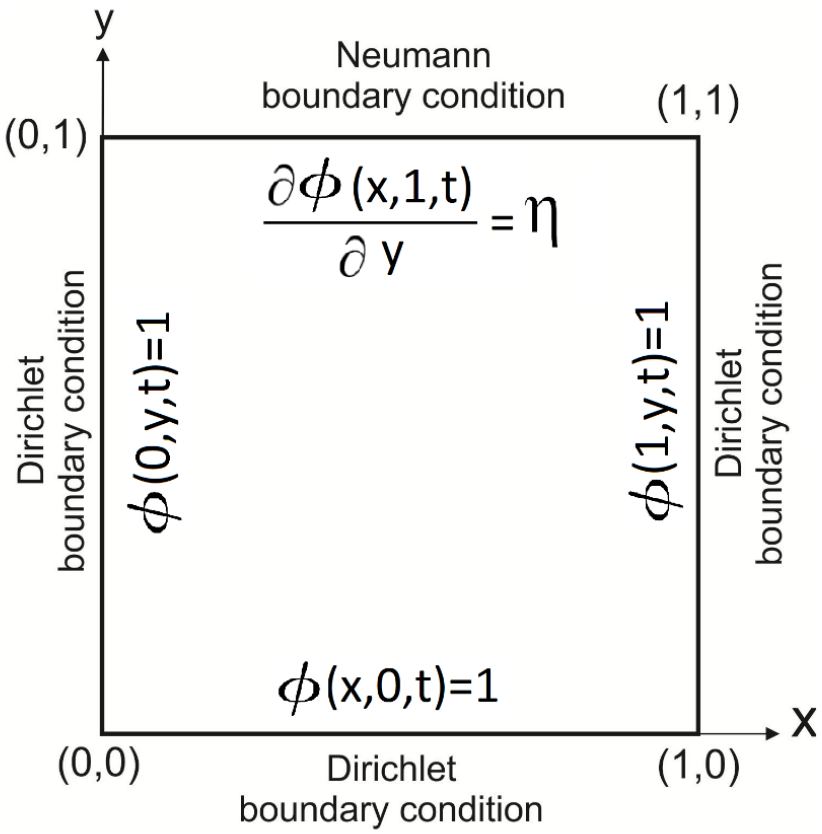

Figure A-2: Schematic of the two-dimensional diffusive problem. Three Dirichlet boundary conditions are defined at $x=0$, $x=1$, and $y=0$; and a Neumann boundary condition is defined at $y=1$.